Aus dem Zentrum für Klinische Tiermedizin

der Tierärztlichen Fakultät

der Ludwig-Maximilians-Universität München

Arbeit angefertigt unter der Leitung von Priv.-Doz. Dr. Nadja Herbach

Angefertigt am Institut für Pathologie der Technischen Universität München

(Univ.-Prof. Dr. Irene Esposito)

Development of a training program for disease modeling and its practical application: morphological characterization of a genetically engineered mouse model for pancreatic cancer

Inaugural-Dissertation zur Erlangung der tiermedizinischen Doktorwürde der Tierärztlichen Fakultät

der Ludwig-Maximilians-Universität München

von Susanne Charlotte Haneder

aus Regensburg

München, 2015

Gedruckt mit der Genehmigung der Tierärztlichen Fakultät

der Ludwig-Maximilians-Universität München

Dekan: Univ.-Prof. Dr. Joachim Braun

Berichterstatter: Priv.-Doz. Dr. Nadja Herbach

Korreferent: Priv.-Doz. Dr. Valeri Zakhartchenko

Tag der Promotion: 31.01.2015

Für meine Familie

"Where the hell is the pancreas, anyway? I don't even know what the damn thing does beside give you cancer." -Hawk Hawkins

TABLE OF CONTENT

ABBREVIATIONS

Ab	Antibody
ADM	Acinar-ductal metaplasia
AFL	Pancreatic atypical flat lesion
AS	Dako Autostainer
cm	Centimeter
DAB	3,3'-diaminobenzidine
DNA	Deoxyribonucleic acid
ECM	Extracellular matrix
EDTA	Ethylenediaminetetraacetic acid
EMT	Epithelial-mesenchymal transition
EtBr	Ethidium bromide
EtOh	Ethanol
FPC	Familial pancreatic cancer
GEM	Genetically engineered mouse
H_2O_2	Hydrogen peroxide
HCl	Hydrogen chloride
hrs	Hours
IPMN	Pancreatic intraductal papillary mucinous neoplasm
KC	LSL-KRAS$^{G12D/+}$;Ptf1a$^{+/Cre(ex1)}$
KC-TNChet	LSL-KRAS$^{G12D/+}$;Ptf1a$^{+/Cre(ex1)}$;TNC$^{+/-}$
KC-TNCko	LSL-KRAS$^{G12D/+}$;Ptf1a$^{+/Cre(ex1)}$;TNC$^{-/-}$
KO	knock-out
mA	Milliampere
man	Manually
MCN	Pancreatic mucinous cystic neoplasm
min	Minute
ml	Milliliter
NaCl	Sodium chloride
ON	Overnight
PanIN	Pancreatic intraepithelial neoplasia
PBS	Phosphate buffered saline
PCR	Polymerase chain reaction
PDAC	Pancreatic ductal adenocarcinoma
rpm	Rounds per minute
RT	Room temperature
SCID	Severe combined immunodeficient
sec	Second
TC	Tubular complex
TNC	Tenascin-C
µg	Microgram
µl	Microliter

I. INTRODUCTION

Experimental animal models of human diseases are increasingly used from basic science to preclinical drug development (Barthold and others 2007, Sundberg and others 2012, Valli and others 2007). This implicates an urgent need for experts being in the position to examine these models for pathophysiological and pathohistological changes and therefore programs to train these experts (Cardiff 2009). Despite the rising need for experts, training programs do not exist in Europe. Therefore, an international, web-based disease model training program for students with a higher university degree was developed within the frame of the Erasmus Lifelong Learning Programme (project N° 517860-LLP-1-2011-1-FI-ERASMUS-FEXI). Specialists in pedagogy, human and veterinary pathology, biochemistry and mouse models of human disease formed the consortium.

As a test run for the training program, morphological phenotyping of a mouse model of pancreatic ductal adenocarcinoma (PDAC) was performed in this thesis using conventional histology, immunohistochemistry and morphometric analysis. For this purpose, a mouse line was generated by crossing the well-characterized mouse line for PDAC, the LSL-KRAS$^{G12D/+}$;Ptf1a$^{+/Cre(ex1)}$ mice (Siveke and others 2007) with mice deficient for the stromal protein Tenascin C (TNC) (Saga and others 1992). Tumor-stroma interactions in PDAC, which is a very lethal disease, play a key role and contribute to the highly aggressive nature of this cancer type (Hwang and others 2008). TNC is overexpressed in the stroma surrounding the precursor lesions of PDAC and in the stroma of PDAC itself. The overexpression of the "large" splice variant of TNC characterizes the invasive and metastatic PDAC (Esposito and others 2006). Exogenous TNC promotes migration and invasion of pancreatic cancer cell lines and a mixed matrix of TNC and fibronectin blocks cell adhesion through activation of the integrin-signaling cascade (Paron and others 2011).

To investigate the functional role of TNC in PDAC progression in vivo, , LSL-KRAS$^{G12D/+}$;Ptf1a$^{+/Cre(ex1)}$;TNC$^{-/-}$ (KC-TNCko) and LSL-KRAS$^{G12D/+}$; Ptf1a$^{+/Cre(ex1)}$;TNC$^{+/-}$(KC-TNChet) mice where compared to LSL-KRAS$^{G12D/+}$; Ptf1a$^{+/Cre(ex1)}$ (KC) mice, focusing on a detailed morphological and histopathological analysis of this newly generated mouse strain. The aim of this

project was to acquire new knowledge of TNC function, in particular in the early phases of PDAC development.

II. LITERATURE REVIEW

1. Web-based learning platform for comparative histology

1.1. Comparative pathology and comparative medicine

The term "comparative pathology" describes the pathology of laboratory animal diseases in comparison to human diseases. The American Heritage Medical Dictionary defines comparative pathology as "the pathology of animal diseases, especially in relation to human pathology" (Dictionaries 2008) meanwhile the Segen's Medical Dictionary offers the description "a field of science which compares specific human pathologies with those seen in natural animal models-e.g., diabetes insipidus in Brattleboro rats, which don't produce vasopressin." (Segen 2005). Whilst in former times authors focused on comparing zoonosis in animals and humans, it was not before the 20th century that animal models for human diseases have been developed (Rader 2004). As animals have been increasingly used in research, in 1967 the National Institute of General Medical Sciences started a comparative medicine program to detect more animal diseases resembling human diseases. The members realized the importance of studying these animals to understand the underlying mechanisms of the particular disease and to gain insight in the disease process in humans. This knowledge would help to identify models for pharmacological, toxicological and drug development studies. The core disciplines of this comparative medicine program were pathology, physiology, psychology, anatomy and pharmacology. It was clearly stated that these basic disciplines and all medical professions should be involved to work hand in hand (Gay 1967, Nielsen 1983). Gay pointed out that comparative medicine is an interdisciplinary science and that it is important that medicine and veterinary medicine should exchange. They defined comparative medicine as "the study of phenomena basic to the diseases of all species" (Gay 1967). Nine years later, Bustad and others described the meaning of comparative medicine as "the study of the nature, cause and cure of abnormal structure and function in people, animals and plants for the eventual application, and benefit of all living things" (Bustad and others 1976).

In the United States, education in laboratory animal medicine can be performed as a residency program or a postdoctoral fellowship. The first training program offered

was at the Bowman Grey Medical School, initiated in 1960. Shortly after, other training programs followed at the Tulane University, the Stanford University, the University of Florida, the Johns Hopkins University, the University of Missouri, the Edgewood Arsenal, Maryland and the Brooks Air Force Base, Texas. The Jackson laboratories started to offer a summer school program already in the year 1924 (Fox 1985). Still, education in comparison of laboratory and human medicine and pathology remains elusive (Sundberg and others 2012).

1.2. Lack of experts in animal modeling and pathology

Over the past century, the laboratory mouse has become the model animal in many laboratories to mimic human diseases (Valli and others 2007). The mouse harbors many advantages – from cheap, small and easy to handle and to breed to the broad similarity of the murine to the human genome. After the human genome was almost completely revealed, the mouse was the first non-human species whose genome was sequenced. Ninety-nine % of the human genes are conserved in the murine genome (Mouse Genome Sequencing and others 2002). Additionally to these genetic similarities, most physiologic and pathologic characteristics have been shown to harbor similarities in mouse and human, as for instance nervous, cardiovascular, endocrine, immune, musculoskeletal and other organ systems (Rosenthal and Brown 2007). Mice and rats comprise 95% of the animals used in biomedical research. The remaining 5% are covered by several animal species as human- and non-human primates, cows, sheep, swine, dogs, cats, birds, rabbits, guinea pigs, hamsters, fish, frogs, nematodes, fruit flies, even yeasts and pea plans (Simmons 2008).

The histopathological evaluation of animal models is a factor that might cause wrong interpretations if not properly carried out by an expert. Additionally, this histopathological evaluation might be frustrating even in simple cases because of unexpected events as leaky promoters, neomorphic or hypomorphic allelic expression instead of allelic deletion, microbial infections, and genetically differences between murine strains, since all these factors may affect the phenotype (Sellers and Ward 2012). Several mouse strains harbor distinct pathological background lesions, as for example the commonly used BALB/cByJ strain displays hepatic steatosis already in young male animals (Serpi and others 2013). Especially these lesions due to a distinct murine background strain might

cause severe differences in the genetically engineered mice (GEM) and should therefore always be considered to influence the result (Sellers and Ward 2012).

Working with an experienced pathologist, educated in murine and human histopathology, is often undervalued. Cardiff and others published in 2008 a statistic depicting an enormous increase in publications working with GEM, meanwhile the number of pathologists working with GEMs is only slightly increasing. In 2003, the ratio publication dealing with knock-out mice to pathologists involved was about 5000 to 1300; meanwhile in 2006 it was over 7000 to not even 2000 pathologists. (Cardiff and others 2008). Several studies and publications reveal a clear need for experts trained in animal models of human diseases and their distinct histopathology as this field has been expanding in the last 20 years (Barthold and others 2007, Bouley and others 2009, Cardiff and others 2008, Sundberg and others 2012).

An important fact is the knowledge to distinguish normal background lesions of various mouse strains from the lesion of interest. Many mouse strains show abnormalities in their physiology without any pathological impact. This gap of pathological knowledge might cause publications of wrong interpretations. For instance, Fu and coworkers misinterpreted abnormally enlarged preputial glands as a teratoma, not knowing about the existence of these glands. The authors wrote an erratum to indicate this fact (Fu and others 2002). Ince and coworkers called this self-evaluation of slides by non-pathologists without involving an expert in comparative pathology a "do-it-yourself (DIY) pathology" (Ince and others 2008). Robert Cardiff addresses this problem in his paper "How to phenotype a mouse?": "Without access to comparative pathologists, how can disease models be analyzed with confidence?". He foresees an aggravation of this problem as e.g. the NIH Knockout Mouse Project (KOMP) generated numerous new mouse models which need to be analyzed histopathologically (Cardiff 2009).

Although in the last years a growing list of resources as books, articles in journals and web pages have been developed to facilitate the pathologic analysis of rodents compared to humans (Bolon and others 2012), this material cannot replace a training course. Inasmuch as there is no specific training program included in the traditionally pathology residency core courses, the only chance to develop skills in this field is to learn by experience, being lucky enough to find a mentor providing the expertise. As these mentors, especially in Europe, are very rare, this might be

tricky. A specialist in comparative pathology not only needs to be trained in basic mouse biology which includes husbandry, pathogens, strain-specific diseases and also in modern biomedical research but also human pathology (Sundberg and others 2012). Modern pathology training programs should include training in differences between mouse strains and their individual background lesions, gender differences, lesion in aging mice and embryonic development (Sellers and Ward 2012). A standardized morphological phenotyping is therefore necessary and it is important to depict differences in murine background strains (Mossbrugger and others 2007). Unfortunately, these requirements are not even completely achieved yet in the training program of veterinarian pathologists. In US, the American College of Veterinary Pathologists (ACVP) offers training in animal models used in biomedical diseases with spontaneous background lesions, and has workshops, which cover the human disease (http://www.acvp.org/). In Europe, the European College of Veterinary Pathologists (ECVP) has only included laboratory animal pathology in their training program, but offers summers schools, symposiums and meetings about comparative pathology (http://www.ecvpath.org/). In Germany, the training program is less defined, but includes laboratory animals (http://www.bltk.de/fileadmin/bltk/user_upload/Dokumente/images/stories/weiter bildung/wb-2003/anlageI/22-0-fta-pathologie.pdf, [date: 01.10.2014]). New technologies as slide scanners and webmicroscopy offer the possibility not only to preserve rare, important material, but also to reach more people over distances and these resources or mentors might be easier to reach (Hamilton and others 2012).

1.3.   Advantages of e-learning

The term e-learning describes a form of electronically supported learning and teaching (Kerres 2013) and has gained significant value in biomedical education. Existing learning strategies can be improved by providing new methods to already existing traditional learning techniques (Boeker and Klar 2006, Dev 2006). Different e-learning strategies have been described: passive, facilitated learning, interactive learner-system, learner-teacher and virtual reality learner-system (Maxwell and Mucklow 2012). E-learning offers the opportunity to improve learning with new tools, even though the participants are not in the same room. This includes animations that can be controlled by the user, exercises with self-assessment and feedback, videos and podcasts that can be streamed on demand. Important assets of e-learning for students are the supply of material, which can be

easily accessed, an improved interactivity and the freedom not to follow time schedules. Web-based learning can be performed any time and in any location with internet-accesses, well suited to the students' needs (Maxwell and Mucklow 2012). Especially in the field of medical education, e-learning offers the opportunity to create case studies which can be attended by the students, as for instance the CASUS system in German veterinarian universities (Borchers and others 2010). The University of Leipzig, Germany, uses Moodle as an e-learning platform to teach their students, offer courses and show curricula. Advantages for the teachers include the wide accessibility of material, which is easy to update once it is established, and the possibility to pursue the students learning activity. Potentially no time restriction interferes with the offered material and teachers are able to update the material any time. The disadvantage of e-learning is the time and personnel needed to set up a course. Nevertheless, e-learning does not exclude the teacher, a personal interaction is possible when needed and necessary. E-learning does not center the teacher, therefore students are able to work according their individual preferences (Salter and others 2014). Even more, e-learning can be individualized, tailored to the students pace of learning, making it a crucial tool for student's education (Masic 2008, Maxwell and Mucklow 2012).

1.4.　　Moodle

Martin Dougiamas developed the user-friendly open-source course management system Moodle in 1999 to improve classical learning platforms. It offers a broad spectrum of tools to work with, for instance wiki, a chatting tool, databases, blogs, calendars and newswire. Moodle is freely available and simple to handle. The program is used in approximately 214 countries for more than 4,784,691 courses with over 45 million students and 1.1 million teachers (Bussieres and others 2012, Seluakumaran and others 2011). This widely used tool is beneficial for the provision of courses in universities, curricula, application of courses and examinations, as well as in the area of medical education to implement case reports, patient cases and macroscopical and histological pictures (Seluakumaran and others 2011).

1.5.　　Webmicroscope

Virtual microscopes are increasingly used in medical education, ranging from dental students to veterinary students in every field of education, as well as

postgraduate programs. By digitalization of histological or histopathological slides, teaching collections can be used for web-based learning (Szymas and Lundin 2011). The usage of virtual slides offers many advantages regarding accessibility, efficiency, pedagogic features and costs. The slide can be accessed from every PC with an internet connection and all students can review the same slide, they do not need to be in the same classroom. Therefore, teachers are able to provide the best slides to all students. A webmicroscope is efficient, as students do not need to adjust the focus, condenser and lightening as with a traditional microscope and can therefore faster access the next slide. Annotations and group discussions offer a broad spectrum for teaching. However, in terms of didactical aspects, it should be considered teaching traditional microscopy as well to train students with the handling of a traditional microscope. Disadvantages of digital microscopy include mainly technical aspects, e.g. less resolution of low magnifications on the PC screen or difficulties in scanning artifacts in tissue (Dee 2009).

1.6. Aim of the project

Aim of this project was to develop a training program for researchers working with animal models and offer an international training course. A combination of animal model pathology and human pathology in this course should help researchers with their future work. To further validate the course system, a deeper morphological phenotyping of a mouse model for PDAC was performed, as described in section 2.

2. Pancreatic cancer and tenascin-C

2.1. Pancreatic cancer

There are many different cancers of the pancreas described, although the term pancreatic cancer is synonymously used for pancreatic ductal adenocarcinoma (PDAC), which accounts for more than 90 % of malignant neoplasia of the human pancreas (Bosman 2010, Maitra and Hruban 2008). PDAC is a tumor of the exocrine compartment of the pancreas, originating from cells with a ductal phenotype and accompanied by a dense stromal reaction, called desmoplasia (Maitra and Hruban 2008). This aggressive solid tumor is highly challenging to treat because of its extensive local invasion, early systemic dissemination, most often in liver, lung and peritoneum (Samuel and Hudson 2012). The desmoplastic stromal is reaction linked with a low perfusion rate leading to a reduced

accessibility of intravenously administered therapeutics (Wilson and others 2014).

2.1.1. Epidemiology

PDAC is a lethal disease with a dismal overall prognosis. In the EU and US it has become the fourth leading cancer death in 2013 and the eight leading cause for cancer related death worldwide. In the past 30 years, PDAC has shown little improvement in survival and cancer mortality and cancer predictions underscore this trend: PDAC is the only major cancer site with no predicted improvement of mortality rates (Malvezzi and others 2013, Siegel and others 2013). In the United States 45,220 patients have been newly diagnosed in 2013, which is an increase of 3 % to the year 2012 (Wang and others 2013). The five year survival rate is below 5 %, which accounts for the very aggressive nature of this cancer (Siegel and others 2013). Known risk factors that have been identified are sex, age, race, rare genetic conditions, smoking, obesity, alcohol abuse, chronic and hereditary pancreatitis, diabetes and infectious diseases (Alsamarrai and others 2014, Wormann and Algul 2013, Yadav and Lowenfels 2013). PDAC is predominantly a disease of the elderly; it is very seldom diagnosed in patients younger than 40 years, the mean age of the patients diagnosed is 73 years (Koorstra and others 2008, Maitra and Hruban 2008).

2.1.2. Prognosis and therapy

In addition to the dismal outlook, patients generally have a poor response to radio- and chemotherapy. Most patients are diagnosed in an advanced stage, as the tumor remains silent until it invades in other structures. Abdominal pain is often the first symptom of the disease, but at this time, the tumor is mostly beyond cure (DiMagno 1999). Surgery is the only treatment with a chance for healing, but only a minor part of patients (15-20 %) qualifies for surgical resection (Sultana and others 2012). The median survival ranges from 2.5 months to 24.1 months, depending on the stage, with a median overall survival of less than 12 months (Bilimoria and others 2007, Siegel and others 2012). To date, the standard chemotherapy is gemcitabine, although the gemcitabine-free FOLFIRINOX regimen (5-FU/folfinic acid, irinotecan and oxaliplatin) showed a higher median survival than gemcitabine alone (Heinemann and others 2012). An early detection of the disease might improve the worse prognosis and serum levels of many enzymes and antigens have been tested, but no reliable marker candidate has been detected so far (Hidalgo 2010, Locker and others 2006). Targeting the tumor stroma might be a promising therapy concept

in PDAC as it is characterized by a poor vascularization and a dense desmoplastic stroma which may contribute to impaired drug delivery and therefore resistance to chemotherapy (Neesse and others 2011).

2.1.3.   Precursor lesions of PDAC

Different distinct precursor lesions of PDAC are described in the literature, including pancreatic intraepithelial neoplasia (PanIN), intraductal papillary mucinous neoplasm (IPMN) and mucinous cystic neoplasm (MCN). Compared to IPMNs and MCNs, PanIN are the most frequent precursor lesions. In contrast to PanIN lesions, IPMNs and MCNs are already established neoplasms (Maitra and Hruban 2008). More recently, another type of precursor lesion was proposed: atypical flat lesions (AFL) (Aichler and others 2012).

Pancreatic intraepithelial neoplasia (PanIN)

PanIN lesions are clearly defined and classified lesions in the WHO classification as follows. PanIN are non-invasive, microscopic proliferative epithelial lesions arising in smaller pancreatic ducts and ductules and are subdivided into PanIN-1A, PanIN-1B, PanIN-2 and PanIN-3, depending on the degree of cytological and architectural atypia, always with a diameter less than 1 cm. PanIN-1A are flat epithelial lesions with minimal atypia. Characteristically, the cells are tall and columnar, containing abundant mucin with basal orientation and small, round to oval nuclei. The similar PanIN-1B lesions harbor additionally a papillary, micropapillary or basally pseudostratified architecture. PanIN-2 lesions are flat or papillary and show nuclear abnormalities as loss of polarity, nuclear crowding, enlarged nuclei, pseudo-stratification and hyperchromatism. Mitoses are a rare finding. PanIN-3 are papillary or micropapillary, lesions with marked atypia. Seldom, this lesions can be flat. Budding of epithelial cells into the lumen of the lesions and luminal necrosis can be found in these lesions. In addition, loss of nuclear polarity, dystrophic goblet cells, abnormal mitoses, nuclear irregularities and prominent nucleoli are a common finding (Hruban and others 2001, Kern and others 2001). These morphological alterations are accompanied by an accumulation of genetic alterations, summarized in Figure 1.

Normal ductal epithelium	→	PanIN1A	→	PanIN1B	→	PanIN2	→	PanIN3	→	PDAC
Genetic alterations		K-ras Her-2/neu				p16		p53 SMAD4 BRCA2		
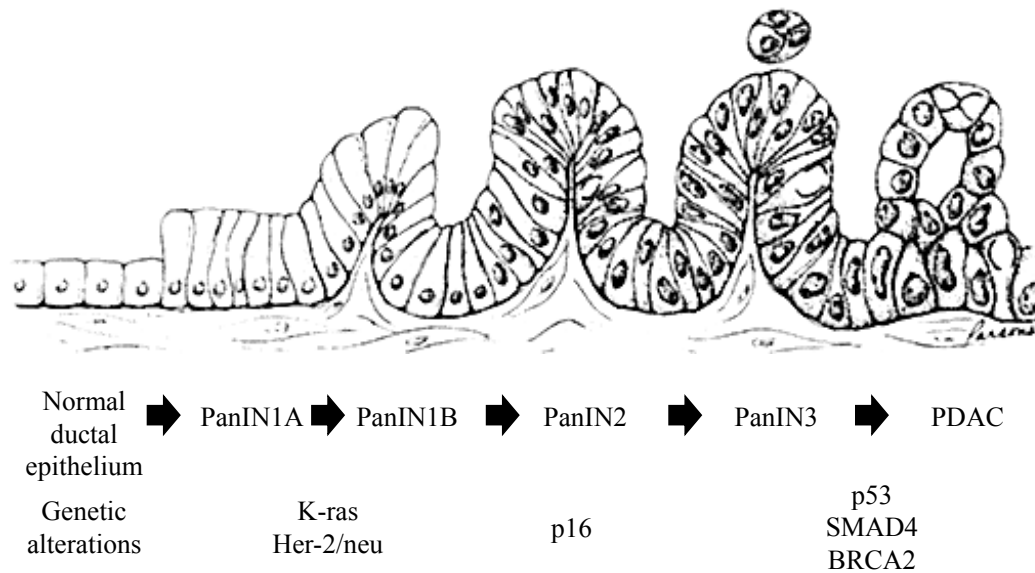
Figure 1: Progression model of pancreatic intraepithelial neoplasia (PanIN) and pancreatic ductal adenocarcinoma (PDAC) formation: Accumulation of genetic alterations leads to PanIN and finally PDAC formation, modified by author (Hruban and others 2006).

Accordingly, murine PanIN are similarly defined as human PanIN (Hruban and others 2006).

Intraductal papillary mucinous neoplasm (IPMN)

In contrast to PanIN, IPMNs are lesions at least 1 cm in size, arising in the main pancreatic duct or branch ducts. Mucin production and papillary architecture are the histologic features of IPMNs (Furukawa and others 2005). IPMNs are subdivided into main-duct (21-36 %), branch-duct (40-48 %) and mixed duct types (16-38 %); branch-duct IPMNs usually have a foveolar appearance and are therefore called "gastric-type", meanwhile main-duct IPMNs are histologically divided into the "intestinal-", "pancreatobiliary-" and "oncocytic-type", depending on morphological and immunohistochemical features. Progression to invasive PDAC is quite common in main-duct IPMNs (48-64 %) and less frequent in branch-duct IPMNs (10-20 %) (Schlitter and Esposito 2012). The 5-year survival rate is depending on the histological subtype and ranges from 52 % (pancreatobiliary-type) to 84 % (oncocytic-type). PDAC arising in the context of IPMN have a better prognosis (Furukawa and others 2011).

Mucinous cystic neoplasm (MCN)

MCNs are mucin producing, cyst-forming epithelial neoplasms without communication with the pancreatic ducts and surrounded by a distinctive ovarian-

type stroma, immunohistochemically expressing hormone-receptor antigens. These lesions are predominantly detected in women (98%). Histologically, MCNs can display low to high-grade dysplasia. One third of MCNs are resected with an associated invasive carcinoma. The 5-year survival for resected patients with noninvasive MCNs is almost 100 % and about 50 % for patients with invasive cancer (Crippa and others 2008, Hruban and Fukushima 2008).

Atypical flat lesions (AFL)

AFL have only recently been described as another type of potential precursor lesions. Discovered in the KC mice, the presence of this lesion was confirmed in non-tumorous specimen of individuals belonging to familial pancreatic cancer (FPC) kindred. AFL are proliferating, non-mucinous, flat ductal lesions with enlarged and hyperchromatic nuclei and prominent nucleoli surrounded by a fibrous and cell-rich stroma that can have a loose, myxoid appearance. Mitoses are a common finding. These lesions seem to arise from tubular complexes (TC) (Aichler and others 2012, Bockman 1997) in areas of tissue remodeling, so called acinar-ductal metaplasia (ADM), and their frequency increases with the age of mice. Compared to PanIN, murine AFL display a higher proliferation activity (10-80 %), p53 positivity and stromal accumulation of αSMA (Aichler and others 2012). The consideration of AFL as precursor lesions might influence the controversial discussion whether PDAC arises from ductal, acinar or centroacinar cells (Guerra and others 2007, McDonald and others 2012). Figure 2 depicts a possible way of PDAC development from acinar and centroacinar cells.
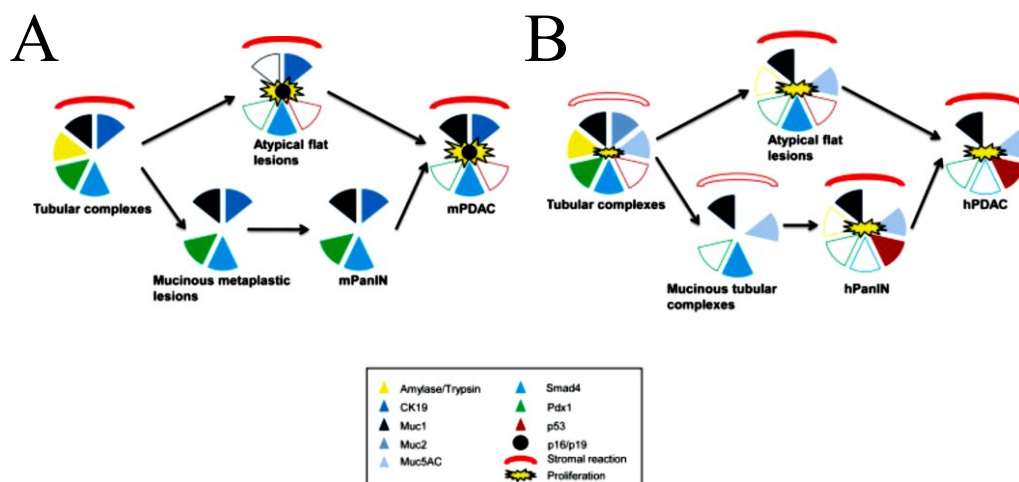
Figure 2: Possible carcinogenesis from AFL lesions, A: mouse, B: human. Atypical flat lesions (AFL) arise in a setting of acinar-ductal metaplasia (ADM) lesions with tubular complexes (TCs)

and mucinous tubular complexes (MTCs), proposing the flat carcinogenesis model, modified by author (Aichler and others 2012).

2.1.4.   Genetic alterations

PDAC develops as a result of successive accumulation of genetic alterations in pre-neoplastic lesions, including mutations in the key driver genes *KRAS*, *P16/CDKN2A*, *TP53* and *SMAD4/DPC4.5* (Hruban and others 2000). The mutation of the oncogene *KRAS* is an early event in the development of PDAC, which can be detected in 92 % of PanIN-1A lesions. More than 95 % of human PDAC contain an activating point mutation in the *KRAS* gene, mainly changing codon 12 from glycine to aspartate or valine in exon 2. Further, mutations in codon 13 and 61 are observed occasionally (Almoguera and others 1988, Biankin and others 2012, Kanda and others 2012). Inactivation of the tumor suppressor gene *CDKN2A* gene is another early event in PDAC. Around 30 % of PanIN-1A lesions harbor a *CDKN2A* mutation, and more than 95 % of PDAC have an inactivated *CDKN2A* gene due to homozygous deletion, inactivation mutation in one allele and loss of heterozygosity or promoter hypermethylation (Ottenhof and others 2011). The subsequent loss of functional p16 protein leads to an increased cell cycle progression (Schutte and others 1997). A late event in the tumorigenesis of PDAC is the inactivation of the *TP53* gene by missense mutation of one allele and subsequent loss of the second allele. It is mutated in about 75 % of PDAC and functional loss of the protein p53 leads to accumulation of further genetic abnormalities through anti-apoptotic effects in the presence of DNA-damage (Bardeesy and others 2006, Rozenblum and others 1997). Similar to *TP53*, inactivation of *SMAD4* is found only in high-grade PanIN, indicating another late event in the progression to PDAC. Fifty-five % of PDAC cases harbor a *SMAD4* inactivation (Hruban and others 2000, Tascilar and others 2001).

2.1.5.   Stromal component and tumor microenvironment

PDAC harbor a characteristic stromal reaction, called desmoplasia. This desmoplastic stroma is mainly found in PDAC, rarely in other pancreatic primary or secondary tumors of the pancreas and represents for up to 90 % of the tumor volume (Kloppel and others 2004). It is characterized by a deposition of extracellular matrix proteins and a cellular component consisting of stellate cells, activated fibroblasts and myofibroblasts, as well as inflammatory cells. The extracellular matrix proteins are synthesized mainly by pancreatic stellate cells

(PSC) and in a lower amount by cancer cells (Neesse and others 2011). The stroma acts as a mechanical barrier to the tumor, restricting the vascularity of the tumor and hereby limiting the effect of anti-cancer drugs. Hereby, it plays an important role in the process of tumor formation, progression, invasion and metastasis, protection from apoptosis and cancer stem cell maintenance (Hwang and others 2008, Korc 2007).

Another important key player of the tumor microenvironment is the immune system. Antigens associated to cancer are expressed by PDAC and competent $CD4^+$ and $CD8^+$ T cells with specific receptors against cancer antigens are expressed in the bone marrow of patients harboring PDAC (Schmitz-Winnenthal and others 2006). Pancreatic cancer cells are known to be able to evade the immune system and cancer associated inflammation evident in the tumor stroma might serve as a barrier to the surveillance of the immune system (Bayne and others 2012).

2.1.6.   Mouse models of pancreatic cancer

Animal models closely mimicking the human disease are helping to understand the pathogenesis of PDAC and to reveal the mechanism leading to invasive cancer. In 2003, Hingorani and others generated a mouse model with a Cre recombinase dependent, endogenous, conditional *Kras* mutant allele on pancreas specific PDX-1 or p48 promoters (see Figure 3). These mouse models develop low-grade and, to a less extent, high-grade PanIN, as well as ADM, closely resembling the human disease.
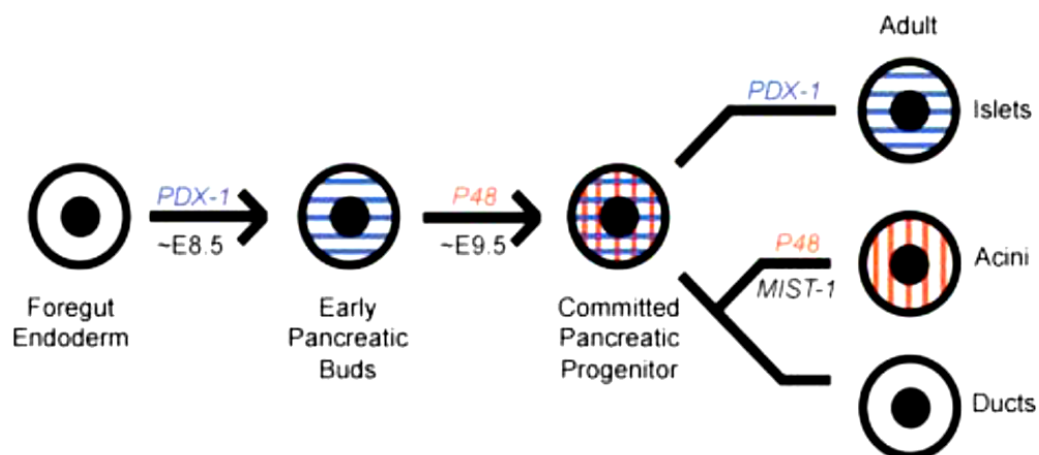

Figure 3: Pancreatic development. Transcription factors that program the early progenitor cells in the developing murine pancreas are indicated. PDX-1 expression starts with embryonic day 8.5 and p48 expression begins with embryonic day 9.5. These progenitor cells develop to all cell linages of

the pancreas, modified by author (Hingorani and others 2003).

As in human PDAC, a single *Kras* mutation leads not necessarily to invasive cancer (Hingorani and others 2003). Therefore, further genetic alterations have to be targeted e.g. *Cdkn2a*, *Tp53*, and *Smad4* on a mutant *Kras* background, leading to fully invasive PDAC with metastases (Aguirre and others 2003, Hingorani and others 2005, Kojima and others 2007). A further breakthrough was the development of a doxycycline dependent, conditionally inducible *Kras* allele in the mouse, showing that the *Kras* mutation is required for the maintenance of ADM, PanIN and PDAC and that the inactivation of *Kras* leads to regression of PDAC (Collins and others 2012a, Collins and others 2012b).

Models other than GEMs used to mimic human disease are heterotopic xenograft models, with subcutaneous implantation of human cancer cells in nude or severe combined immunodeficient (SCID) animals. Another possibility is the orthotopic xenograft model, with tissue grafted in the pancreas. The limiting factor of these two models is that the recipients are immunocompromised animals to avoid rejection of human tissues, so modulation of the tumor growth by the immune systems is lacking. Furthermore, these mice show only a minimal or no stromal reaction (Capella and others 1999, Ding and others 2010).

In summary, transgenic mouse models of precursor lesions and PDAC offer new possibilities to test the validity of early detection methods and of therapeutic strategies and to investigate cellular origins and molecular pathways involved in the development, progression and invasion of PDAC.

2.2.   Tenascin-C

Tenascin-C belongs to a family of large oligomeric extracellular matrix proteins, the tenascins (TN), displaying a distinct expression pattern during development, tissue maintenance and disease. TNC was detected by different working groups independently and former names include glioma mesenchymal ECM antigen (GMEM) (Bourdon and others 1983), hexabrachion (Erickson and Inglesias 1984), myotendinous antigen (Chiquet and Fambrough 1984), J1 glycoprotein (Kruse and others 1985) and cytotactin (Grumet and others 1985) until in 1986 Chiquet-Ehrismann and others introduced the name tenascin (Chiquet-Ehrismann and others 1986). TNC was the first tenascin described more in detail before other TNs even have been detected in humans including tenascin-R (TNR, restrictin, janusin), tenascin-X (TNX, gene X) and tenascin-W (TNW, tenascin-N), and additionally

tenascin-Y (TNY) in chicken (Jones and Jones 2000a). Tenascin was chosen as common name as it is a protein enrolled in the adhesion of cells (lat. "tenere", to hold) (Mackie 1997) and the C in TNC stands for "cytoactin" (Chiquet-Ehrismann and Tucker 2011).

The human TNC gene is localized on chromosome 9 in band q32-q34 (Rocchi and others 1991). TNC, as all TNs, consists of a common set of structural motifs, including heptad repeats, EGF-like repeats, fibronectin type III (FNIII) domains and a C-terminal globular domain. The disulfide linked oligomer consists of an 180- and an 300-kD subunit, linked together in a central core composing a hexabrachion (Figure 4) (Vaughan and others 1987).
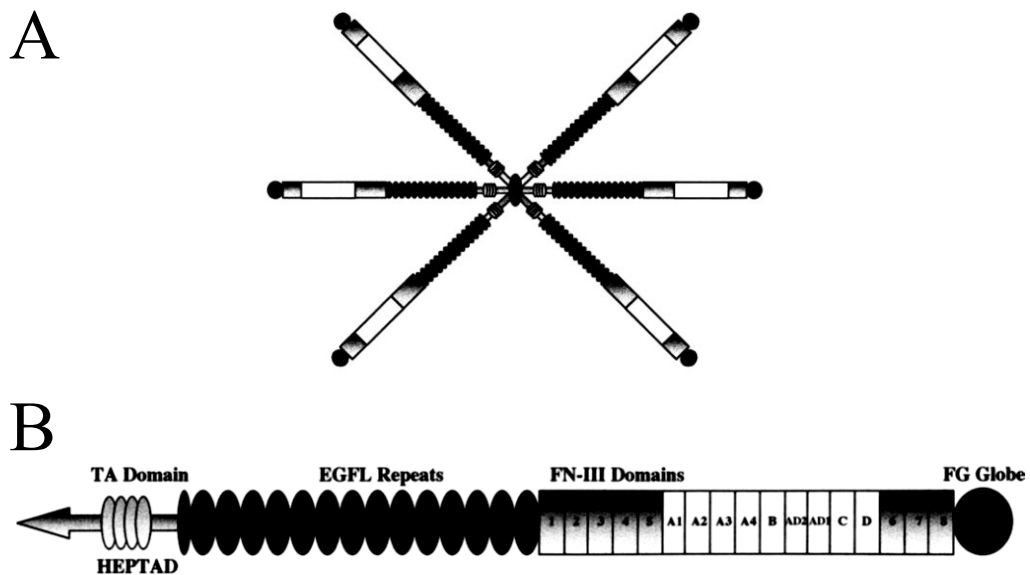
Figure 4: Structure of TNC: Schematic presentation of the hexameric TNC (A), and the TNC oligomer (B). The six oligomers are linked together at the tenascin assembly (TA) domain by coiled-coil interactions in the HEPTAD region. The left arrow represents terminal cysteine residues. Mammalian TNC contains 14 EGFL repeats and 8-17 FNIII domains (black: conserved, white: alternatively spliced variants). The fibrinogen globe represents the C-terminal end, modified by author (Jones and Jones 2000b).

Every arm contains an aminoterminal tenascin assembly (TA) domain in which the TNC polypeptides can be linked together by terminal cysteine residues and 3-4 α-helical heptad repeats (Conway and Parry 1991). The TA domain is followed by 14.5 epidermal growth factor-like (EGFL) repeats, each containing six cysteine residues, which participate in intrachain disulfide bonds. These EGFL repeats are important for the adhesion to fibroblasts and neurons (Fischer and others 1997). In

the carboxy-terminal direction, 8-17 fibronectin-III (FN-III) repeats are present, 8 conserved and up to 9 alternatively spliced FN-III repeats (Pas and others 2006). The domains are arranged in two sheets of seven anti-parallel β-strands (Baron and others 1992) and account for the flexibility of TNC (Carr and others 1997). The FN-III repeats are altered by alternative splicing of TNC mRNA and distinct expression pattern of these slice variants have been described in development and disease, modulating the biological function of TNC (Esposito and others 2006, Jones and Jones 2000a). Interestingly, TNC promotes adhesive and anti-adhesive actions, depending on the binding to different EMC proteins or cell surface receptors. Alternative splicing does influence this binding, as it has been shown for the cell surface receptor annexin II, which binds to the alternatively spliced FN-III region A-D of the large TNC splice variant (Chung and Erickson 1994).

The C-terminal end of TNC is represented by the fibrinogen (FG) globe, which contains polypeptide loops, formed by two disulfide bonds and has an Ca^{2+}-binding site (Jones and others 1989). This domain interacts with other proteins of the ECM and cell surface receptors, e.g. collagens, integrins and heparins (Milev and others 1997). These interactions promote TNC dependent activities, like migration, proliferation and regulation of cell adhesions (Orend 2005). Proteins like TNC, that contain binding sites for major structural proteins in the ECM and specific cell surface receptors are called "matricellular" proteins (Roberts 2011). Various effects of TNC on cell behavior are mediated through the existence of specific receptors. Different cell types are able to produce TNC, for instance stromal cells (Oskarsson and Massague 2012). In human brain, e.g. oligodendrocytes and astrocytes express different splice variants of TNC, oligodendrocytes the larger ones, meanwhile astrocytes the smaller ones (Garwood and others 2004).

2.2.1.   Tenascin-C in development and the adult organism

TNC is expressed in a restricted pattern during embryogenesis and early postnatal development. It was detected at sides of tissue remodeling, in the mesenchyme around the epithelium undergoing differentiation, for instance in the mammary gland, the tooth bud formation, the early tubulogenesis in the kidney and the urogenital sinus at the sites of formation of prostatic buds and vagina. Organs that express highest levels of TNC are thymus, lung and cerebellum (Saga and others 1991).

In the adult organism, TNC is tightly regulated and restricted to tissues which undergo either mechanical stress, such as tendons, ligaments and smooth muscles or exhibit a high cell turnover as lymphoid organs and hair buds in the skin (Chiquet-Ehrismann and others 2014). Examples for areas of restricted TNC expression in the adult organism are the basement membrane of the skin, mucosa of the colon, ductal salivary glands, vessel walls of various organs, visceral smooth muscle, the mammary gland after lactation and the uterus during estrus cycle and pregnancy (Juuti and others 2004, Saga and others 1992). Reappearance of TNC in adult tissue is triggered by injury and tissue regeneration as well as in healing wounds, arteriosclerosis and cancer (Chiquet-Ehrismann and Tucker 2011). As *in vivo*, TNC expression of most cultured cells is dependent on certain growth factors and hormones. For instance, TNC expression in cultured fibroblasts is only detectable after incubation with factors associated with inflammation and wound healing, like transforming growth factor-β, basic fibroblast growth factor and interleukin-1 (Chiquet-Ehrismann and others 1995).

2.2.2.   Tenascin-C and cancer

Strong expression of TNC in the adult organism is found in the tumor microenvironment (Orend 2005). In most epithelial tumors, tumor-associated fibroblasts are the source of TNC, not the epithelial tumor cells themselves. Interestingly, in non-epithelial derived tumors, such as melanoma or glioblastoma, the tumor cells are the source of TNC. In epithelial tumors, immunohistochemistry reveals a fibrous network of TNC immunoreactivity surrounding tumor cell nests. A correlation between elevated expression of TNC and local infiltration of adjacent normal tissue and increased metastasis in many types of cancer was observed (Chiquet-Ehrismann and Tucker 2011). Moreover, TNC expression is upregulated during angiogenesis in inflammatory and neoplastic diseases. TNC concentrations have been linked to tumor recurrence and prognosis, but the findings are contradictory, underscoring the several functions of this protein (Orend and Chiquet-Ehrismann 2006). In breast cancer and colorectal cancer TNC expression is connected with worse prognosis, whereas in cervical and gastric cancer patients have a better prognosis with a TNC immunoreactivity in immunohistochemistry of tumor samples (Juuti and others 2004). TNC expression in breast cancer was investigated intensively. Here, it induces an epithelial-mesenchymal transition (EMT)-like change in breast cancer cells by binding of αvβ1 and αvβ6 integrins

(Katoh and others 2013). Another interesting feature is the fact, that often the large splice variant of TNC is associated with tumors. Borsi and others found that the extracellular matrix pH influences the splicing of TNC mRNA in normal fibroblasts, meanwhile malignant cells exclusively produce the large TNC mRNA (Borsi and others 1996). Antibodies against these splice variants might therefore play a role in diagnosis and therapy (Chiquet-Ehrismann and Chiquet 2003).

2.2.3.   Distribution and function of tenascin-C in pancreatic cancer

Compared to normal tissue, the distribution of extracellular matrix proteins such as TNC differs in PDAC. TNC expression was found to be upregulated in PDAC, mostly in the stroma, surrounding tumor cells (Juuti and others 2004, Linder and others 2001). Juuti and others correlated immunohistochemical TNC detection with patient survival rate. They showed that TNC expression was associated with poorly differentiated tumor grades and patients age. No correlation between the expression of TNC and stage, tumor size, lymph node status, metastasis or tumor location could be detected. Interestingly, in male patients, TNC expression seemed to correlate with a higher survival (Juuti and others 2004). Gong and others detected a correlation between high levels of spliced TNC in sera of patients and gemcitabine resistance (Gong and others 2010). Esposito and others reported in 2006 that PSC are the main source of TNC, not the pancreatic cancer cells themselves. Here, they could show that the expression is induced by tumor necrosis factor alpha (TNFα) and transforming growth factor beta (TGF-β) (Esposito and others 2006).

Large TNC splice variants have been found in precursors of PDAC and PDAC as well as in chronic pancreatitis, but not in normal pancreas and the expression intensity increases from low-grade PanIN to invasive PDAC. In normal pancreatic tissue, the distribution of TNC is restricted to the muscular wall of blood vessels and the stroma surrounding interlobular ducts (Esposito and others 2006).

Functional analysis of TNC *in vitro* showed that TNC increases growth and adhesion of poorly differentiated pancreatic cancer cell lines. Moreover, using TNC as growing substrate the cell lines exhibited higher migration rate. Proliferation of pancreatic tumor cells was enhanced by TNC (Paron and others 2011). The role of TNC on apoptosis is not clear and results are sometimes controversial (Midwood and others 2011). However, these results indicate a possible tumor supportive role

of TNC in PDAC. Unfortunately, little is known about the role of TNC in the pancreas harboring only precursor lesions.

2.2.4. Mouse models of tenascin-C

In 1992, Saga and others succeeded in developing mutant mice lacking TNC. They replaced two-thirds of exon 2 and parts of intron 2 of the TNC gene with a lacZ gene, which induces lacZ expression instead of TNC. To their surprise, the mice developed normally and showed no obvious abnormalities (Saga and others 1992). Finally, in 1996, Forsberg and others independently generated a different mutant mouse model lacking the TNC gene and confirmed previous findings. TNC was deleted by switching the coding region of exon 2 to a neomycin gene (Forsberg and others 1996). However, TNC null mice showed some abnormalities as low body weight and low pregnancy rates. Fukamauchi and others first described abnormal behavior of TNC knockout mice. The mice exhibited a prolonged exploratory behavior in a new surrounding and had problems to habituate to the unknown circumstances (Fukamauchi and others 1996). Further, abnormalities in the central nervous system, development of lung and prostate as well as regenerative processes after injury and stress have been detected (Cifuentes-Diaz and others 2002, de Chevigny and others 2006, El-Karef and others 2007, Garcion and others 2004, Ishii and others 2008, Nakao and others 1998, Roth-Kleiner and others 2004). Moreover, it has been found that the TNC knockout mouse has a reduced inflammatory response (Chiquet-Ehrismann and Tucker 2011). Interestingly, knockout of other genes like Bcl-2, Smad8, Msx2 and MMP-19 seem to influence the expression of TNC and therefore the phenotype (Chiquet-Ehrismann and Tucker 2011), making it important to generate mouse models for special cancer types to elucidate the role of TNC in several cancer sites.

2.3. Aim of the project

Aim of this work was to compare an ablation of TNC in a mouse model of PDAC to a well-established mouse model of PDAC. Hereby, the focus was set to acquire new knowledge of TNC function, in particular in the early phases of PDAC development as this dismal disease has still a worse prognosis.

III.   MATERIAL AND METHODS

1.   Web-based learning platform for comparative histology

1.1.   Material

Material used during the course is listed in the annex.

1.2.   Methods

1.2.1.   Human tissue

Tissue samples were obtained from the archive of the Institute of Pathology, Technische Universität München, Germany. After surgical removal, tissue samples were fixed in 4 % buffered formalin and embedded in paraffin after 24 hrs in a paraffin embedding machine. For routinely diagnostic purposes, histochemical and, if necessary, immunohistochemical stainings were performed, as described in detail in 2.2.2-2.2.6. The use of human material for this project was approved by the local ethics committee of the Technische Universität München, Germany, and written informed consent was obtained from all patients.

1.2.2.   Murine tissue

Murine tissue slides of wild type mice were kindly provided by the mouse platform of the German Mouse Clinic (GMC), Helmholtz Zentrum München, Germany. The mice were housed and bred at the animal facilities of the GMC, in accordance with the German Animal Protection Law with permission from the responsible veterinary authority. Wild type mice were euthanized in a CO_2 chamber, tissues were harvested, fixed in 4 % buffered formalin and embedded in paraffin after 24 hrs. H&E staining of organ tissue sections were performed.

1.2.3.   Consortium

The project was financed by ERASMUS Lifelong Learning, 517860-LLP-1-1-FI-ERASMUS-FEXI. A network of universities teaching disease model pathology has been developed through the project. The consortium was composed by the Institute of Pathology, Technische Universität München, Munich, Germany, the Palmenia Centre for Continuing Education, University of Helsinki, Finland, Turku Center for Disease Modeling, University of Turku, Finland and the College of Medical, Veterinary and Life Sciences, University of Glasgow, Scotland. The members of

the consortium offered a broad knowledge and included specialists in pedagogy, medical and veterinary pathology and mouse models of human diseases.

1.2.4. Development of a curriculum

A curriculum for the web-based course content was developed. The structure for the overall curriculum was planned together by the members of the consortium using Moodle as an interactive web-based tool. Further discussions were hold by videoconferences and in face-to-face meetings. Quality criteria for a comprehensive learning, the e-learning content, the online tutoring and mentoring, the webinars, and the scanned slides utilized, have been applied in order to ensure that the curriculum was based on the latest research and pedagogical knowledge.

1.2.4.1. Normal murine tissue

Murine tissue slides from the mouse strains BALB/cByJ, C3HeB/FeJ, 129P2OlaHsd, C57BL6/N, FVBNJ and C57BL6/J were obtained from the mouse platform of the Helmholtz Zentrum München. At least one representative female and male example with strain-specific background lesions was selected. H&E sections included murine brain (cerebrum, cerebellum, brainstem), neck (esophagus, trachea, thyroid, parathyroid), thoracic and abdominal organs (lung, heart, thymus, liver, kidney, spleen), reproductive organs (ovaries with fallopian tube, uterus, vagina, bladder, testes, epididymis, prostate), glands and lymph nodes (adrenal glands, salivary glands, lymph nodes) and gastrointestinal tract with skin (stomach, small intestine, large intestine, pancreas, skin).

1.2.4.2. Basic lesions

To highlight basic pathological lesions, appropriate human tissue sections were screened from the archive of the Institute of Pathology, Technische Universität München, Germany and interesting cases were selected. Tissue sections of animal models fitting to the human tissue sections were used from the mouse tissue archive of Prof. Dr. Esposito. Representative H&E slides as well as histochemical and immunohistochemical stains were used if important to understand the case. In detail, the chosen examples comprised cell adaptation reactions (hypertrophy, hyperplasia, atrophy and metaplasia), cell injury and death (apoptosis, necrosis), inflammation (acute, chronic, granulomatous) and tissue repair. Table 1 contains a detailed description of the murine and human lesions included in the course.

	Cell reaction	*Human example*	*Murine example*
Cell adaptations	Hypertrophy	Cardiac hypertrophy	Leydig cell hypertrophy (AROM+ mouse model)
	Hyperplasia	Prostatic hyperplasia	Adrenal subcapsular cell hyperplasia (incidental finding in a female BalbcbyJ mouse)
	Atrophy	Testis atrophy	Testis atrophy (incidental finding in normal 129P2OlaHsd male mouse)
	Metaplasia	Gastric intestinal metaplasia	Pancreatic acinar-ductal metaplasia (cerulein induced acute pancreatitis, C57BL6N mouse strain)
		Squamous epithelial metaplasia cervix	
Cell injury and death	Apoptosis	Apoptotic bodies in viral hepatitis	Wilson disease (Atp7b$^{-/-}$ rat model) (Zischka and others 2011)
		Lichen ruber	Acute pancreatitis (cerulein induced acute pancreatitis, C57BL6N mouse strain)
	Necrosis	Acute liver failure	Toxic liver necrosis (C57BL6N mouse strain, unexpected toxicity after experimental drug administration)
		Colliquative necrosis in acute pancreatitis	Tumor necrosis liver (Wistar rat treated with Diethylnitrosamine to achieve hepatocellular carcinoma)
		Cardiac infarction	
Inflammation	Acute inflammation	Acute bronchopneumonia	Acute bronchopneumonia (incidental finding in a normal C57BL6N mouse)
		Acute pancreatitis	Acute pancreatitis (cerulein induced acute pancreatitis,

			C57BL6N mouse strain)
		Ascending cholangitis	Ascending cholangitis (mouse model for sclerosing cholangitis, C57BL6N mouse strain) (Fickert and others 2002)
	Chronic inflammation	Autoimmune pancreatitis	Chronic pancreatitis (mouse model of immune modulated form of chronic pancreatitis, courtesy of Bo Kong, Surgical department, TUM)
		Primary sclerosing cholangitis	Chronic cholangitis (mouse model for sclerosing cholangitis, C57BL6N mouse strain) (Fickert and others 2002)
	Granulomatous Inflammation	Granulomatous hepatitis	Granulomatous hepatitis (Helicobacter hepaticus infection in a female BalbcbyJ mouse)
		Foreign body reaction skin	
Tissue repair	Fibrosis	Liver cirrhosis	Liver cirrhosis (chemically induced liver cirrhosis, Wistar rat with oral administration of dibromoacetic acid)
		Keloid	

Table 1: Detailed content of the Webmicroscope module "Basic lesions"

1.2.5.   Digitalization

Digital images of appropriate histochemical and immunohistochemical sections for the use in the Webmicroscope were obtained with a five-slide scanner (ScanScope CS, Aperio) at 40X magnification (0.25 µm/pixel resolution). Images were saved in the fastest to process .svs file format with a .jpg compression to minimize the file size. Images were stored on small hard drives and sent to the partners in Finland to upload them in the Webmicroscope.

1.2.6. Annotation of slides in the Webmicroscope

Annotation of the slides was performed after uploading to the Webmicroscope server. Four different signs (circle, rectangle, polygon and arrow) and five colors (yellow, red, green, blue and black) were available in the Webmicroscope slide viewer. A new annotation was opened and the lesions were described by using the signs and colors. Normal murine histology of organs and relevant background lesions were highlighted in the common mouse strains BALB/cByJ, C3HeB/FeJ, 129P2OlaHsd, C57BL6/N, FVBNJ and C57BL6/J. In the basic lesions part, important features of the changes seen in the particular organs were highlighted and short introductions towards cases, mouse strains and background information of the underlying diseases were prepared. Additional features were annotated as well.

1.2.7. Pilot Course

A part of the developed curriculum was carried out in the Pilot Course, which was run from 15.04.2013 to 30.06.2013. Additionally, two final examinations in July and in August were hold. Students were recruited in January 2013. After the Pilot Course, feedback was collected from the students. Each module of the Pilot Course was evaluated separately in terms of quality of the instruction, the course material and the organization of the course modules. Additionally, the students evaluated their own learning progress and improvement and the relevance of the course for their work. Moodle was used as an e-learning environment for the course platform and internal communications of teachers and students. The content of the Pilot Course focused on comparative pathology in mice and humans. This included PowerPoint presentations linked to a virtual microscope (Webmicroscope, hosted by the University of Turku, Finland, prepared by the Technische Universität München), video clips (prepared by the University of Turku and Helsinki), recorded lectures (prepared by every partner, voice over spoken by Prof. VD Janet Patterson-Kane, University of Glasgow, Scotland) and interactive exercises (prepared by every partner in the corresponding module). Information about the Pilot Course was distributed *via* a public website designed for the project (http://pathpath.eu) by the University of Helsinki, Finland.

2. Example for phenotyping of a mouse strain: The TNC

model

2.1. Material

Material used during the course is listed in the annex and relevant material as follows.

2.1.1. Antibodies

Primary antibodies

Product	Application/Dilution	Company
Anti-claudin-18	IHC (1:1000)	Life Technologies GmbH, Darmstadt
Anti-cleaved caspase-3	IHC (1:1000)	New England Biolabs, Frankfurt
Anti-E-cadherin	IHC (1:100)	New England Biolabs, Frankfurt
Anti-HES1	IHC (1:50)	Biozol Diagnostica Vertrieb GmbH, Eching
Anti-Ki-67	IHC (1:200)	BD Transduction Laboratories, Heidelberg
Anti-notch2	IHC (1:10)	DSHB, Iowa (USA)
Anti-p16	IHC (1:200)	Santa Cruz Biotechnology, Inc., Heidelberg
Anti-tenascin-C	IHC (1:1000)	Abcam plc., Cambridge (UK)
Anti-TROMA III (CK19)	IHC (1:800)	DSHB, Iowa (USA)
Anti-β-catenin	IHC (1:500)	BD Transduction Laboratories, Heidelberg

Secondary antibodies

Product	Application/Dilution	Company
Biotin-labeled goat anti-mouse IgG	IHC (Ready to use)	KPL, Inc., Gaithersburg (USA)
Biotin-labeled goat anti-rabbit IgG	IHC (Ready to use)	KPL, Inc., Gaithersburg (USA)
Dako EnVision+ System-HRP, Labelled Polymer Anti-Mouse	IHC (Ready to use)	Dako Deutschland GmbH, Hamburg
Dako EnVision+ System-HRP, Labelled Polymer Anti-Rabbit	IHC (Ready to use)	Dako Deutschland GmbH, Hamburg
Biotinylated anti-rat IgG (H+L)	IHC (1:300)	Vector Laboratories Inc., Burlingame (USA)

2.1.2.   Primer pairs

Primer sequences used for genotyping of mutant mice:

Primer *Tenascin-C* genotyping

TN-G-1-2 (FW)	5'-GAA GTC ACT AGA AAC TAG TGG ACA ACT C-3'
TN-150R (~3'TN) (RE)	5'-AAG CTA GAA AGA TGC CTG GC-3'
TN-lacZ (RE)	5'-CTC CAT GCT TGG AAC AAC GAG CGC AGC-3'

Primer *Kras^{G12D}* genotyping

K004 (FW)	5'-GTC GAC AAG CTC ATG CGG GTG-3'
K005 (FW)	5'-AGC TAG CCA CCA TGG CTT GAG TAA GTC TGC A-3'
K006 (RE)	5'-CCT TTA CAA GCG CAC GCA GAC TGT AGA-3'

Primer *Cre/Ptf1α* genotyping

C001 (FW)	5'-ACC AGC CAG CTA TCA ACT CG-3'
C002 (RE)	5'-TTA CAT TGG TCC AGC CAC C-3'
C003 (FW)	5'-CTA GGC CAC AGA ATT GAA AGA TCT-3'
C004 (RE)	5'-GTA GGT GGA AAT TCT AGC ATC ATC C-3'

2.2.   Methods

2.2.1.   Animals

All mice were housed and bred at the animal facilities of the German Mouse Clinic, Helmholtz Zentrum Munich. All work with the mice was carried out in accordance with the German Animal Protection Law with permission from the responsible veterinary authority. *TNC$^{-/-}$* animals were breed with *LSL-Kras$^{G12D/+}$* and *Ptf1a$^{+/Cre(ex1)}$* mutant mice on a C57BL6N background to obtain triple mutant mice (*KC-TNChet* and *KC-TNCko*). *LSL-Kras$^{G12D/+}$* and *Ptf1a$^{+/Cre(ex1)}$* mice were breed to obtain double mutant mice (*KC*). Relevant mice and corresponding littermate controls were euthanized in a CO_2 chamber. Mutant pancreata were harvested after 15, 12, 9, 6, 3, 2 and 1 months.

2.2.2.   DNA extraction from mouse tails

At weaning, three weeks old mice were anesthetized with isoflurane for identification with ear punching and tail clipping for DNA analysis. 0.2 - 0.5 cm of the tail were cut and bleeding was stopped with silver nitrate. For evaluation of

mutant mice, each mouse tail was incubated with 250 µl tail lysis buffer (50 mM TRIS-HCL pH 8.0, 100 mM EDTA, 100 mM NaCl, 1 % SDS, 0.5 mg/ml proteinase K) at 55 °C overnight on a gently rocking platform (700rpm). 200 µl of aqua ad iniectabilia and 200 µl phenol-chloroform-isoamyl alcohol were added to the tissue lysate, mixed by repeated inversion and centrifuged for 15 min at 13.000 rpm at RT. The upper aqueous layer was transferred to a new tube and 200 µl chloroform isoamyl alcohol (24:1) was added. The lysate was mixed and centrifuged as described above. The upper aqueous layer was transferred to a new tube. DNA precipitation was performed with 800 µl of cold ethanol 100 %. The precipitated DNA was centrifuged for 15 min at 13.000 rpm at 4 °C and the supernatant discarded. The same step was repeated with 400 µl of ethanol 70 %. After removing the supernatant, DNA was dried at 40 °C and resuspended in 30 µl aqua ad iniectabilia. DNA concentration and quality was measured by reading absorbance at 230, 260 and 280 nm and diluted to 100 ng/µl for further PCR analysis.

2.2.3.   PCR for mouse genotyping

Genotyping Master Mix	1.16X
10X buffer (15 mM Mg^{2+})	1.74 mM
dATP	232.56 µM
dCTP	232.56 µM
dGTP	232.56 µM
dTTP	232.56 µM
Cresol Red sodium salt	46.51 µg/ml
Sucrose	6.98 %

For the *TNC* (wild-type presence) PCR a 25 µl reaction was set as follows:

Genotyping Mastermix	21.5 µl
Primer G1-2	1.0 µl
Primer 3'TN	1.0 µl
Taq polymerase	0.5 µl
DNA	1.0 µl

For the *LacZ* (TNCko presence) PCR a 25 µl reaction was set as follows:

Genotyping Mastermix	21.5 µl
Primer G1-2	1.0 µl
Primer lacZ	1.0 µl
Taq polymerase	0.5 µl
DNA	1.0 µl

The amplification parameters were set as following:

95 ° C	5 min initial denaturation

35 cycles with:

94 °C	1 min denaturation
60 °C	2 min annealing
72 °C	1 min elongation
72 °C	10 min final elongation

For the *wtKras* (*Kras* wild-type presence) PCR a 25 µl reaction was set as follows:

Genotyping Mastermix	21.5 µl
Primer K004 (FW)	1.0 µl
Primer K006 (RE)	1.0 µl
Taq polymerase	0.5 µl
DNA	1.0 µl

For the *mutKras* (*Kras*$^{G12D/Lox}$ presence) PCR a 25 µl reaction was set as follows:

Genotyping Mastermix	21.5 µl
Primer K005 (FW)	1.0 µl
Primer K006 (RE)	1.0 µl
Taq polymerase	0.5 µl
DNA	1.0 µl

The amplification parameters were set as following:

95 ° C	5 min initial denaturation

35 cycles with:

95 °C	1 min denaturation
60 °C	1 min annealing
72 °C	1:30 min elongation
72 °C	10 min final elongation

For the *Cre/Ptf1α* (Cre presence and internal PCR control) PCR a 27 µl reaction was set as follows:

Genotyping Mastermix	21.5 µl
Primer C001 (FW)	1.0 µl
Primer C002 (RE)	1.0 µl
Primer C003 (FW)	1.0 µl
Primer C004 (RE)	1.0 µl
Taq polymerase	0.5 µl
DNA	1.0 µl

The amplification parameters were set as following:

95 ° C   5 min initial denaturation

35 cycles with:

95 °C   1 min denaturation
60 °C   1 min annealing
72 °C   1:30 min elongation
72 °C   10 min final elongation

Each PCR set included a positive and a negative control. The amplification product was visualized by gel electrophoresis on 1 % agarose gel in TBE containing 0.5 µg/ml ethidium bromide. Gel images were taken with a gel documentation system.

2.2.4.   Murine tissue collection

Tissue samples were obtained from mice after euthanasia. After resection, the harvested pancreas was cut parallel to the longitudinal axis of the organ. One half was fixed in 4 % neutral buffered formalin and embedded in paraffin after 24 hrs with a paraffin embedding machine (Medite GmbH, Burgdorf) for subsequent histological and immunohistochemical analysis. The other half was submerged in RNAlater® and stored at -80 °C for future molecular analyses.

2.2.5.   Hematoxylin and eosin stain (H&E)

For H&E staining, 3 µm tissue sections were were cut on a microtome, mounted on microscope slides and dried overnight. After heating in the oven for 30 min at 65 °C, sections were dewaxed in xylene and rehydrated with ethanol and distilled water. Subsequently, the sections were stained for 5 min with hematoxylin for nuclear staining. The slides were washed with running tap water for 5 min to obtain differentiation. Eosinophilic structures were stained for 5 min with eosin. Finally, the slides were washed in running tap water and dehydrated in alcohol and xylene. To protect the tissue, coverslips were mounted with a drop of mounting medium.

2.2.6.   Masson-Goldner trichrome stain

Paraffin fixed tissues were dewaxed and rehydrated as described above. Then the sections were stained for 10 min with Weigert's iron hematoxylin for nuclear staining. Between each staining the sections were rinsed in distilled water and differentiated in 1 % acetic acid. The slides were stained with Ponceau S dye for

4 min, with phosphotungstic acid hydrate-Orange G for 4 min and with light green for 4 min. Dehydration and tissue protection was performed as described above. Muscle fibers were stained red, fibrin pink, collagens green, nuclei black and erythrocytes red.

2.2.7.   Alcian Blue-Periodic acid-Schiff reaction (PAS) stain

Paraffin fixed tissues were dewaxed and rehydrated as described above. Subsequently, the sections were dipped in 3 % acidic acid for 2 min and stained for 5 min with Alcian Blue stain. The slides were rinsed with tap water for 1-2 min and transferred to an automatic stainer. Here, the sections were immersed in sodium-periodate for 5 min and 15 sec in 70 % ethanol before staining them with PAS with for 6 min. Before and after staining with Mayer's hematoxylin, the slides were rinsed with running tap water. Dehydration and tissue protection was performed as described above. Acidic mucins were stained blue, neutral mucins magenta, mixed mucins blue to purple and nuclei blue.

2.2.8.   Movat's pentachrome stain (Verhoeff)

Paraffin fixed tissues were dewaxed and rehydrated as described above. Subsequently, the sections were pretreated in 3 % acetic acid for 30 sec and stained for 30 min with 1 % Alcian Blue stain. The slides were rinsed with tap water for 2 min and stained for 8 min with Verhoeff solution for nuclear staining. Following this, the slides were differentiated in 1% aqueous ferric chloride for 1 min and rinsed in tap water for 10 min. Subsequently, the slides were stained for 6 min in crocein scarlet-acid fuchsine for cytoplasmic staining, followed by differentiation in 1 % acetic acid. Then the slides were placed in 2 % phosphotonungstic acid, differentiated in 1 % acetic acid for 1 min and treated in 99 % ethanol for 3 and 15 min. Last step was a stain for 15 min in safron du gatinais for staining of fibers. Dehydration and tissue protection was performed as described above. Nuclei and elastic fibers are stained blue-black (in the murine pancreatic tissue nuclei are stained grey-red), collagen fibers and reticular fibers yellow, matrix and mucin blue, elastic fibers and muscle red.

2.2.9.   Immunohistochemistry

For immunohistochemistry, 2-3 μm tissue sections were mounted on Superfrost® Plus microscope slides and dried overnight at 37 °C. After heating in the oven for 30 min at 65 ° C, sections were dewaxed in xylene and rehydrated in a graded series

of ethanol (2x 100 %, 2x 96 %, 2x 70 %) and distilled water. Heat induced epitope retrieval (HIER) was performed in a pressure cooker with citrate buffer or in a water bath with EDTA buffer for each 20 min (see table 2), slides were then allowed to cool down in the buffer for 30 min. Staining was either performed manually or with the Dako Autostainer Universal Staining System (AS) in a humified chamber. Endogenous peroxidase activity was blocked in 3 % H_2O_2 for 10 min or with Universal Block for 20 min. Non-specific binding sites were blocked by either rabbit serum or goat serum diluted in TBS (manually) or washing buffer (AS) for 30 min according to the host species of the secondary antibody. Primary antibodies with adequate dilution in antibody diluent were applied over night at 4 °C (manually) or for 2 hr at room temperature (RT) (AS), dilution see table 2. Positive and negative controls were used to determine a successful result. Subsequently, the slides were washed three times in TBS/washing buffer and the matching biotinylated secondary antibody was added for 30 min at RT. Slides were washed again three times with TBS/washing buffer before streptavidin-horseradish peroxidase was added, when needed, for 30 min at RT. If a polymer detection system was used, the last two steps were replaced by adding Dako Envision for 30 min at RT. After another washing step colorimetric detection was performed using diaminobenzidine (DAB). The color reaction was observed under the microscope and stopped with distilled water. Counterstaining with hematoxylin for 10 min was performed followed by differentiation under running tap water. Dehydration and tissue protection was achieved as described above.

Antibody	Type	Dilution	HIER	Serum blocking	Secondary antibody
Anti-β-catenin	AS	1:100	citrate buffer	3 % goat serum	Envision anti-Mouse
Anti-claudin-18	AS	1:1000	citrate buffer	3 % goat serum	goat-anti-rabbit
Anti-cleaved caspase-3	man.	1:800	citrate buffer	3 % goat serum	goat-anti-rabbit
Anti-E-cadherin	AS	1:200	citrate buffer	3 % goat serum	goat-anti-rabbit
Anti-HES1	man.	1:50	citrate buffer	10 % rabbit serum	rat-anti-rabbit

Anti-Ki-67	AS	1:200	citrate buffer	3 % goat serum	goat-anti-rabbit
Anti-notch2	man.	1:50	citrate buffer	10 % rabbit serum	rat-anti-rabbit
Anti-p16	man.	1:200	citrate buffer	10 % goat serum	goat-anti-rabbit
Anti-TROMA III (CK19)	AS	1:800	EDTA buffer	3 % rabbit serum	rat-anti-rabbit

Table 2: Primary antibodies used for murine tissue sections

2.2.10. Markers for PDAC in humans and mice

p16

P16 can be seen as a connection between the control of cell cycle and cancer development (Serrano 1997). In physiological conditions, p16 controls the G1-S check-point of the cell cycle by inhibiting the kinase activity of the CDK4/6, thus preventing the phosphorylation of Rb. The expression of p16 is increased by different factors, including aging, exposure to DNA-damaging agents, and oncogenes and it is an important regulator of senescence (Rayess and others 2012). In PDAC and in its precursor lesions genetic and epigenetic events inactivate the p16 tumor suppressor, thereby overcoming the induction of cell senescence (Ottenhof and others 2011).

Ki67

Ki67 is a nuclear antigen. The protein is absent in quiescent cells in G0, but universally expressed in cells that proliferate. Therefore, Ki67 serves as a proliferation marker (Pathmanathan and Balleine 2013). The evaluation of proliferation in mice has to be performed carefully, taking into account that the rate of cell division in pancreatic mice parenchyma reaches its maximum between 15 and 30 days after birth. In this period of rapid growth, centroacinar, ductal and acinar cells exhibit similar mitotic indices (Dore and others 1981).

Cleaved caspase-3

Cleaved caspase-3 can be used as a marker of apoptosis. Sequential activation of caspases is a central step in both pathways of the apoptotic process. Caspase-3 is an apoptosis related cystein-aspartic acid protease and an effector caspase. After

cleavage through initiator caspases, caspase-3 activates downstream targets. Antibodies against cleaved caspase-3 detect cells that undergo apoptosis (Kuribayashi and others 2006).

<u>CK19</u>

Cytokeratin 19 belongs to the keratin family, and is an important marker for immunohistochemical evaluation of tumors. Under normal conditions, CK19 is expressed in normal ductal epithelium. PanIN lesions, MTCs and PDAC express CK19 (Jain and others 2010). PanIN lesions are defined as ductular lesion with a size less than 1 mm, arising of pancreatic ducts in a setting of unaffected acinar parenchyma (Hruban and others 2006).

<u>Claudin-18 and other adhesion molecules</u>

Claudin-18 (CLN-18), a tight-junction protein, is under physiological conditions only expressed in human body in the gastric epithelial cells and lung. The splice version 2, CLN-18.2 was described as a novel, specific marker for precursor lesions of PanIN and PDAC. Normal human acinar parenchyma, ductal cells and islet cells show no membranous immunoreactivity for CLN-18 (Tanaka and others 2011, Woll and others 2014). The Wnt signaling pathway components E-Cadherin and β-catenin are important for epithelial-to-mesenchymal transition (EMT). EMT acts as an important factor in fibrosis of tissue and in development of cancer (Tian and others 2011).

<u>Notch signaling</u>

In cancerous tissue, the embryonic signaling pathway Notch is reactivated and leads to progression of the tumor growth and promotes insensitivity towards chemotherapy. Wörmann and Algül showed that in PDAC Notch ligands and receptors are upregulated when compared to normal pancreatic tissue. The Notch components seem to promote development of PanINs and PDAC (Wörmann and Algül, 2013). Although the *Notch* signaling pathway is apparently necessary in the early development of the pancreas, it is suppressed in the adult organ (Jensen and others 2000). The transcription factor *Hes1* is a downstream target gene of the *Notch* pathway. It is nuclear expressed by an activation of *Notch* pathway. Hingorani and others described the PanIN lesions of their mutant mice to be strongly positive for nuclear und weakly positive for cytoplasmic *Hes1* expression, but not in the normal

pancreas except in centroacinar cells (Hingorani and others 2003, Miyamoto and others 2003).

2.2.11.   Analysis of histo- and immunohistochemical stainings and reactions

Stainings and immunoreactions were analyzed either semi-quantitatively or quantitatively, as described below.

<u>Masson-Goldner-Trichrome</u>

Analysis of Masson stain was performed in collaboration with Raisa Serpi, PhD, Biocenter Oulu, Finland. In detail, slides were scanned at 20X magnification, computer aided analysis was performed by discrimination of stained pixels and percentage of architectural distorted areas (stained green) to whole tissue area (stained red and green) was calculated.

<u>Alcian Blue-PAS</u>

Analysis of Alcian Blue-PAS stain was done in collaboration with Jussi Kupari, MSc, Institute of Biomedicine, University of Helsinki, Finland. In detail, digital images were captured from five random areas filled with ductular lesions at 10X magnification from three different slides per animal to achieve a total number of 15 images/animal. ImageJ with the "color deconvolution"-plugin (http://www.mecourse.com/landinig/software/cdeconv/cdeconv.html) was used to analyze the slides, as this plugin can discriminate between different histochemical stains. Vectors for Alcian Blue (AB) and hematoxylin (H) and PAS and H were used to analyze the AB and PAS staining on the sections (Ruifrok and Johnston 2001). The images were transformed to grayscale (8-bit) and opened with the "color deconvolution"-plugin. The analysis was first performed on AB and H and then repeated for PAS and H. The information received for hematoxylin was not used. The threshold was set on the level where minimum nonspecific signal was seen. The area covered by AB and PAS was then measured and the full tissue area of the image was calculated. The ratio of mucin covered (PAS, AB) area/total tissue area was calculated for all images.

<u>Movat pentachrome stain</u>

Movat pentachrome stain was analyzed in collaboration with Dr. rer. nat. Annette Feuchtinger, Helmholtz Zentrum München, Germany. Slides were scanned at 20X magnification and Definiens software (Tissue Studio, Definiens) was used to

discriminate colors of different stained areas. Normal ductular structures and vessels were excluded from the analysis. Architectural distorted areas with fibrosis were calculated and set in percentage to the completely analyzed area. Figure 5 shows an example of the color deconvolution.
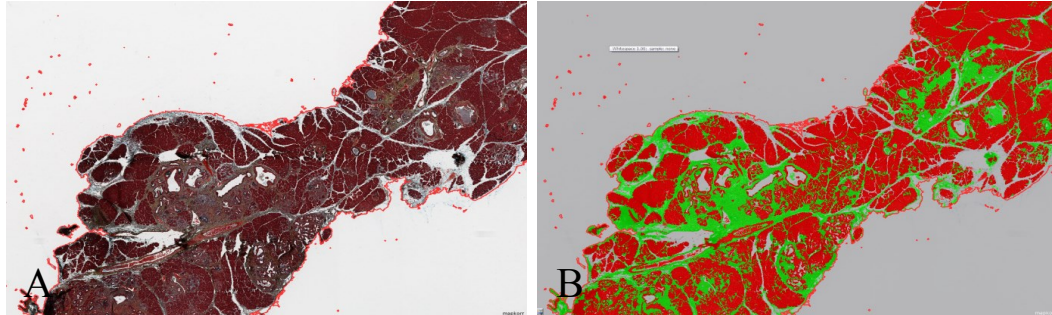

Figure 5: Mutant pancreata of a KC animal, stained with Movat stain, 10x, B: Color deconvolution to calculate fibrotic areas, 2x

Anti-TROMA III (CK19), Anti-claudin-18, anti-E-cadherin, anti-β-catenin

These proteins showed a membranous staining pattern and had therefore been selected for computer based analysis. Slides were scanned at a 20X magnification with the Aperio CS System and evaluated with Aperio's Area Quantification Color Deconvolution Software (Spectrum, Aperio). Percentage of stained area to whole area was measured. Anti-TROMA III (CK19) analysis was performed in collaboration with Raisa Serpi.

Anti-Ki-67, anti-cleaved caspase-3, anti-p16, anti-notch2, anti-HES1

The expression of these markers was evaluated focusing on regions of interest. In detail, five random areas of architectural distortion or precursor lesions were selected and at least 100 cells were counted. The percentage of positive cells was then assessed.

2.2.12.   Data evaluation and statistical analysis

Results are expressed as arithmetic mean ± standard error of the mean. Statistical analysis was performed in cooperation with Dr. Alexander Hapfelmeier, Institut für Medizinische Statistik und Epidemiologie, TUM, using the software IBM SPSS Statistics 21 for Windows and Microsoft Excel software. Normality was tested and two-way analysis of variance student's t-test was used to determine the significance and p-values < 0.05 were considered significant. Graphs were generated using Microsoft Excel software.

IV. RESULTS

Aim of this project was to develop a web-based online course for disease model pathology, which is reported in section 1. With the knowledge gained during development and hosting of the course, a subsequent characterization of a tumor model for pancreatic cancer was performed. The results of this characterization are presented in section two.

1. Web-based learning platform for comparative histology: The PATHPATH project

1.1. Pilot course

1.1.1. Recruitment of students

In February 2013, 36 postgraduate students with at least masters' degree in the medical or natural science field were enrolled from the partner universities. Eight students came from Germany, 11 from Finland, 16 from UK and 1 from Denmark. Their countries of origin were Denmark, Finland, Germany, Greece, Poland, Sweden, England, Scotland, Brazil, China, India, Iran and Pakistan. Twenty-four students had a natural science background (M.Sc., biochemistry or biology) and eight students had a medial background (MD). 32 students started the course. As the students' backgrounds varied from medical to biochemical, they had high differences in background knowledge. Medical students were more comfortable in histology, but less in biomedical aspects as creation of genetically engineered mice and *vice versa* for biochemical students. Students had to fill in a questionnaire and wrote a short letter of motivation about their reasons for participating in the course. The motivation of most students' was to deepen their knowledge about murine histology and background lesions of different mouse strains, as they were working on mouse projects.

1.1.2. Content of the course

The course content offered a composition of basic knowledge in mouse and human biology, biochemistry and histology, important for everyone working with mouse models of human diseases and in particular disease model pathologists. The content of the modules is displayed below. An examination at the end of each module tested

the learned knowledge of the students.

1.1.2.1. Modules

The pilot course was divided into the following specific modules:

Module 1: Basics in experimental animals and how to create genetically engineered mice

Module 2: Basic histology of different mouse strains: Webmicroscopy-self studying

Module 3: Basic histology of different mouse strains: exercises

Module 4: Mouse necropsy and sample collection

Module 5: Processing and staining of histological samples

Module 6: Description of the gross pathology

Module 7: Basic pathological lesions

Module 8: Histological description of neoplasms

Final examination

The collected material presented in the Moodle platform, included Webmicroscope slides, recorded lectures with voice-over technology including video clips, recorded interactive live lectures, discussion forums, learning exercises and material of the final examination. Figure 6 shows the timeline of the pilot course, outlining the time frames given to the students to complete each module and to finish the examination. Module 1 was prepared by the group of the University of Turku and covers principals of the creation of GEM. The group of the Technische Universität München (TUM) developed module 2 and 3. In particular, they cover the basic histology and histopathology of the commonly used mouse strains C57BL/6N and C57BL/6J (module 2) and BALB/cByJ, C3HeB/FeJ, 129P2/OlaHsd and FVB/NJ (module 3). These modules are described in detail under 1.1.2.2. Module 4 was covered by the group of the University of Glasgow and includes general guidelines for necropsy, sample collection and preparation of mice. Module 5 was developed by the groups of the Universities of Turku and Helsinki and covers the basic handling of histological samples. This includes tissue processing, embedding and histochemical and immunohistochemal stainings. The group of the University of Glasgow took care of module 6, which deals with gross pathology. Module 7 was prepared by TUM and deals with basic lesions in human and murine histopathology, described in detail under point 1.1.2.3. The group of the University of Glasgow

developed module 8; it covers principles in murine neoplasia. A final examination completed the course, which was held in July and August. Figure 6 gives a detail overview of the time table of the pilot course.
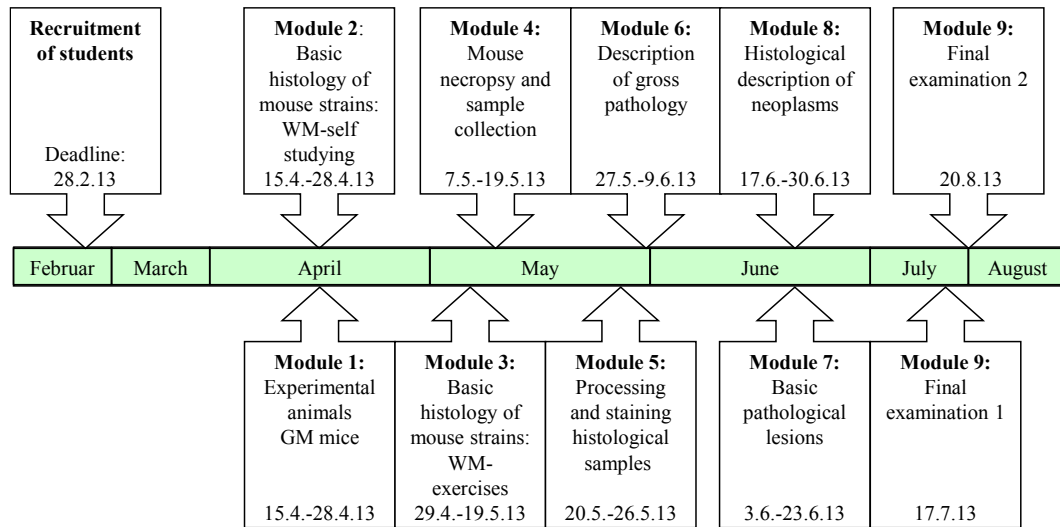

Figure 6: Time bar with recruitment of the students and a timetable of the pilot course. WM (Webmicroscope).

1.1.2.2. Module 2 and 3

In module 2, histological descriptions and slides of the commonly used C57BL/6N and C57BL/6J mouse strains were available for self-studying. In module 3, the mouse strains BALB/cByJ, C3HeB/FeJ, 129P2/OlaHsd and FVB/NJ were introduced. The contents of module 2 and 3 could be used to complete the examination. Students accessed the link to the Webmicroscope *via* Moodle.

1.1.2.2.1. Content module 2

Here, students were able to examine extensively annotated histological slides stained with H&E from a male and female mouse. Each strain contains slides listed below. Aim of this module was to get all students familiar with the basic histology of a murine model and learn basic histologic expressions. Furthermore, physiologic correlations were explained and presented in the particular context.

Brain

Brain slides contain a section of the cerebrum, approximately at the high of diencephalon to mesencephalon and a section of the cerebellum or brain stem.

Reproductive organs

Slides of female reproductive organs include the ovaries, fallopian tube, uterus, cervix, vagina with fornices, ureter and urinary bladder. Slides of male mice include testis, epididymis, vas deferens, prostate, seminal vesicle, urethra and urinary bladder.

Neck

The sections of the neck contain trachea, esophagus, thyroid gland and parathyroid.

Thoracic and abdominal organs

This slide shows heart, lung, thymus, liver, spleen and kidney.

Glands and lymph nodes

This slide contains sections of the salivary glands, the adrenal glands and a lymph node.

Gastrointestinal tract and skin

This section contains the forestomach with limiting ridge and the glandular stomach, sections of small and large intestine, pancreas and skin.

In general, relevant structures of these sections were annotated, as well as artifacts and pathological abnormalities. Figure 7 indicates an example of an annotation of normal histology.
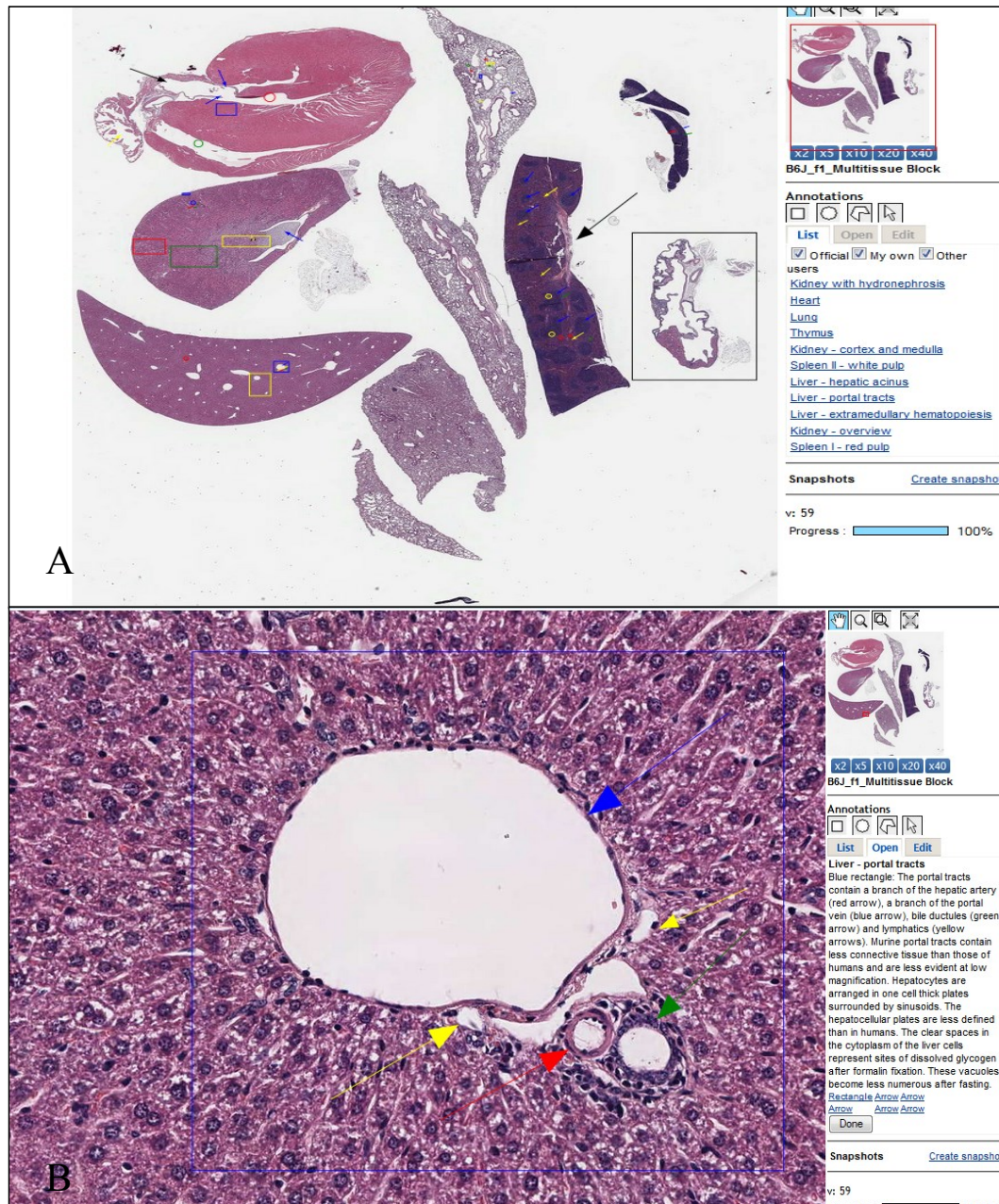
Figure 7: Tissue slide with annotations A: Complete slide with annotations on the right side, B: Annotation of normal liver tissue.

1.1.2.2.2. Content module 3

In this module, in addition to the mouse strains of module 2, BALB/cByJ, C3HeB/FeJ, 129P2/OlaHsd and FVB/NJ mouse strains are presented. The focus of this module was to point out differences in background lesions between the different mouse strains as well as differences between female and male mice and the similarities and differences to human histology. Furthermore, physiologic correlations were presented and discussed. Whenever possible, age-related lesions were included. Figure 8 show annotated examples of different background lesions

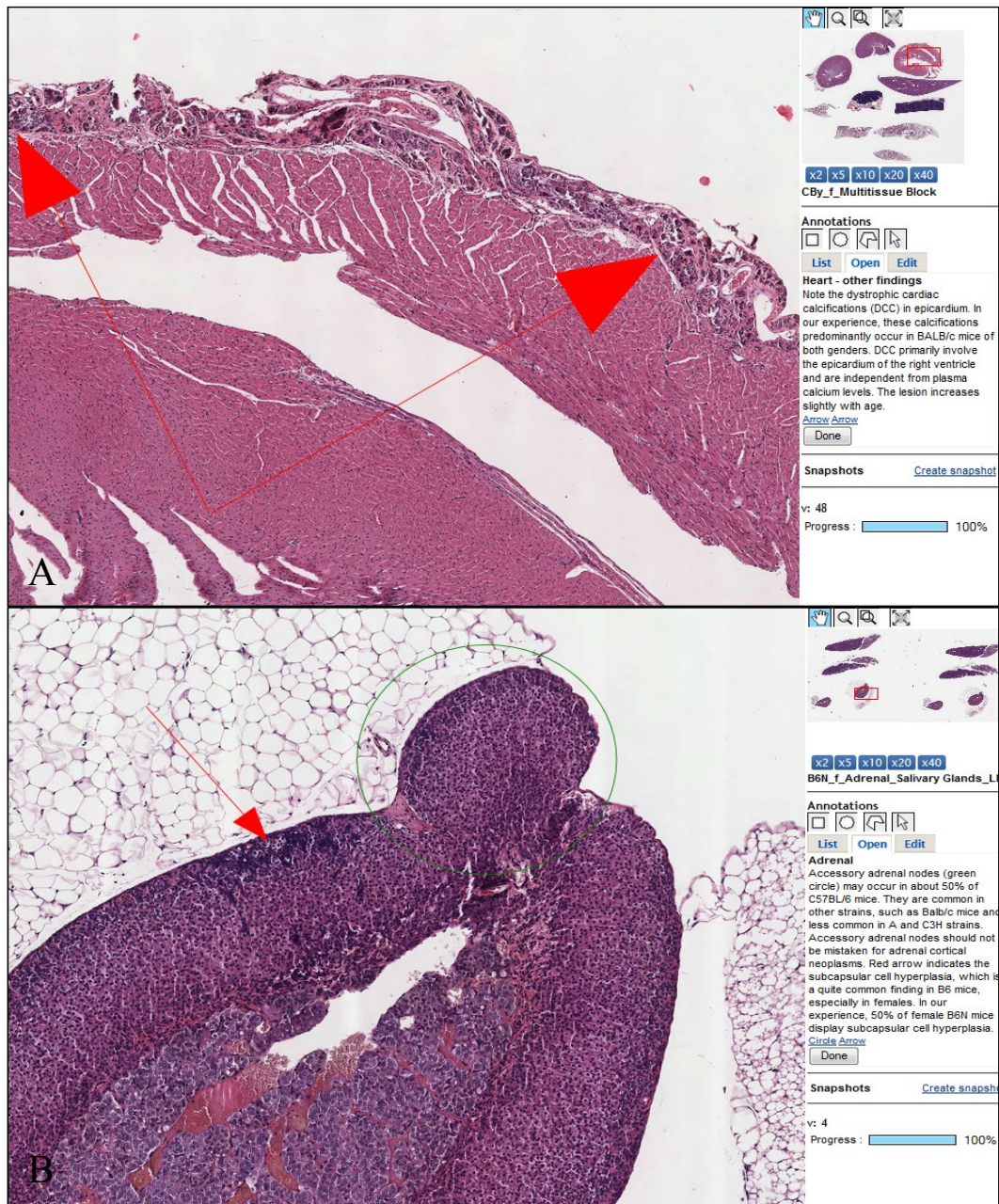in the mouse strains; Table 3 gives an overview of background lesions.

Figure 8: A: Annotation of dystrophic cardiac calcification in a female BALB/cByJ mouse, B: Annotation of accessory cortical node and subcapsular cell hyperplasia in a female C57BL/N mouse.

Strain	Lymphoid organs	Heart	Adrenal glands	Corpus callosum	Liver	Pancreas
C57BL/6J	-	-	Female: no fat cells at all, instead area of increased vascularization between cortex and medulla subcapsular cell hyperplasia	-	Small non-specific infiltrates	-
C3HeB/FeJ	Better developed lymphoid organs - Peyer's patches intestine - BALT - B-cell marginal zone spleen - extramedullary hematopoesis in spleen (erys, megakaryocytes)	-	Female: rare fat cells between cortex and medulla increased vascularization area less conspicious subcapsular cell hyperplasia male: subcapsular cell hyperplasia	-	Rarely infiltrates increased number of necrotic foci	Lipomatosis
Balb/cAnPt	-	Male: calcifications in epicardium	Female: fat cell zone between cortex and medulla increased vascularization area not existing	-	Rarely infiltrates	-
S129/J	-	-	Female: rare fat cells between cortex and medulla increased vascularization area less conspicious no subcapsular cell hyperplasia	Without corpus callosum	Rarely infiltrates	-
BALB/cByJ	Female: BALT, peyer's patches	Epicardial calcifications	Subcapsular cell hyperplasia	Without corpus callosum	Male: liver steatosis	-
C57BL6/Ntac	-	-	Female: subcapsular cell hyperplasia	-	-	-
129P2/OlaHsd	-	-	No subcapsular cell hyperplasia	-	-	-
FVB/N	-	-	-	-	Female: multifocal hepatocellular necrosis	Lipomatosis

Table 3: Background lesions and gender differences in strains presented in modules 2 and 3 (Serpi and others 2013).

1.1.2.2.3. Examination module 2 and 3

For evaluation of the student's learning progress, short tests had been prepared. They included 19 questions, which had to be answered by annotating a picture taken by the students themselves (part I, questions 1-19) and four open questions (part II, questions 20-23). In part I, students had to recapitulate their learned knowledge about normal histological structures of organs, physiological context, background lesions in mice and gender differences in mouse strains. The didactic goal was to make them familiar with histological and pathohistological structures. Part II challenged the students to utilize their new knowledge use-oriented. For instance, they had to discuss why they should use a certain background strain for a clearly defined project and avoid other strains. Figure 9 shows an example of each type of

question. Students were allowed to use the course material to answer the questions. Detailed solution to the questions were provided afterwards. Additionally, students received a personal feedback about their positive results and explanation of their mistakes.
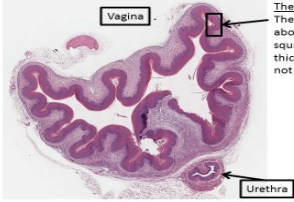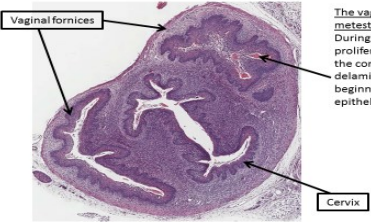

Figure 9: Examples for questions to module 2 and 3. The examination tests the knowledge of the students in terms of murine basic histology and histopathology, differences between mouse strains and differences to human histology. Answers were provided after the deadline.

1.1.2.3. Module 7

Module 7 covers basic pathological lesions in humans and mice. Before assessing the Webmicroscope slides, students had to listen to a module related lecture consisting of PowerPoint-presentations with voice-over. To facilitate this module, the content was split in two parts, as indicated below, ending with an examination.

1.1.2.3.1. Content module 7

The content of module 7 covered the following topics: Cell adaptations, cell injury and death, as well as inflammation and tissue repair. The module started with a

lecture about cell adaptations and cell injury with corresponding virtual human and murine tissue sections. The questions for the examination were released two days later. The second lecture about inflammation and tissue repair was opened one week later and virtual slides were provided. The second part of the questions was available two days after opening of the lecture.

Figure 10 depicts an example of comparative lesions in mouse and human.
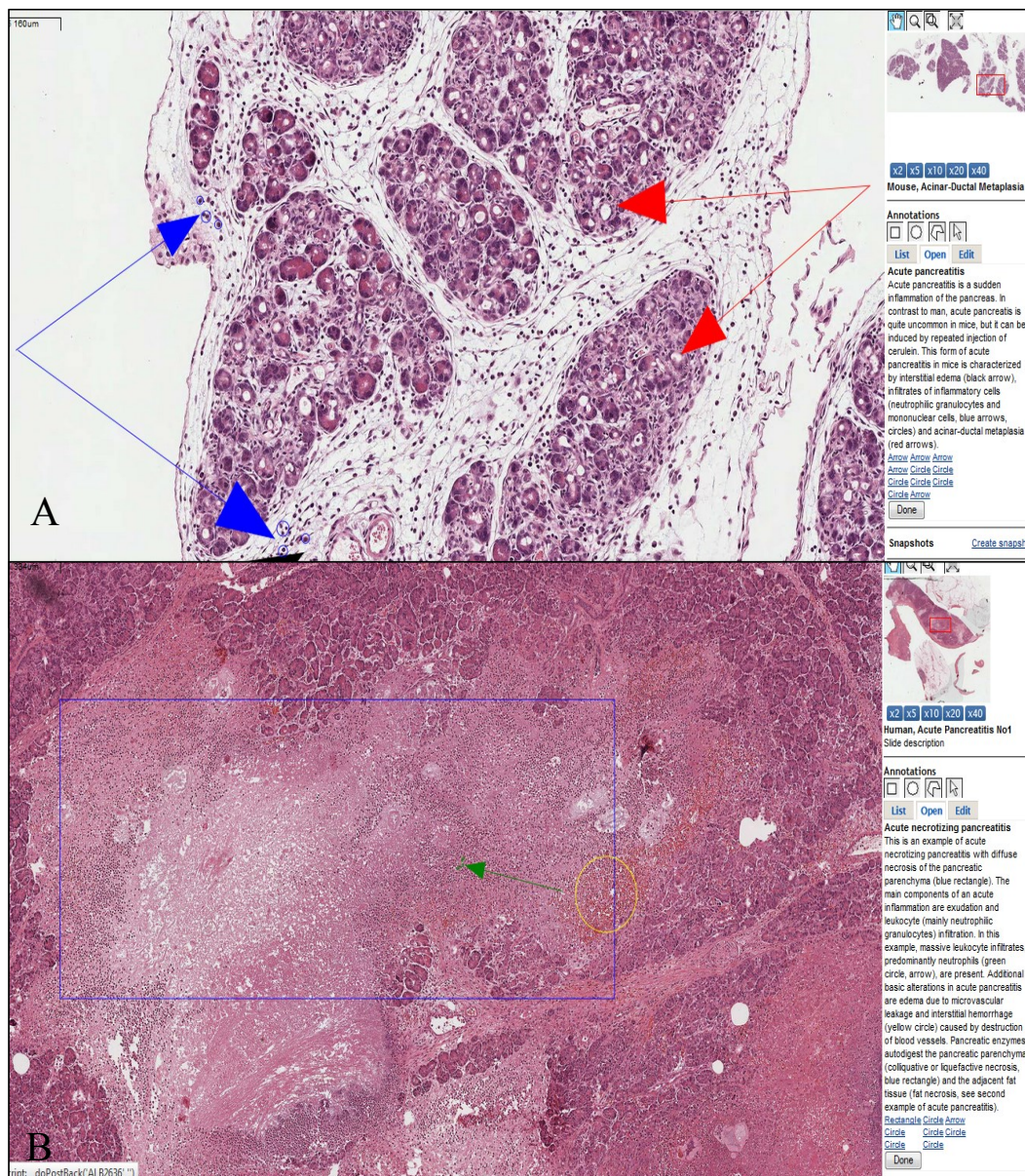
Figure 10: Example of murine (A) and human (B) acute pancreatitis. The murine pancreatitis can be classified as interstitial, meanwhile the human pancreatitis is a necrotizing pancreatitis.

1.1.2.3.2. Examination module 7

For every subtopic of the module, three question were prepared. The first questions covered theoretical knowledge about general pathology, e.g. a definition of

metaplasia. The second and third question were covering human and murine pathohistology. As in the previous pathohistology modules, students had to annotate slides and compared the lesions seen in human and murine tissue.

1.1.3.   Final examination

The final test was held twice 3 and 4 months after the beginning of the pilot course. Questions about histology topics were similar to questions prepared in modules 2, 3 and 7. The test included eight interactive questions, one question per module. A maximum of 24 points was reachable and most students performed very well. Out of 21 participating students, 20 passed the exam, one student needed a second try. Figure 11 shows an example of the final examination.

The final examination of the pilot course "Basics in mouse modelling and pathology"

The 20th of August, 2013

1. **Describe shortly**
    a. Chimeric mouse (2p)
    b. Pseudopregnant female (2p)
    c. Homologous recombination (2p)

2. **Gastrointestinal tract**
    Take a picture of the stomach. Mark the forestomach, the glandular stomach and the limiting ridge.

3. **Salivary glands**
    Name the salivary glands. Which salivary glands show a sexual dimorphism in mice? Shortly describe the differences in this gland between females and males.

4. **Open the Power-point presentation entitled "Question 4" in this Moodle section.**
    a. Describe the macroscopic abnormality in the mouse shown in the second slide. Use the descriptors we have covered in Module 6, i.e. location, size, shape, color, consistency (take a guess if the appearance indicates it), number/extent and distribution. Please note: we have also provided a photograph of a normal mouse in the first slide, which does not need to be described. It is only for your reference.
    b. Briefly describe the samples you would take to help you obtain a diagnosis in this case.

5. **Abnormality in brain structure**
    129P2/OlaHsd mice frequently show an abnormality in their brain structure. Take a picture of the brain of the 129P2/OlaHsd mouse and name this abnormality.

6. **Metaplasia**
    Briefly describe the term metaplasia and give examples for metaplasia in man and mice.

7. **Chronic inflammation**
    Briefly define the term chronic inflammation. What are the main inflammatory cells in chronic inflammation?

8. **Open the link to a Webmicroscope slide entitled "Question 8".**
    Write a microscopic description of the neoplasms in the organ section outlined by a blue rectangle. Use the description method provided in our Module 8 lesson. Make sure you look at all of the masses in this organ section before completing your description".

Figure 11: Final examination of the Pilot Course.

1.1.4. Collection of students' feedback

The Pilot Course was advertised and started with 32 students of whom 21 finished the course successfully. After completion of the course, students were asked to fill in a feedback-sheet, which 18 students completed. Feedback was collected as points, ranging from 0 to 5.0 points, with 5.0 points being the highest score. This grading schema was used, as it was already successfully implemented at the University of Helsinki, Finland (http://www.helsinki.fi/law/studies/general/credits_grading.html) [date: 01.10.2014].

Generally, the students rated the course in average with 4.2 points, and with 4.5 points as the course being useful for their work. In addition, there was a significant improvement of students' knowledge in murine pathology (32 %); students rated themselves before the course in average with 2.3 points and after the course with 3.9 points. Figure 12 shows a part of the students' feedback questionnaire.

Course results

Please indicate your level of agreement with the statements listed below (Strongly disagree=1, Strongly agree=5)

	Strongly disagree	Disagree	Neutral	Agree	Strongly agree	Average
a) The course lived up to my expectation			2	11	5	4,2
b) The activities in this course gave me sufficient practise		1	5	8	4	3,8
c) The course was useful for my work			1	7	10	4,5

How would you rate your level of understanding before and after taking this course?

	0 - 20	21 - 40	41 - 60	61 - 80	81 - 100	Average
Before	3	9	3	3		2,3
After			2	15	1	3,9

How would you rate the training overall?

	Very poor	Poor	Average	Good	Excellent	Average
			2	11	5	4,2

Figure 12: Students evaluation on the course in general

Concerning module 2 and 3, the average of points was > 4.0 points, except for the time given to finish module 3 (3.7 points). Importantly, the students gave high points for quality of the content (4.5 and 4.3 points) and usefulness of exercises (4.3 and 4.6 points), see Figure 13.

Module 2: Basic histology of different mouse strains: WebMicroscopy -self studying

Please indicate your level of agreement with the statements listed below (Strongly disagree=1, Strongly agree=5)

	Strongly disagree	Disagree	Neutral	Agree	Strongly agree	Average
a) The objectives of the module were clearly defined			2	9	7	4,3
b) The learning activities were appropriate		1		10	7	4,3
c) The learning activities were interactive			4	7	7	4,2
d) The quality of instructions was good		1	2	11	4	4,0
e) The course material distributed was high-quality		1	1	4	12	4,5
f) The module-based exercises were useful		1	3	3	11	4,3
g) The time allocated for the training was sufficient			2	12	4	4,1

Module 3: Basic histology of different mouse strains: WebMicroscopy -exercises

Please indicate your level of agreement with the statements listed below (Strongly disagree=1, Strongly agree=5)

	Strongly disagree	Disagree	Neutral	Agree	Strongly agree	Average
a) The objectives of the module were clearly defined			0	12	6	4,3
b) The learning activities were appropriate			1	10	7	4,3
c) The learning activities were interactive			3	8	7	4,2
d) The quality of instructions was good			2	11	5	4,2
e) The course material distributed was high-quality		1	0	10	7	4,3
f) The module-based exercises were useful				8	10	4,6
g) The time allocated for the training was sufficient		2	5	8	3	3,7

Figure 13: Students' evaluation of module 2 and 3

As in modules 2 and 3, students' rating of module 7 was > 4.0 points, with the exception of the allocated time (3.6 points). Here, as well the quality of the content (4.2 points) and the usefulness (4.4 points) was rated high, indicated in Figure 14.

Module 7: Basic pathological lesions

Please indicate your level of agreement with the statements listed below (Strongly disagree=1, Strongly agree=5)

	Strongly disagree	Disagree	Neutral	Agree	Strongly agree	Average
a) The objectives of the module were clearly defined		1	1	10	6	4,2
b) The learning activities were appropriate				12	6	4,3
c) The learning activities were interactive			6	5	7	4,1
d) The quality of instructions was good		1	1	10	6	4,2
e) The course material distributed was high-quality			3	9	6	4,2
f) The module-based exercises were useful			1	9	8	4,4
g) The time allocated for the training was sufficient		3	4	9	2	3,6

Figure 14: Students' evaluation of module 7

Asked for their interest in participating in a comparative, human-mouse organ-specific course out of 18 students 17 answered with positively (94 %).

An open text form was also provided in the feedback catalogue, asking the students for the most relevant issue concerning the course, many students answered that the

histology part was most useful for them. Examples for students' comments were:

"Basic histology as well as pathological lesions and their description were most relevant to me. The other modules also added some new information to my preexisting knowledge."

"I learned a lot about microscopical structure of different organs, and that there are differences between mouse strains. Also, the description of the neoplasms I found very useful."

"For me it was most important to learn about mouse histology and the analysis of histological samples to help me with my future analysis of my models. This course has covered this in great detail and has very much helped me to improve my approach of histological analysis from start (organ collection) to finish (staining and analysis) as it covers every aspect during this process as well as the initial development of mouse models."

As already seen in the general evaluation, the biggest issue students had with the course, was the time allocated with the different modules:

"The only issue for me was the time allotted for each module"

1.1.5.   Differences between medical or natural science students

As previously reported, students had differences in background and therefore not the same basic knowledge about pathohistology. After the final examination, students were grouped into natural science background and medical background. Even though natural science students performed very well in the pathohistology part (mean of correct answers: 87 %), the medical students showed in significantly average higher points (mean of correct answers: 97 %, p-value < 0.05). Additionally, medical students had more often full marks. In general, medical students showed more consistent results, meanwhile students with a natural science background differed in the group itself. Figure 15 shows the differences in marks between medical and natural science students.
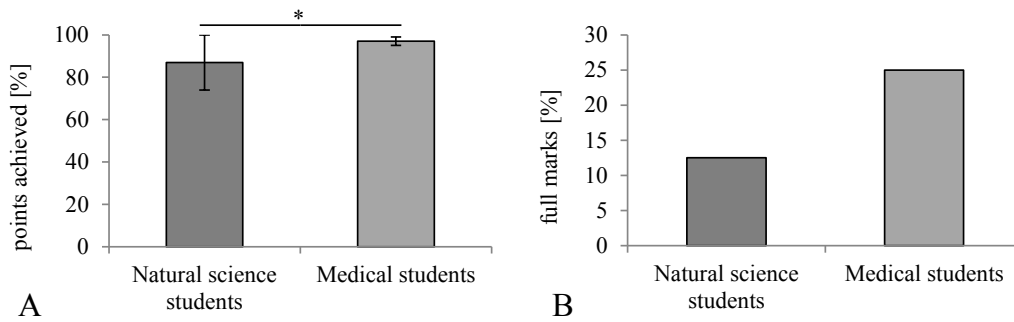
Figure 15: Differences in background between natural science students and medical students. A: Medical students achieved higher points in the pathohistology part of the final examination. The maximum of points was 12. B: Medical students reached more often full marks than natural science students did.

1.1.6. Dissemination and exploitation strategy and activities

Information about the course was available on a public website, which had been created for the project (http://pathpath.eu/). The course content was advertised during a poster and various talks in international congresses (Haneder and others 2013, Haneder and others 2014, J.C. Patterson-Kane and others 2013, Strauss and others 2013).

2. PDAC and TNC

2.1. Practical application of the course: PDAC project

Together with the feedback collected from the students, the PDAC project was used to evaluate the course content. After the successful run of the pilot course, the morphological characterization of a genetically engineered mouse model for pancreatic cancer with a depletion of the stromal protein TNC was conducted. The results are presented and the usefulness of the course for the mouse project is discussed below.

2.2. TNC expression in *KC* mice

In human PDAC tissue, immunohistochemistry reveals a selective stromal accumulation of TNC (Esposito and others 2006). To validate whether the same is true for murine precursors of PDAC and murine PDAC, pancreata of *KC* mice were stained for expression of TNC. A moderate to intense accumulation of stromal TNC can be observed around ductal lesions in areas of ADM, murine PanIN lesions (Figure 16) as well as in the invasive front of murine PDAC, thus confirming the selective expression of the *Tnc* gene in the mouse model.
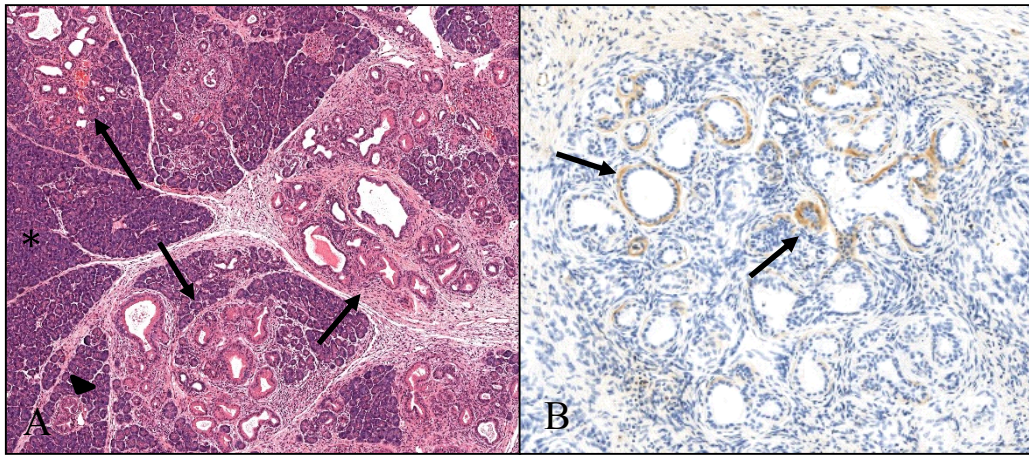
Figure 16: A: A *KC* mouse mimicking human precursor lesion of PDAC. Areas of ADM (arrows) and murine PanIN-1 lesions (arrowhead) are present next to unaffected acinar areas (asterisk), 5x, HE, B: Immunohistochemistry with an antibody against TNC on pancreatic tissue of a *KC* mouse. Pronounced expression of TNC (brown DAB stain, arrows) around ductular lesions in areas of ADM, 10x.

2.3.   Architectural distortion and classification of precursor lesions

To assess the influence of an absence of TNC protein on the development of murine pancreatic precursor lesions, triple mutant mice lacking TNC were generated. This was performed by crossbreeding TNC null mice with *KC* mice, both on a C57BL6N background, to achieve *KC-TNChet* and *KC-TNCko* mice. *KC-TNChet* and *KC-TNCko* mice were smaller than their TNC bearing littermates and more prone to biting by their siblings, as seen on their fur and adnexa and were found more often dead in their cages. HE stained serial sections of pancreata of *KC*, *KC-TNChet* and *KC-TNCko* mice were evaluated semi-quantitatively in different age groups, ranging from one to 15 months (1 month, 2 months, 3 months, 6 months, 9 months and 12-15 months), including appropriate controls. At least four animals per group were analyzed. *KC* mice alone develop the complete spectrum of precursor lesions as well as invasive PDAC (Hingorani and others 2003). Diseased pancreata of TNC knockouts and KC mice were compared and architectural distortion of pancreata as well as the number and type of precursor lesions and frequency, histological subtype and grading of PDACs was calculated. In addition, murine AFL were counted (Aichler and others 2012). Figure 17 shows precursor lesions of PDAC that develop in *KC* mice, but also TNC mutant mice. Control animals did not show any phenotype in their pancreatic sections.

Altogether, 106 mutant mice with the following genotypes

KC-TNCko   n=28

KC-TNChet   n=46

KC   n=32

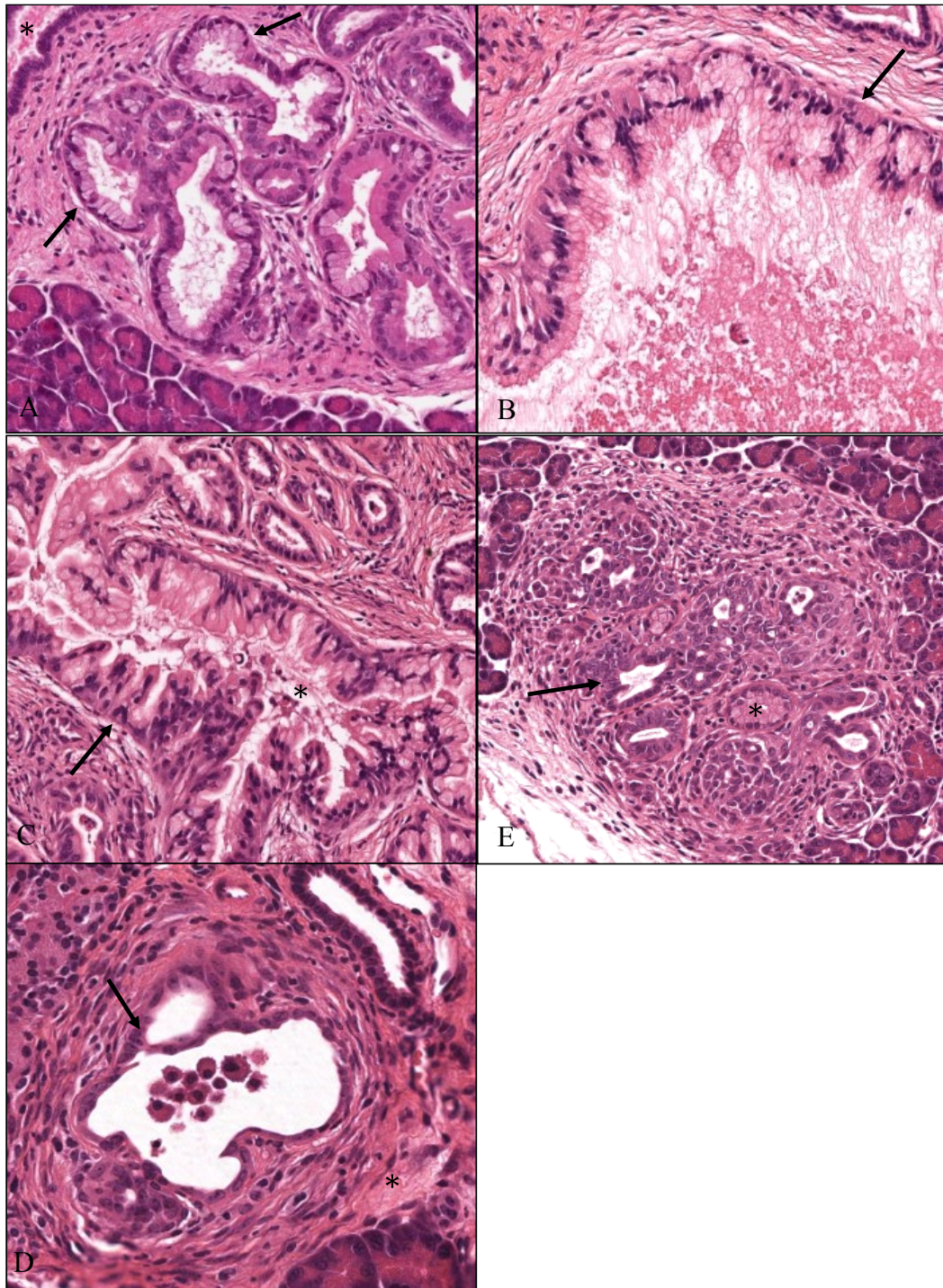were used for histopathological evaluation.

Figure 17: A: Murine PanIN-1 lesion, with basally oriented nuclei and mucinous cytoplasm (arrows)

next to an unaffected duct (asterisk) in a *KC-TNCko* mouse, 20x; B: murine PanIN-2 lesion, with nuclear stratification (arrow) in a *KC-TNCko* mouse, 20x; C: murine PanIN-3 lesions, with marked nuclear atypia, loss of basal orientation of nuclei (arrow) and budding of cells in the lumen (asterisk) in a *KC-TNCko* mouse, 20x; D: area of ADM with TCs (arrow) and MTCs (asterisk) in a *KC-TNCko* mouse, 10x; E: murine AFL with flat cells (arrow), a ductal-like morphology and the typical onion shaped stroma surrounding the lesion (asterisk) in a *KC-TNCko* mouse, 40x

2.3.1.　One month-old mice

Mutant pancreata belonging to the group of one month-old mice showed beginning areas with acinar-ductal metaplasia and invasion of inflammatory cells, mainly lymphocytes and plasma cells. In small tissue areas, the acinar cells formed luminal spaces and changed their morphology to a more ductal like phenotype with cuboidal cells. Mucinous tubular complexes, ductal lesions with mucin containing columnar cells were distributed within areas of ADM. These lesions are morphologically not distinguishable from PanIN-1 lesions. PanIN-1 lesions were a rare finding, and were not connected to a specific phenotype. Single AFL lesions were already present in some mice at the age of one month. No differences of number of AFL between all phenotypes could be observed. All mice exhibited only few lesions, which accounted for less than 5 % of the pancreatic tissue. Control animals did not show any morphological alteration in pancreatic tissue (Figure 18 at 2.2.3.).

2.3.2.　Two months-old mice

Compared to the group of one month, pancreata show a more pronounced architectural distortion (ranging von 10 % to 20 %) with formation of ADM areas containing TCs and MTCs, a distinct inflammatory reaction and fibrosis. PanIN-1 lesions also increased in number. Animals belonging to group *KC-TNChet* and *KC-TNCko* showed a slightly higher percentage of architectural distortion compared to *KC* mice, even if not significant (Figure 18 at 2.2.3.).

2.3.3.　Three months old mice

Here, distinct differences between genotypes were readily apparent. This age group was therefore chosen for further analyses.

Mutant pancreata showed a pronounced architectural distortion with AFL and PanIN-1 as well as PanIN-2 formation. One animal belonging to the *KC-TNCko* displayed a PanIN-3 lesion. As in two months-old animals, mice belonging to group

KC-TNChet and *KC-TNCko* showed a slightly higher mean percentage of architectural distortion compared to *KC* mice (Figure 18).
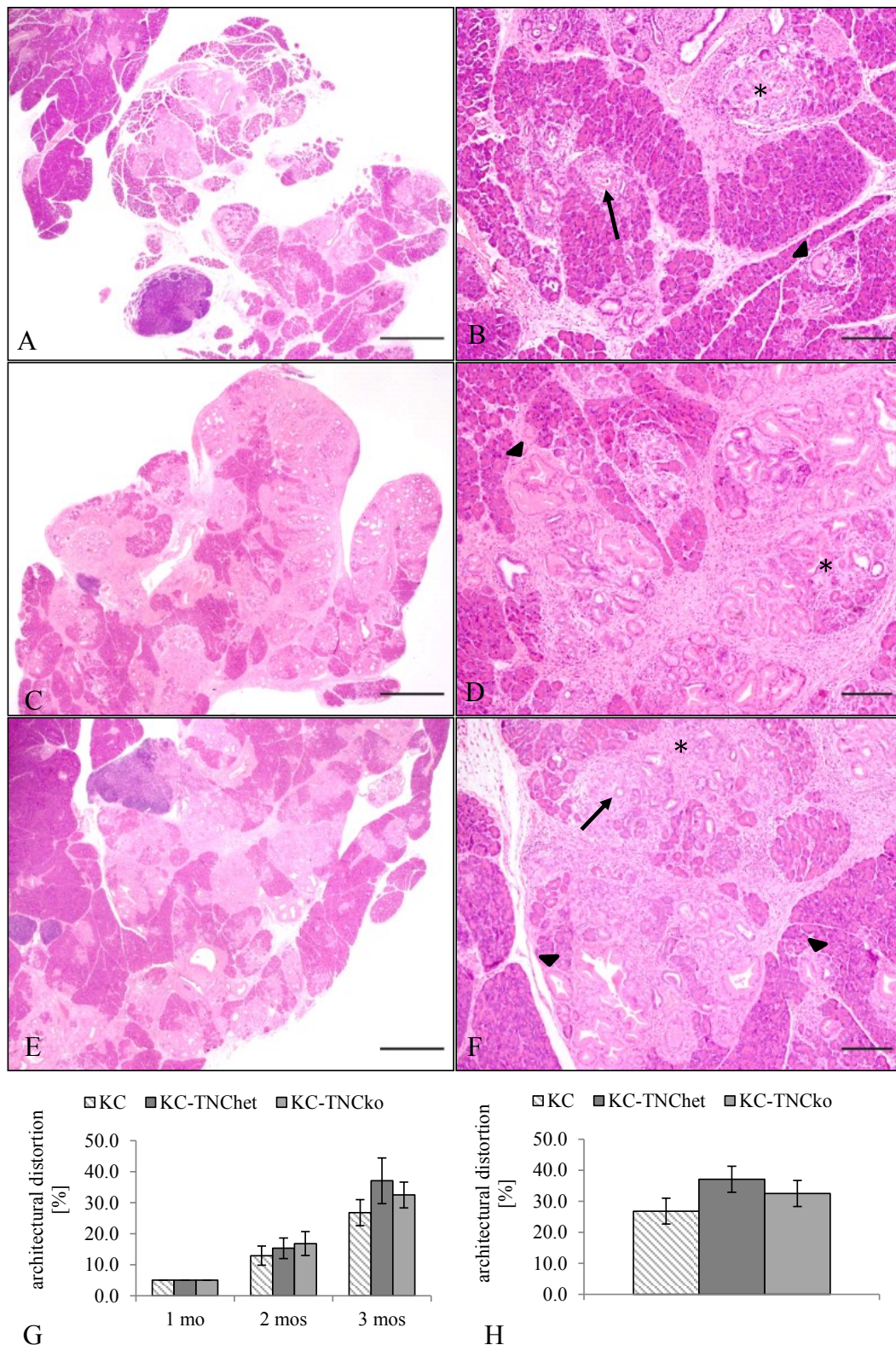

Figure 18: A: Mutant pancreata of three months old mice, A, D: Representative pancreas of a *KC* mouse, B, E: *KC-TNChet*, C, F: *KC-TNCko*. Murine pancreata show loss of acinar parenchyma and architectural distortion (asterisks), PanIN (arrowheads) and AFL (arrows) formation. Architectural distortion is more pronounced in *KC-TNChet* and *KC-TNCko* mice; A-C: 2x, D-F: 5x; G:

Architectural distortion of pancreatic of young animals bearing precursor lesions of PDAC. Compared to *KC* mice, *KC-TNChet* and *KC-TNCko* mice display a higher architectural distortion. H: Comparison of mutant animals of age group three months.

2.3.4.   Six months-old mice

Mice of all genotypes exhibit around 70 % architectural distorted tissue with extended areas of ADM containing AFL, TCs and MTs and a lymphoplasmacellular inflammatory cell infiltrate. Many PanIN-1 and PanIN-2 were detectable in all genotypes, as well as one PanIN-3 lesion in an animal belonging to the *KC-TNCko* group. At this time point, there was a high degree of architectural distortion in all groups and no difference could be identified.

2.3.5.   Nine months-old mice

Similar to 6 months old mice, all mutant mice displayed an architectural distortion of about 95% of the tissue with fibrosis, PanIN-1 and PanIN-2 and AFL. PanIN-3 were detected in mice of the *KC-TNChet* and *KC-TNCko* group and one mouse of the *KC-TNChet* group developed PDAC with invasion in the stomach and liver metastases. The tumor consists of densely packed, moderately differentiated glandular structures surrounded by a desmoplastic stromal reaction. The tumor showed a central necrotic area with infiltration of neutrophil granulocytes.

2.3.6.   Twelve to fifteen months-old mice

As in nine months-old mice, all mutant mice displayed an architectural distortion of at least 95% with fibrosis, PanIN-1 and PanIN-2 and AFL. PanIN-3 were observed in all groups and some animals developed metastatic PDAC. PDAC was twice as frequent in *KC-TNCko* and *KC-TNChet* as in *KC* mice at the age of 12 months, as shown in Figure 19.
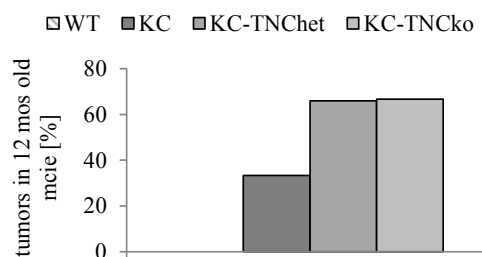

Figure 19: PDAC in mutant mice. At the age of 12 months, more *KC-TNChet* and *KC-TNCko* mice

harbor PDAC than *KC* mice.

2.4. Fibrosis in mutant pancreata

Additionally to the progression of precursor lesions, an increasing fibrosis accompanied tumor development. To validate and further characterize the observations, Masson Goldner trichrome and Movat stains were performed in 3 months-old mice and quantified as described in Methods. In the Masson Goldner stain, the pattern of fibrotic deposition was similar in all groups and mostly displayed a perilobular and perilesional (i.e. around ADM/precursor lesions) distribution. Mice of the *KC-TNChet* and *KC-TNCko* groups showed a higher percentage of fibrosis (17.4 % and 18.2 %, respectively) when compared with the *KC* group (12.7 %). The difference between the *KC* and *KC-TNChet* group at the age of three months was significant (p-values KC-TNCko to WT < 0.01, KC-TNChet to WT < 0.01, KC to WT < 0.01; KC-TNCko to KC 1.45 and KC-TNChet to KC < 0.05 respectively). Figure 20 shows representative pictures of mice at the age of three months.
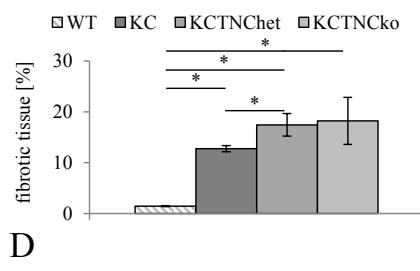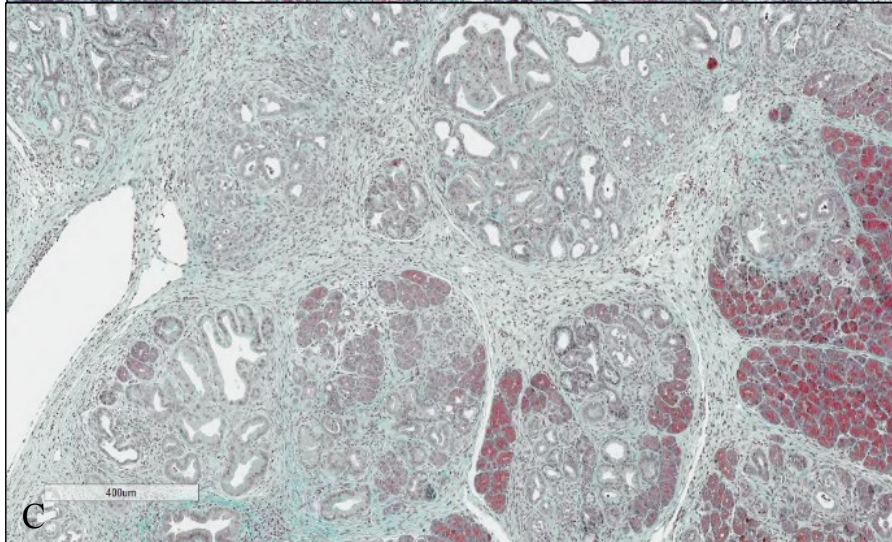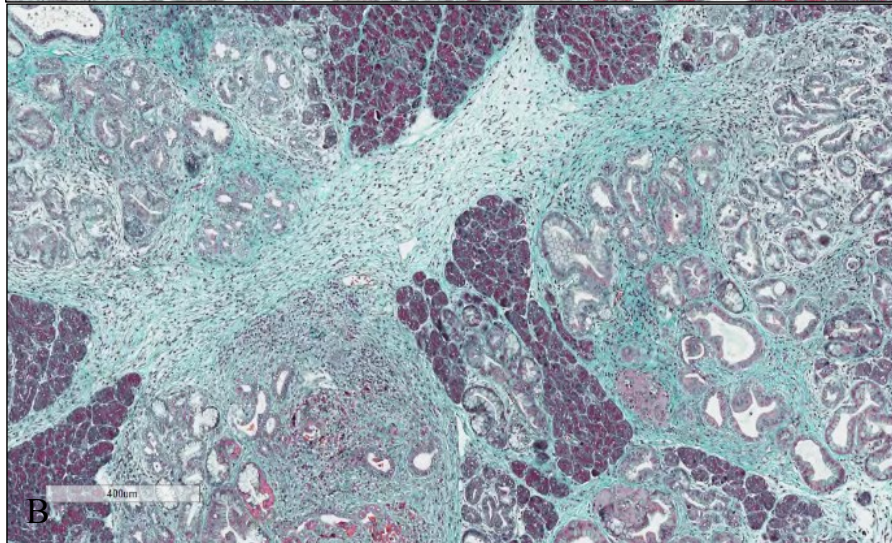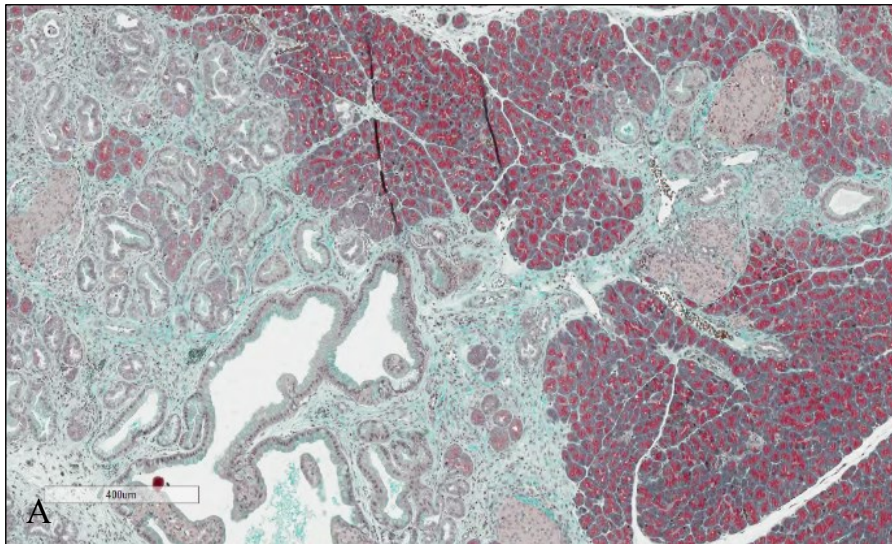
Figure 20: Masson Goldner stain of mutant mice at the age of three months, A: *KC* mouse with red stained residual acinar tissue and islets and green fibrotic area, 5x, B *KC-TNChet* mouse with perilobular and perilesional accumulation of fibrotic tissue, 5x C: *KC-TNCko* mouse with widely remodeled tissue, 5x, D: Calculation of fibrotic areas in pancreata of wild type and mutant mice at the age of three months. *KC* mice show less fibrotic areas when compared to *KC-TNChet* and *KC-TNCko* mice.

With the Movat pentachrome stain immature connective tissue stains blue due to the high content in mucopolysaccharides, whereas older fibrotic lesions, containing mature collagens, are stained yellow (Doello 2014). In general, in beginning ADM lesions, a blue colored layer of mucopolysaccharides containing extracellular matrix encircled remodeled acinar parenchyma, and more advanced lesions with TCs, MTCs and AFL are surrounded by mature collagen. This could be observed in animals of all genotypes. Interestingly, in *KC-TNChet* and *KC-TNCko* mice, an earlier switch to the mature fibrotic tissue could be observed, as depicted in Figure 21. As already seen in the Masson Goldner stain, Movat's stain underscored the tendency of animals lacking TNC towards a more fibrous phenotype.
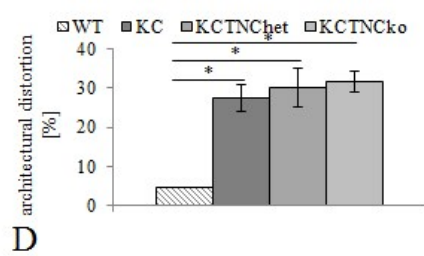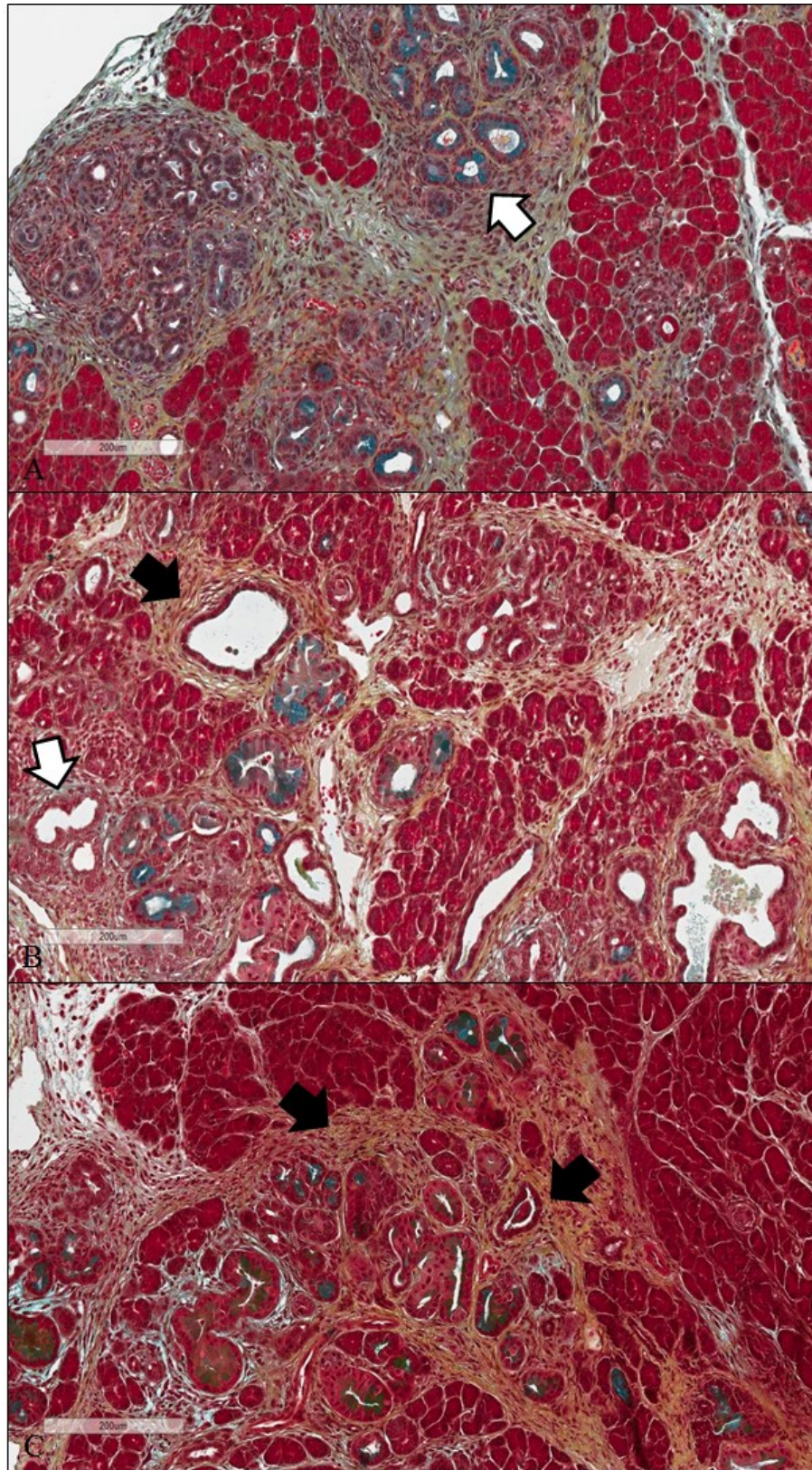
Figure 21: A: Mutant pancreata of a *KC* animal, stained with Movat stain, 10x, B: Mutant pancreata of a *KC-TNChet* animal, stained with Movat stain, 10x, C: Mutant pancreata of a *KC-TNCko* animal, stained with Movat stain, 10x, white arrow pointing to blue colored layer of mucopolysaccharides, black arrow shows mature collagens with a yellow color; D: Result of Movat stained mutant pancreata compared to control animals at the age of three months, results as mean values and SEM. All mutant mice show a clearly higher percentage of fibrotic tissue when compared to *WT* animals. As in Masson Goldner stain, there is a tendency towards a higher percentage of fibrosis in *KC-TNChet* and *KC-TNCko* animals.

2.5.   Mucin

As the previous stains revealed an influence of TNC on the architectural distortion of mutant pancreata, further stains were used to assess the lack of TNC on precancerous lesion development. In order to check the influence of the prevalence or absence of TNC on the development and character of mucinous lesion, mucin staining was used. Cytoplasmic mucin content of PanINs and MTCs can be highlighted by Alcian blue stain and PAS reaction (Muller-Decker and others 2006). The apical mucinous cytoplasm within the lesions stains violet to blue, depending on the pH of the containing mucin. Computer aided analysis was used to calculate mucin content, and results are stated as percentage of mucin to completely pancreatic tissue area. In comparison to *KC* mice, *KC-TNChet* and *KC-TNCko* mice show a slightly higher percentage of mucinous containing structures (Figure 22). The staining pattern was comparable in all groups.
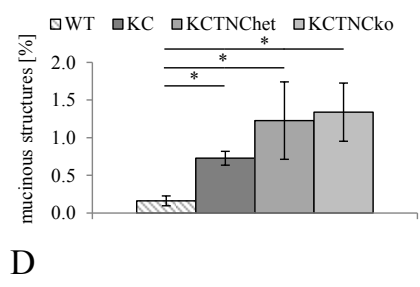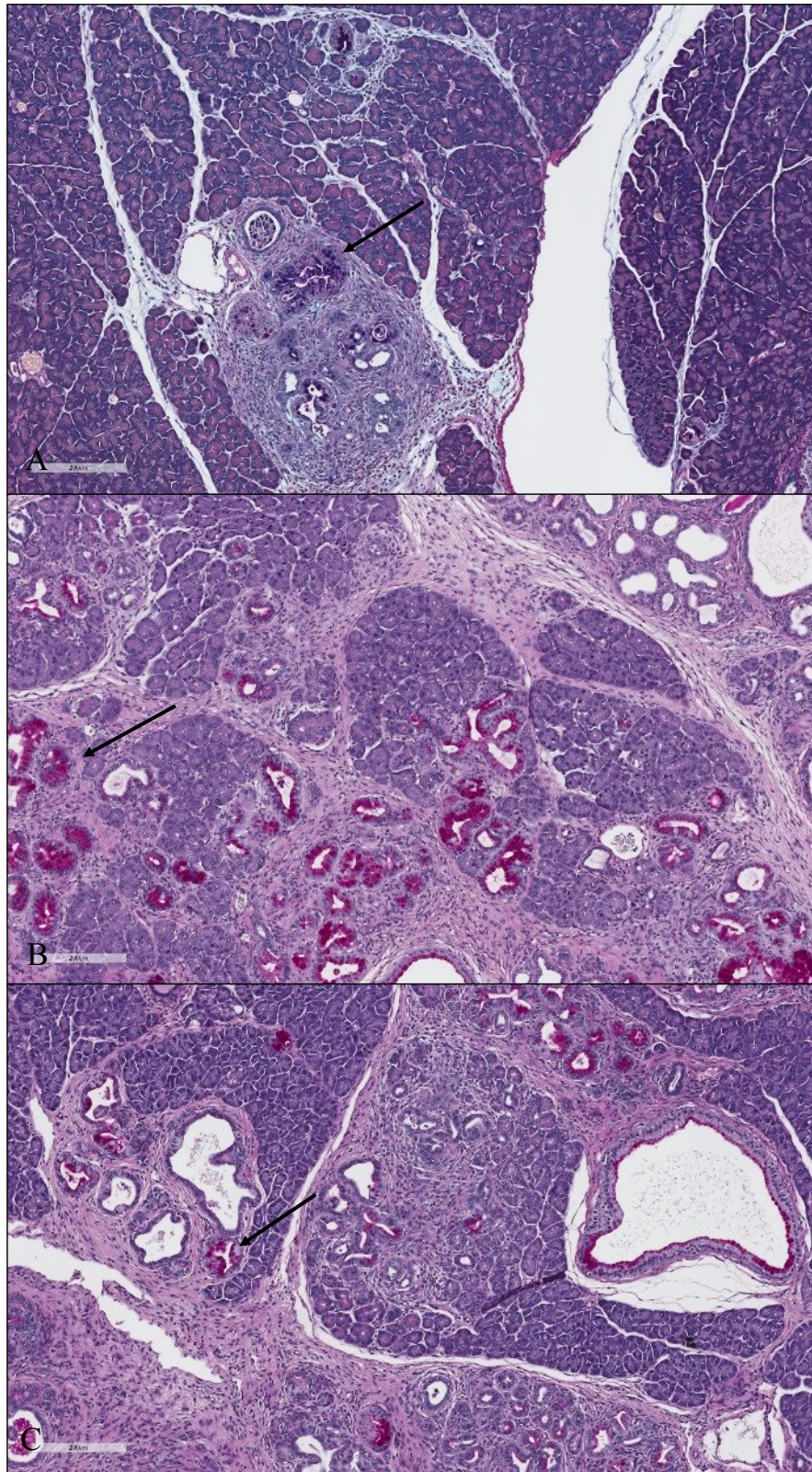
Figure 22: Computer aided calculation of mucin containing lesions, mice at the age of three months. A: *KC* mouse, 5x; B: *KC-TNChet* mouse, 5x; C: *KC*-TNCko mouse, 5x; D: *KC-TNChet* and *KC-TNCko* mice show a higher content of mucinous lesions compared to *KC* mice.

2.6.　　　 **Ductular structures and PanIN**

The impact of TNC on the development of tubular structures, independently from the mucin content, was further assessed by CK19 staining. Normal ducts, PanIN, TCs, MTCs and AFL were all positive for CK19, as expected; acinar cells and islets were negative (Aichler and others 2012). In comparison to *KC* mice, *KC-TNChet* and *KC-TNCko* mice showed a significantly higher percentage of ductular structures, as depicted in Figure 23 (p-values *KC-TNCko* to *WT* < 0.01, *KC-TNChet* to *WT* < 0.01, *KC* to *WT* < 0.01; *KC-TNCko* to *KC* 0.03 and *KC-TNChet* to *KC* 0.05 respectively).
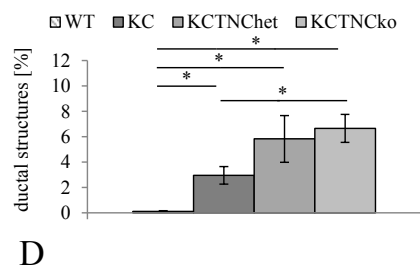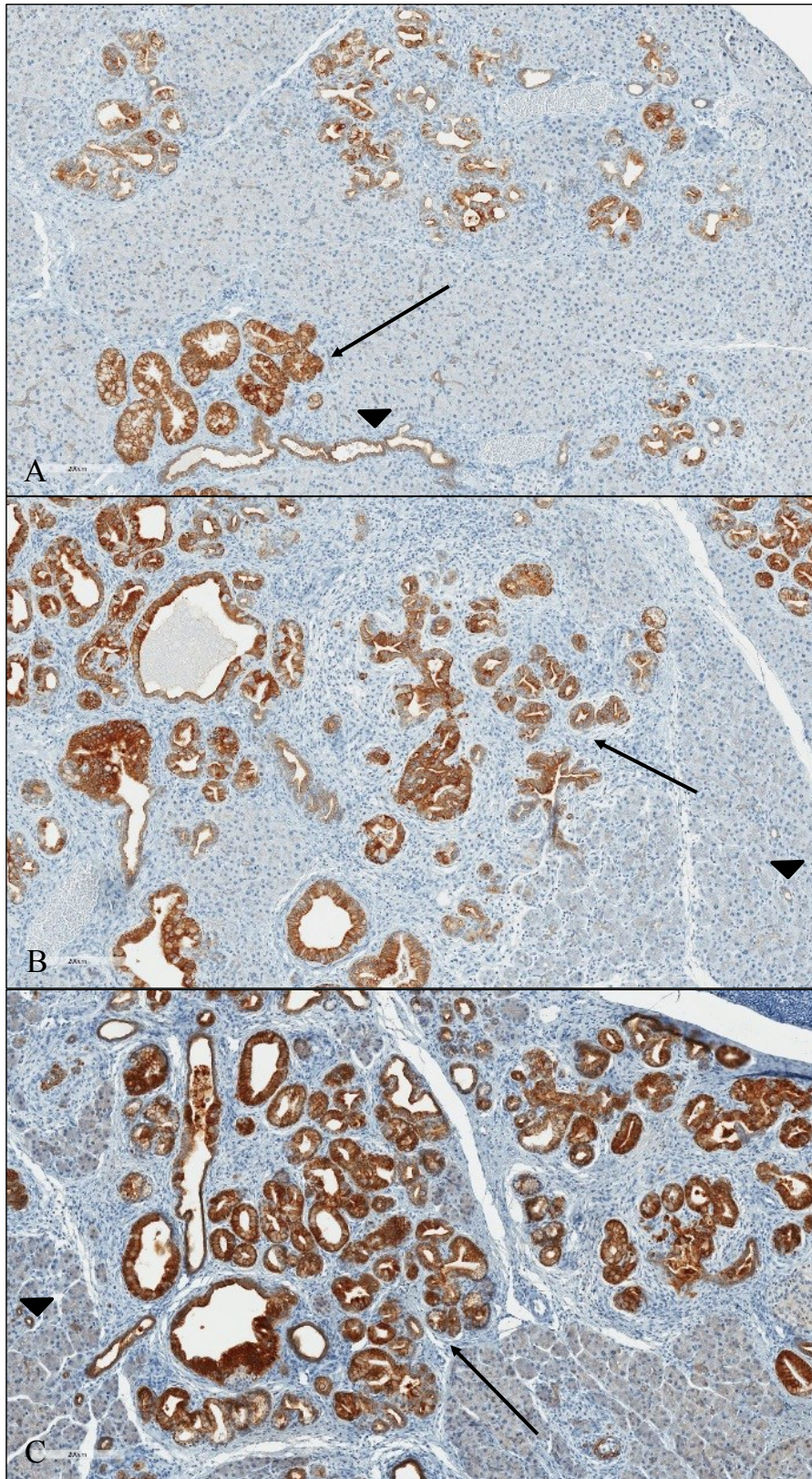
Figure 23: Ductular structures, assessed by CK19 stain, mice at the age of three months. A: KC mouse 5x; B: *KC-TNChet*, 5x; C: *KC-TNCko*, 5x, all diseased (arrows) and normal (arrowheads) ductular structures are detected by CK19 staining; C: Compared to *KC* mice, *KC-TNChet* and *KC-TNCko* mice show a higher percentage of ductular structures.

MTC and PanIN were further assessed by Claudin18 (CLN-18) immunoreactivity. All murine PanIN-1 to PanIN-3 and MTCs showed strong membranous staining for CLN-18, as expected. Here, the *KC-TNCko* group showed a higher rate of PanIN when compared to the *KC-TNChet* and *KC* groups at the age of three months, as shown in Figure 24 (p-values *KC-TNCko* to *KC* 0.13 and *KC-TNChet* to *KC* < 0.01 respectively).
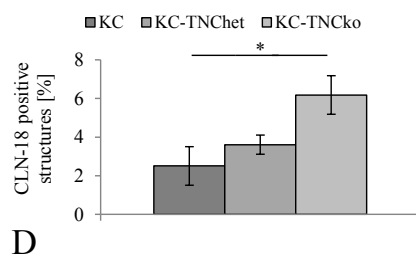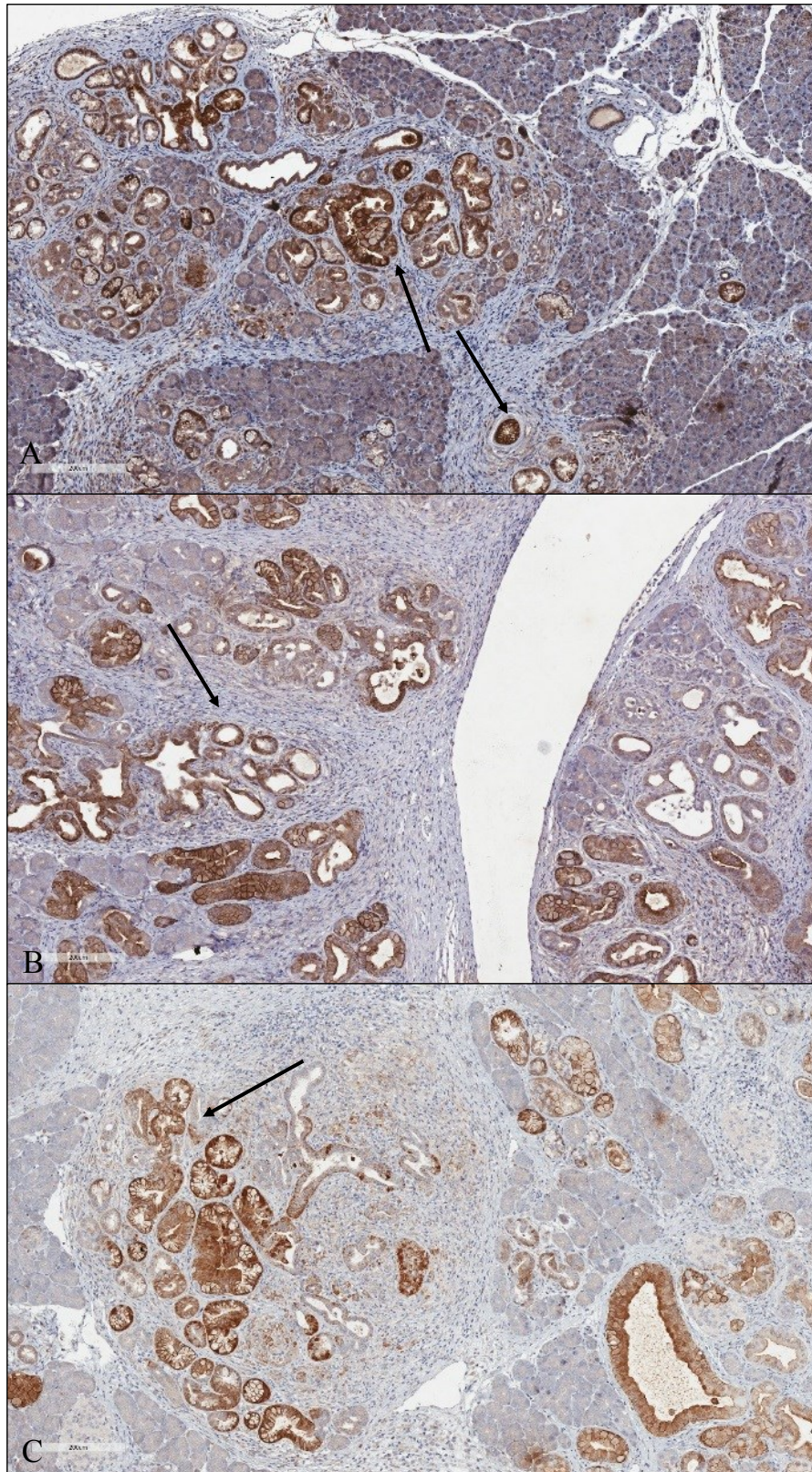
Figure 24: Assessment of ductular structures with CLN-18 staining in the age group of three months. A: KC mouse with membranous CLN-18 positivity (arrows), 5x; B: *KC-TNChet*, 5x; C: *KC-TNCko*, 5x; D: *KC-TNChet* animals show slightly more CLN-18 expression, meanwhile *KC-TNCko* animals exhibit significantly more diseased structures than *KC* animals at the age of three months.

2.7.   Proliferation and apoptosis

In order to assess if the described differences in the frequency of ductular structures and precursor lesions was related to differences in cell proliferation or apoptosis/senescence, staining for Ki67, cleaved caspase-3 and p16 were performed and semi-quantitatively assessed.

In general, areas of ADM showed an increased number of Ki67-positive cells when compared to normal acinar parenchyma. AFL lesions could be easily detected by their high expression of Ki67-antigen, underscoring their highly proliferative nature. In contrast, PanIN-1 lesions exhibited only few Ki67 positive cells (see Figure 25). Interestingly, in areas of ADM, mice belonging to the *KC-TNCko* and *KC-TNChet* groups showed significantly higher proliferative indices than those of the *KC* group (p-values *KC-TNCko* to *KC* < 0.01 and *KC-TNChet* to *KC* 0.01 respectively). In AFL, PanIN-1 and PanIN-2 lesions, no differences between the genotypes could be detected.

Only a small number of apoptotic cells were detected by cleaved-caspase 3 stain. In areas of ADM, few apoptotic cells were present with high differences between mice of the single groups so that no differences in genotypes were found. AFL and PanIN-1 lesion contained hardly any apoptotic cells; therefore, no differences in genotypes could be observed (Figure 26).
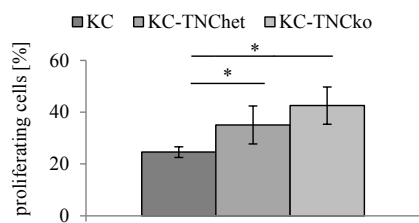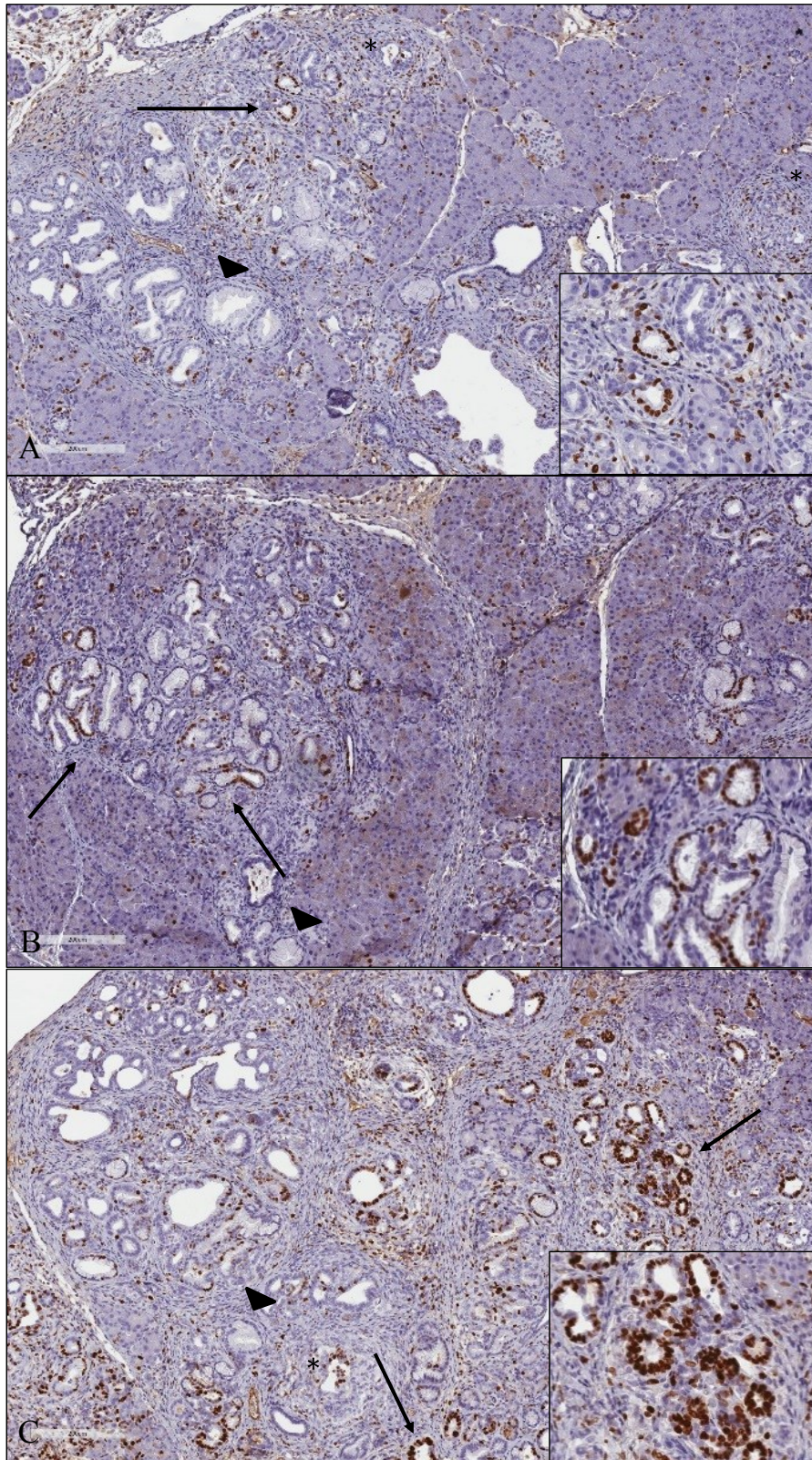
Figure 25: Calculation of proliferation of lesions in areas of ADM, mice at the age of three months, A: *KC* mouse with proliferating cells in areas of ADM (arrow), a low proliferation index in PanIN-1 lesions (arrowhead) and high proliferation in AFL (asterisks), 5x, inset with nuclear details in areas of ADM, 20x; B: *KC-TNChet* mouse with highly proliferating cells in an area of ADM (arrows) and low proliferation in PanIN-1s (arrowhead), 5x, inset with nuclear details in areas of ADM, 20x; C: *KC-TNCko* mouse with highly proliferating cells in ADMs (arrows) and AFL (asterisk), low proliferation in PanIN-1s (arrowhead), 5x, inset with nuclear details in areas of ADM, 20x; D: Compared to *KC* mice, *KC-TNChet* and *KC-TNCko* mice at the age of three months exhibit a

significantly higher proliferation activity.
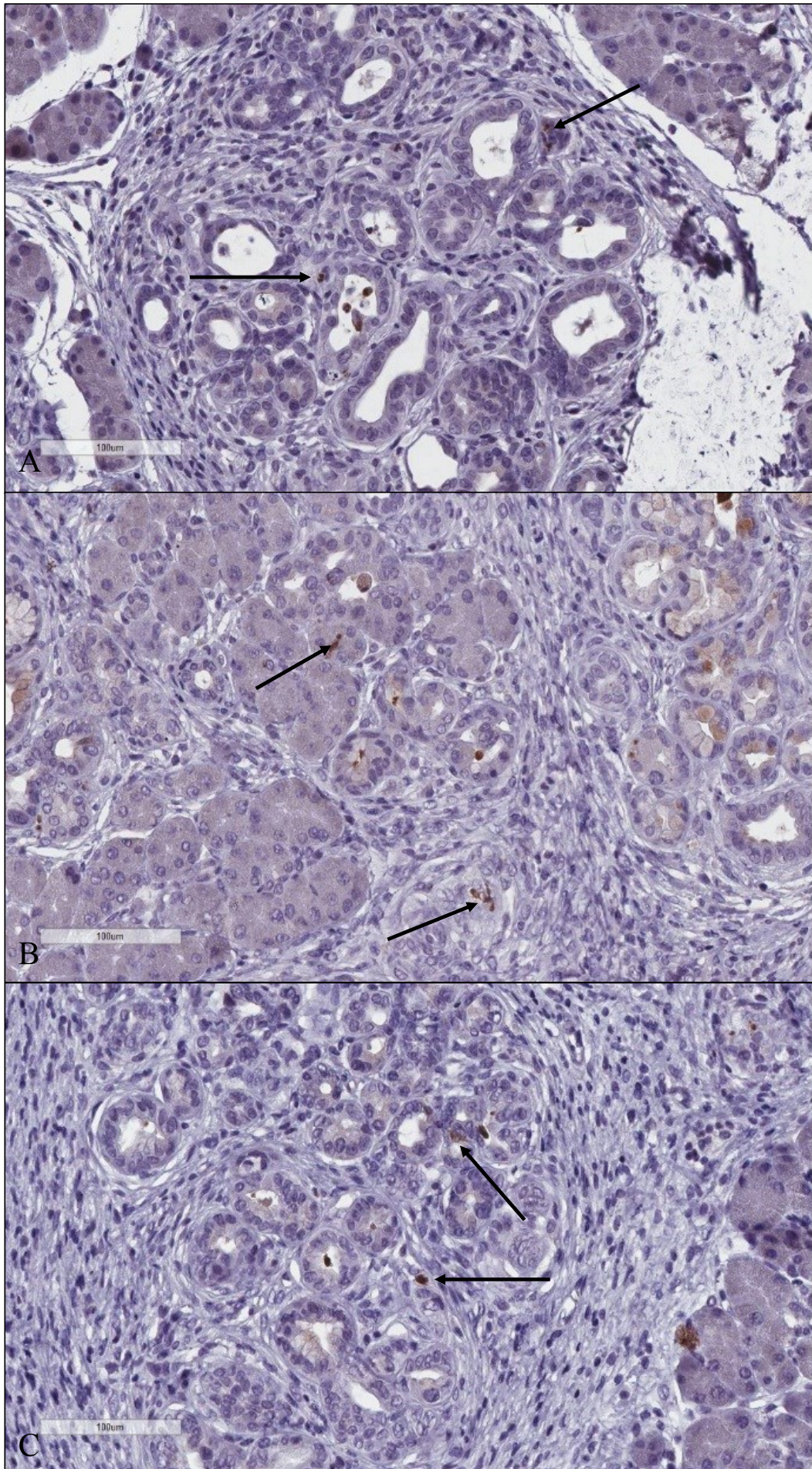
Figure 26: Representative pictures of mutant pancreata with apoptotic cells, pancreata of mice at the age of three months A: KC, B: KC-TNChet, C: KC-TNCko mice, 20x, arrows pointing to apoptotic cells in areas of ADM adjacent to not affected acinar parenchyma.

All genotypes showed an accumulation of p16 protein in nuclei of epithelia in ADM areas and PanIN lesions, indicating an upregulation of *Cdkn2a,* most likely related to increased proliferation. AFL lesions showed a reduced intensity of the nuclear staining, and a slight cytoplasmic staining, as previously observed. Taken together, when compared to each other, no obvious differences in the genotypes could be detected at the age of three months (Figure 27).
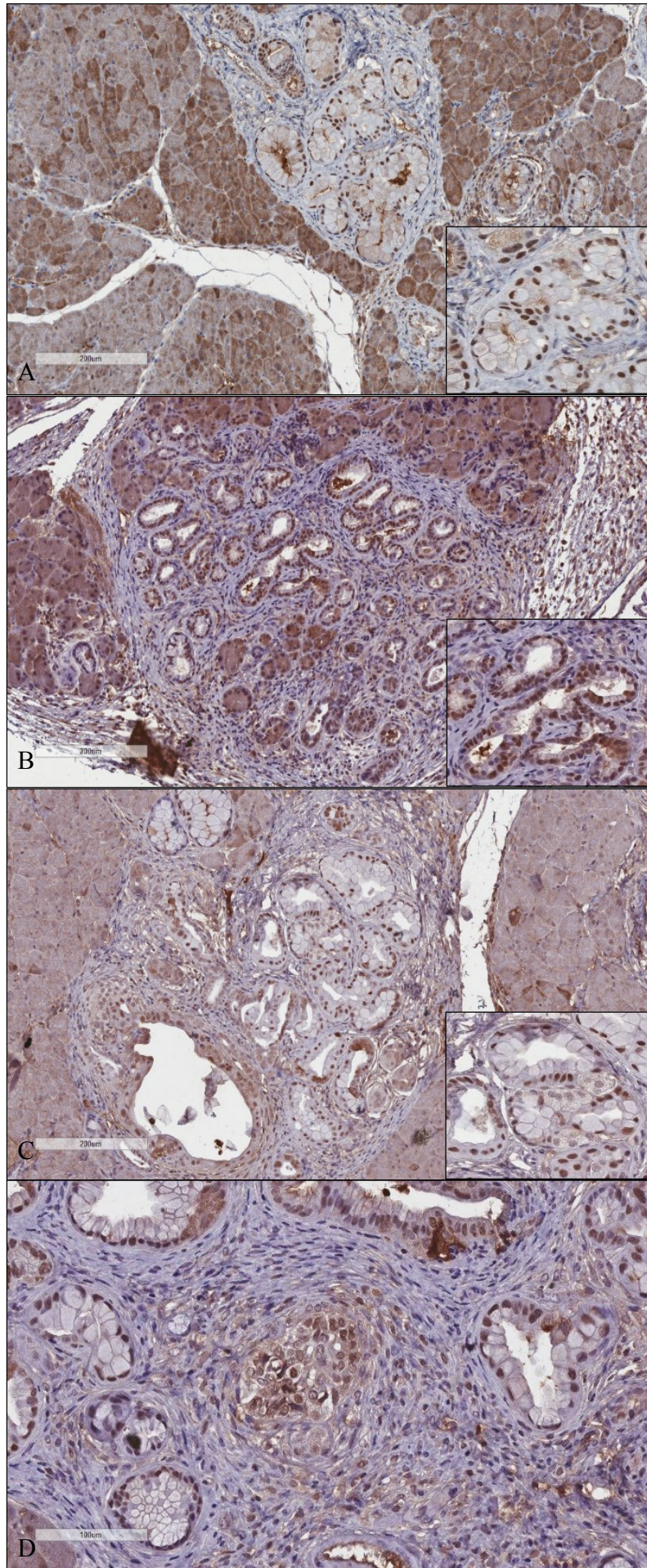
Figure 27: Representative pictures of mutant pancreata with p16 accumulating cells, pancreata of mice at the age of three months, A: *KC*, B: *KC-TNChet*, C: *KC-TNCko* mice, 5x, insets with 20x, D: AFL in a *KC-TNCko* mouse with light nuclear positivity.

2.8.   Wnt signaling pathway

Since TNC and proteins of the Wnt signaling pathway are known to interact during developmental processes and cancer (Hendaoui and others 2014, Saupe and others 2013), the expression of E-cadherin and β-catenin was investigated. In all genotypes, all normal and diseased structures display a membranous staining of E-cadherin and β-catenin with the exception of PDAC. Here a loss of E-cadherin and β-catenin was observed in some of the cancer cells. However, the absence of TNC did not to influence the expression of these proteins (Figure 28).
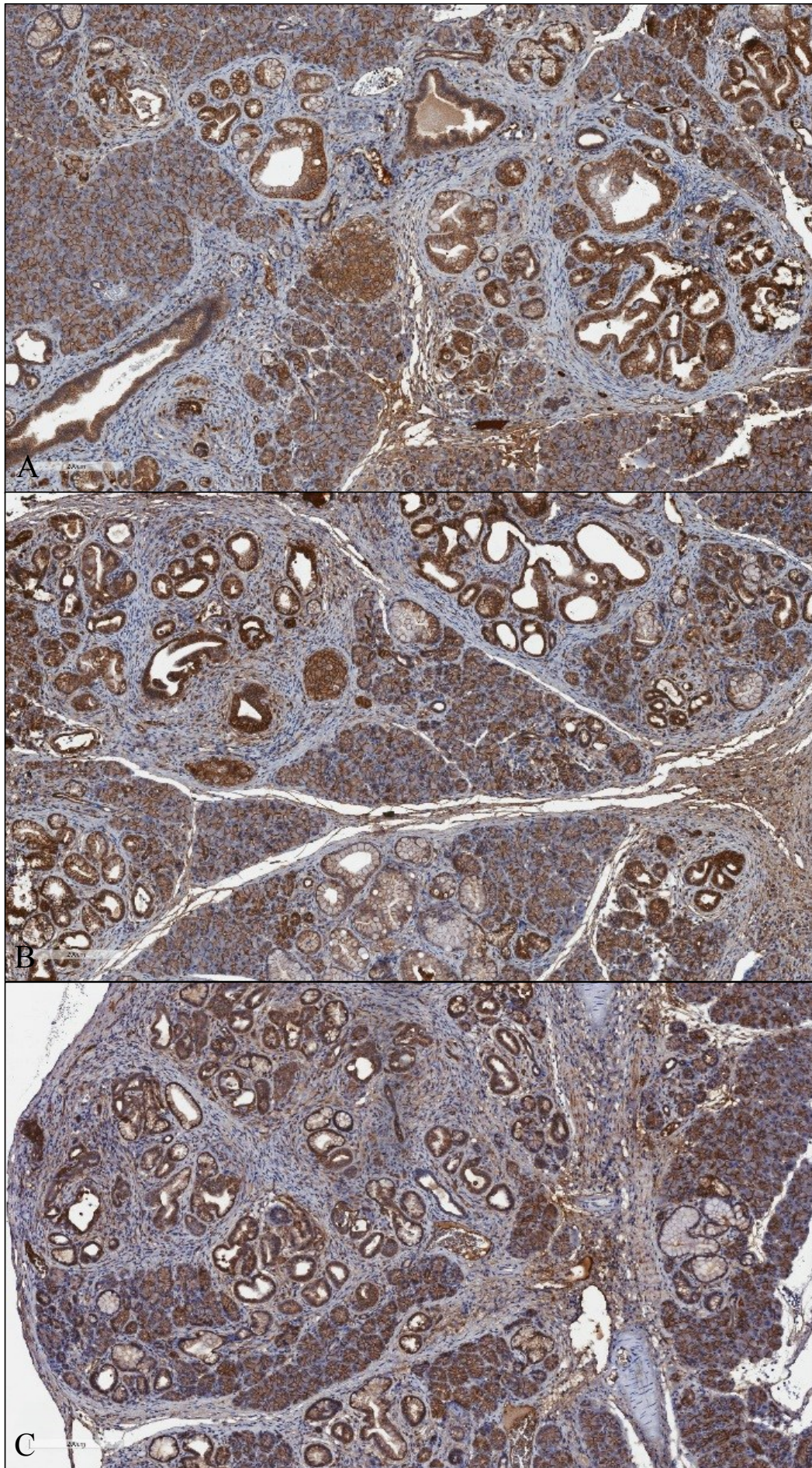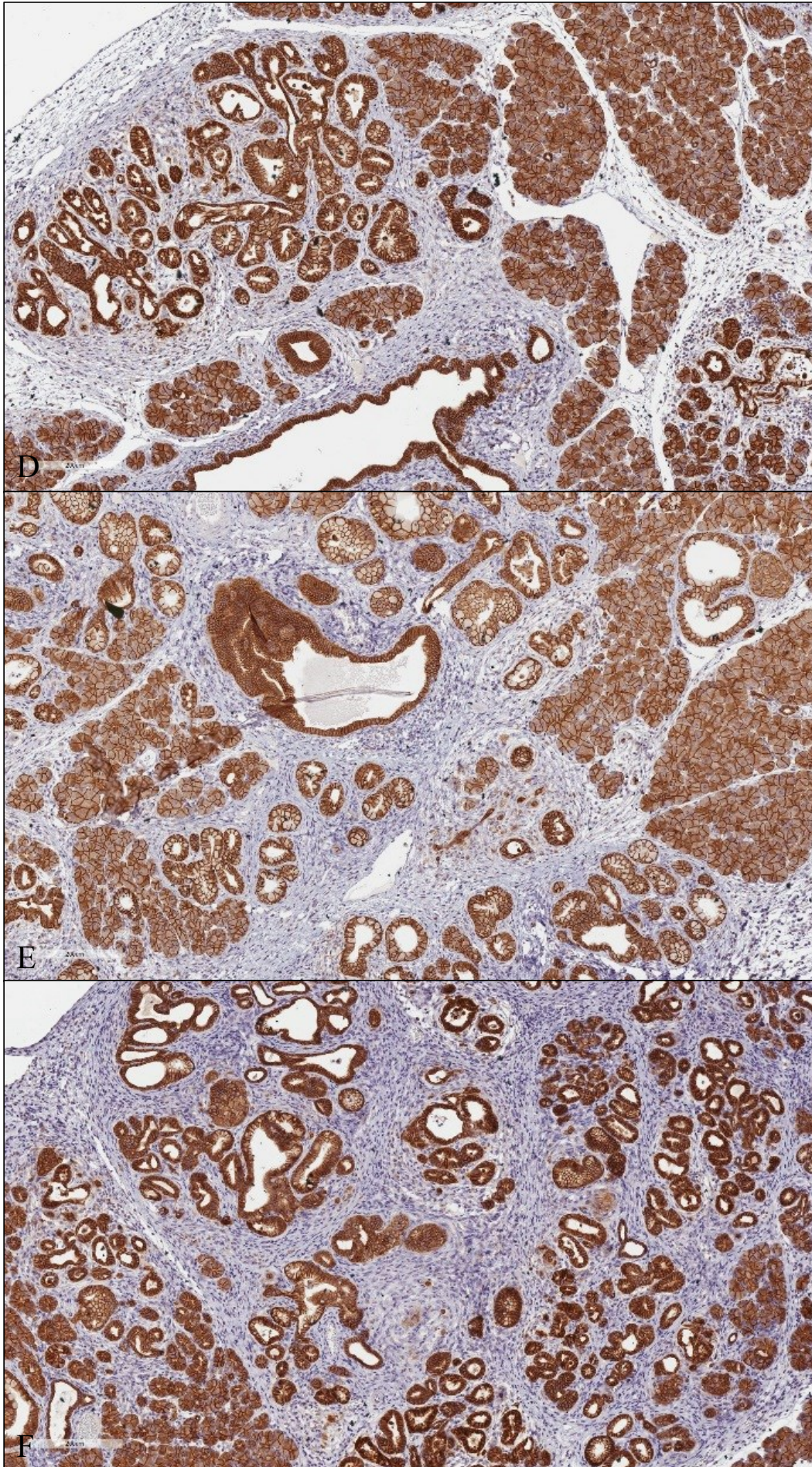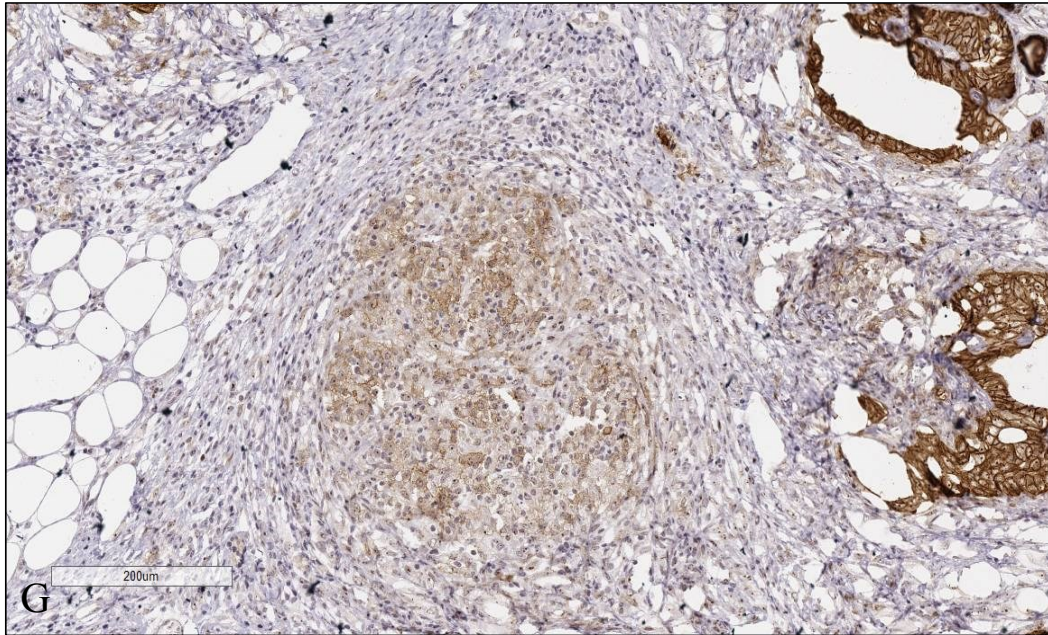
Figure 28: Absence of TNC does not influence the expression of β-catenin and E-Cadherin in mice at the age of three months. A: membranous expression of β-catenin and D: E-Cadherin in a *KC* mouse, B, E: in a *KC-TNChet* mouse, C, F: in a *KC-TNCko* mouse, all 5x, G: partial loss and lower staining intensity of E-Cadherin expression in mouse bearing PDAC, 10x.

2.9. NOTCH/HES1 signaling pathway

2.9.1. NOTCH2

Finally, due to the known role of the Notch pathway in ADM and given the significant differences observed in the extension of ductular structures between the groups, the expression of NOTCH2 and its downstream protein HES1 were investigated. For NOTCH2 staining, normal ductal epithelium and centroacinar cells served as an internal control. Unaffected acini and islets were negative for NOTCH2 staining. In all genotypes, in areas of ADM more than 50% of nuclei were positive for NOTCH2 protein. Similar results could be observed for PanIN-1 lesions. Interestingly, AFL lesions showed a weaker nuclear staining with less positive cells. No differences in NOTCH2 expression between the genotypes could be observed (Figure 29).
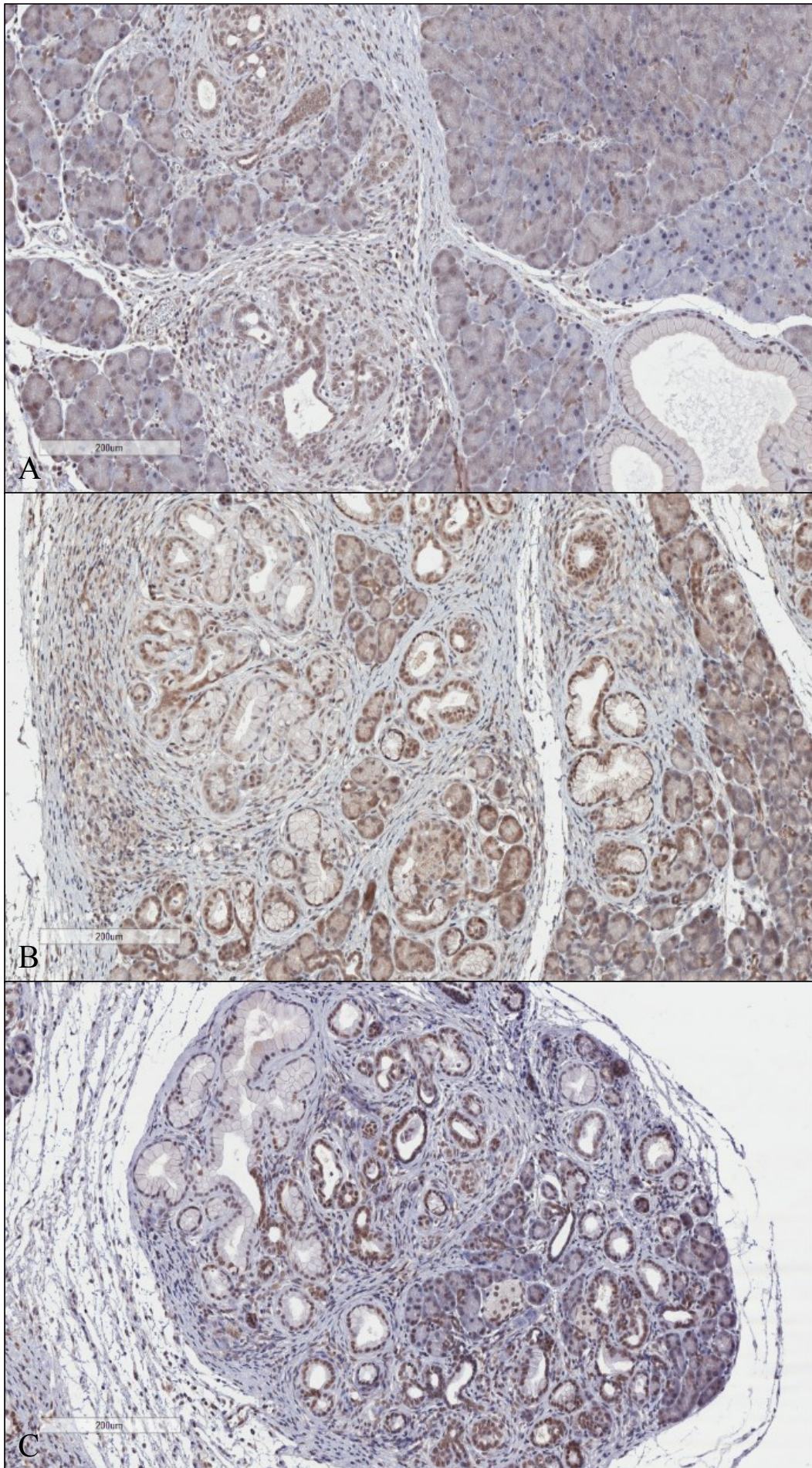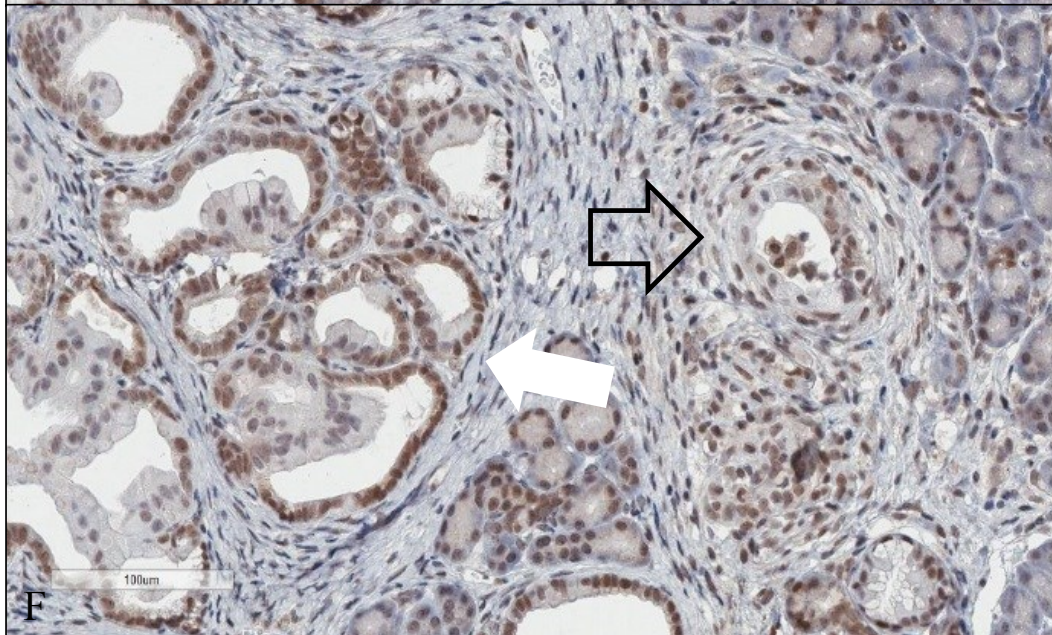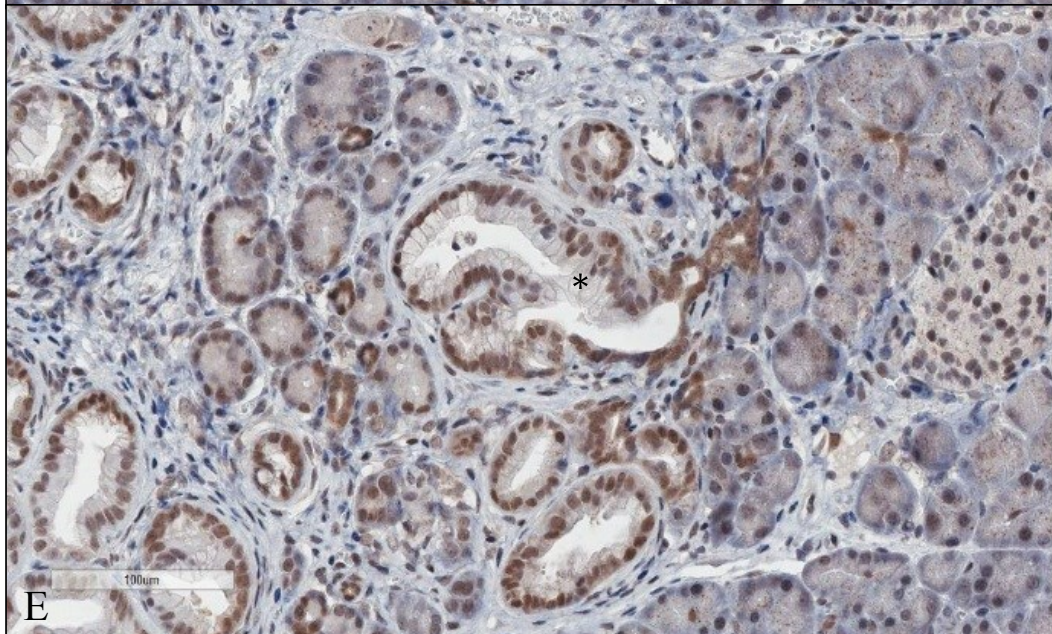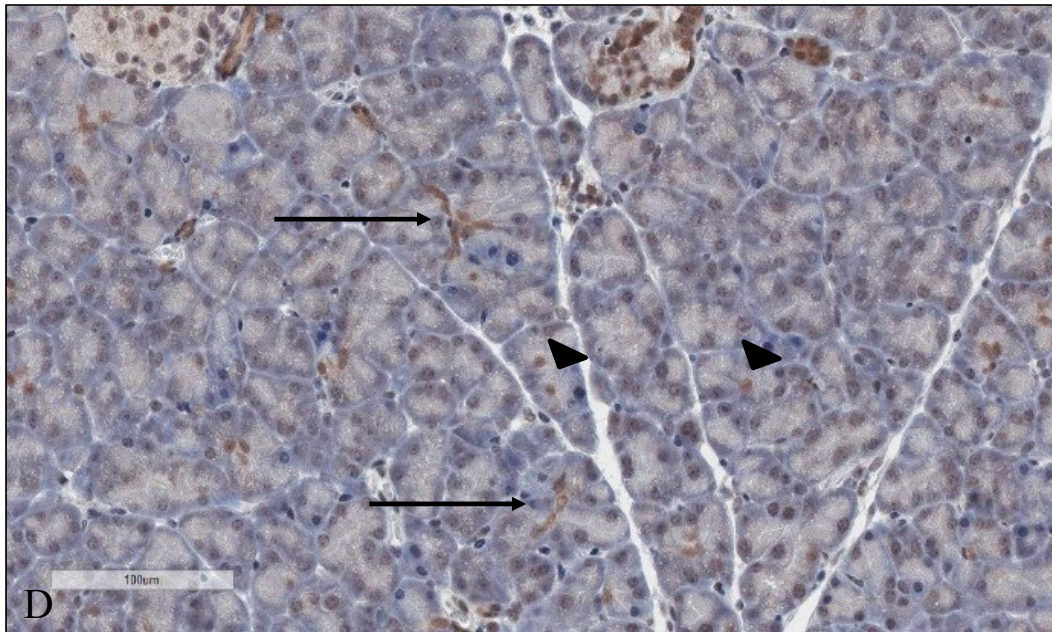
Figure 29: Nuclear and cytoplasmic NOTCH2 expression of PanIN, ADM, AFL lesions and centroacinar cells in mice at the age of three months, A: *KC* mouse, 5x, B: *KC-TNChet*, 5, C: *KC-TNCko*, 5x, D: *KC-TNCko* mouse with unaffected acinar parenchyma, arrows pointing to small, nuclear NOTCH2 positive ducts, arrowheads indicating nuclear positivity in centroacinar cells, 20x, E: *KC-TNCko* mouse with nuclear NOTCH2 positive duct with arising PanIN-1 (asterisk), 20x, F: *KC-TNCko* mouse with NOTCH2 positive nuclei in areas of ADM (white arrow) and weak nuclear positivity in AFL (black arrow), 20x.

Centroacinar cells served as an internal control for HES1 staining. Ductular cells, acini and islets were negative for HES1. In all genotypes at the age of three months, in areas of ADM more than 50 % of nuclei were positive for HES1 protein. Similar results could be observed for PanIN-1 lesions. Interestingly, AFL lesions showed a weaker nuclear staining with less positive cells. In concordance to NOTCH2 expression, no differences between genotypes can be observed in the expression of HES1 (Figure 30).
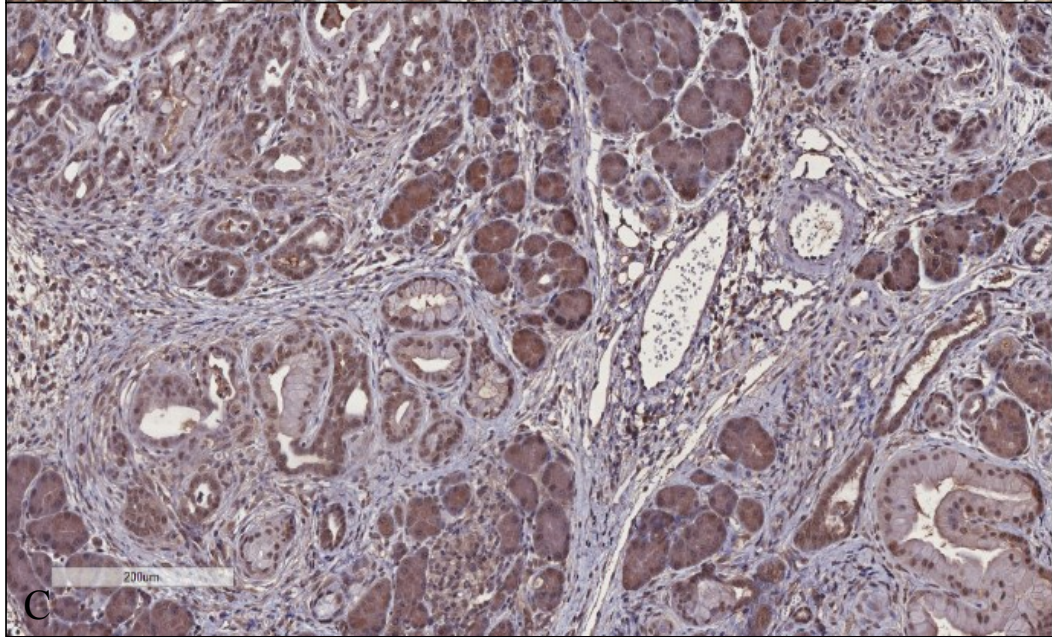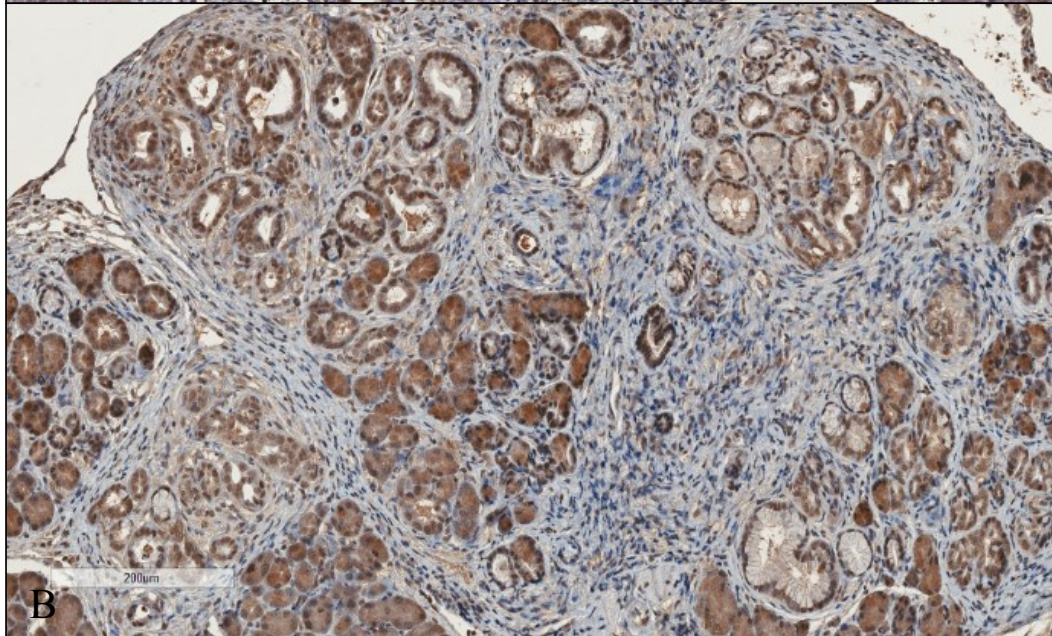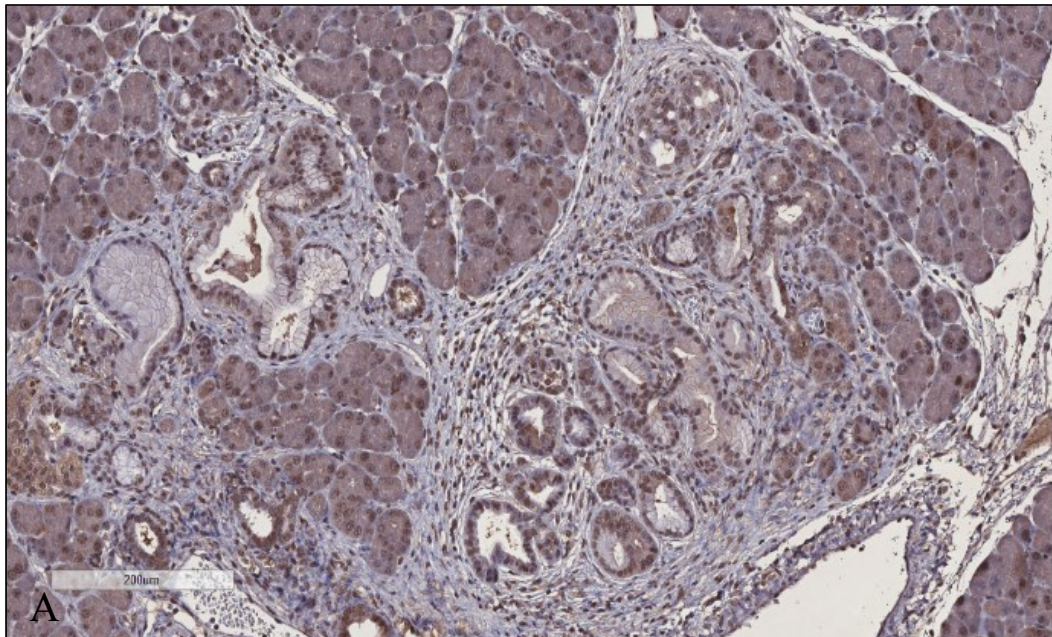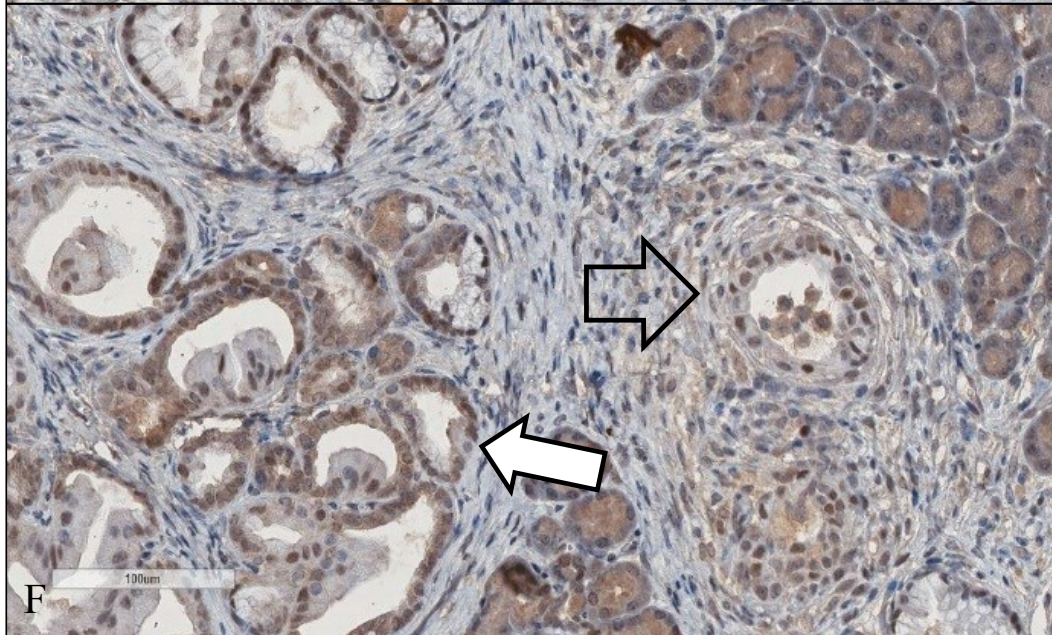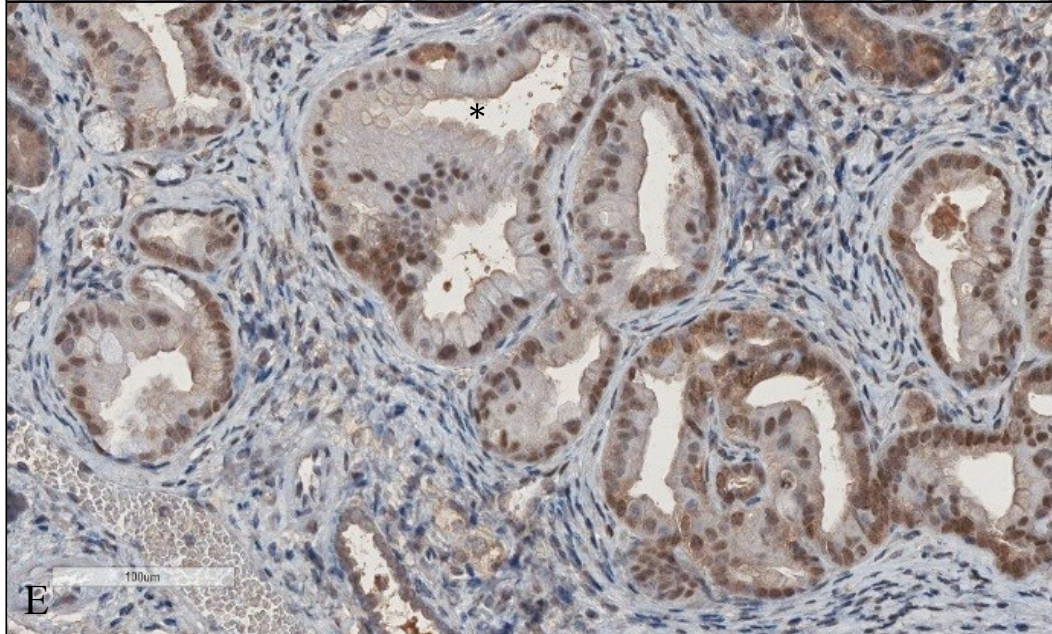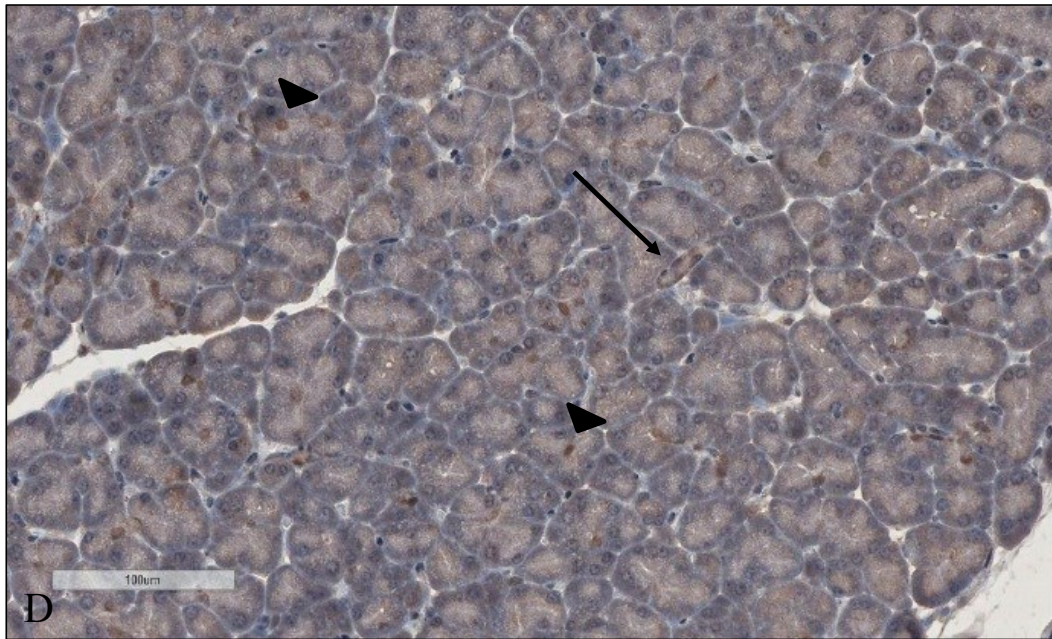
Figure 30: Nuclear HES1 expression of PanIN, ADM, AFL lesions and centroacinar cells in mice at the age of three months, A: *KC* mouse, 5x, B: *KC-TNChet*, 5x, C: *KC-TNCko,* 5x, D: *KC-TNCko* mouse with unaffected acinar parenchyma, arrows pointing to small, HES1 negative ducts, arrowheads indicating nuclear positivity in centroacinar cells, which served as internal positive control 20x, E: *KC-TNCko* mouse with nuclear HES1 positive PanIN-1 cells (asterisk), 20x, F: *KC-TNCko* mouse with HES1 positive nuclei in areas of ADM (white arrow) and weak nuclear positivity in AFL (black arrow), 20x.

V. DISCUSSION

1.   The PATHPATH project

This project was conducted since several studies revealed a great need of trained researchers in the area of comparative pathology (Barthold and others 2007, Cardiff and others 2008, Sundberg and others 2012). The great interest in the training course underscores the need for a training that educates specialists in histopathology of animal models as well as in human pathology. In addition to the development of the training course, the project aimed also to strengthen the collaboration at the European level in the field of disease model pathology, and thereby enhanced the quality of education and possibilities for student exchange.

A web-course offers the possibility to reach many students all over the world, although in this project the pilot course was restricted to a European level due to the rather tight time frame. Our training program has clearly shown that e-learning is an optimal setting for the distribution of knowledge over wide distances and to a large number of students at the same time. This is consistent with previously reported experiences (Ruf and others 2008). Interestingly, Ruf and others identified the lack of a prompt availability of other students and teachers as a disadvantage of the e-learning (Ruf and others 2008). However, this was not identified as a problem in the present project. By using live lectures, chat functions, discussion forums and availability of teachers per mail, a good level of interaction was achieved. Moreover, as students had the possibility to upload descriptions or questions about their own mouse models and get feed-back both from the teachers and from other students, a team-spirit was created. Many students used the possibility to ask questions per mail or discussed their problems in the chat function. Actually, this indirect interaction offers the students the chance to think over their questions and better reflect their problems. However, a rapid communication between teachers and students is necessary in order to promptly solve problems and constructive feed-back of the students' performance should be also delivered fast (McKimm and others 2003). A commitment of the teachers to be reachable and available at least at defined time points and, on the other side, the self-discipline of the students are fundamental elements for the success of a web-based learning environment. The traditional learning is usually pre-structured, but the web-based learning improves

the capability of self-organizing in students (Masic 2008). Web-based learning can be therefore offered as the solely learning platform to more experienced, post-graduate students, meanwhile it could integrate traditional learning methods for pre-graduate students (Masic 2008). Since only post-graduate students were included in our course, we can confirm the suitability of web-based learning for this type of audience.

An important issue in a web-based program is the need for broadband access and the associated costs (Parisky and Boulay 2013). Slow internet connection impairs e-learning, as long downloading-times are frustrating (Masic 2008). Many students claimed that they had only limited time to complete the course while working and time-consuming internet problems would have been a major problem. Costs are another negative factor, as all students need a computer that is able to process the images uploaded in the Webmicroscope. As technology is continuously and rapidly advancing in many countries, it seems likely that these problems can be overcome.

1.1.　　　Evaluation of the pilot course

As shown by the students' feed-back, the pilot course ran very successfully. The rating system of the different parts of the feedback forms was very helpful to assess specific aspects; the anonymous free text evaluation was also very helpful, since students freely wrote their subjective positive and negative opinions about the course.

Nevertheless, several issues were identified during the pilot course. An important aspect, which was underscored both by students and by teachers was the differences in education and training of the students. In particular, students with medical background need less guidance and support in histopathology than student with biochemical background. There is therefore the necessity to clearly define the scopes of the course, but also the pre-requisites to attend it. In order to achieve a larger audience, a possibility would be to split the course in two levels (gene-modified topics plus modeling and normal histology), depending on the education level and background of the students. At the beginning of the course, students had to fill in a questionnaire and write a motivation letter. The data gained from this approach offer a good possibility to structure the course more appropriately according to the background and training level of applicants.

Another general complaint was the time dedicated to each module. This aspect

certainly depends on the work pace of the single student, as well as on the individual knowledge. Nevertheless, more time should be considered in a regular course, as many students choose e-learning platforms so that they can attend them along with normal work.

1.2.   Discussion of tools used in the course

Several didactical tools have been used in the pilot course. A major advantage of this course was the use of the Webmicroscope, as students could examine slides using tools normally present in a standard microscope, which is by far more informative than a static picture in a book. Szymas and others could observe similar findings in five years of dental education with a Webmicroscope (Szymas and Lundin 2011). As discussed before, live lectures, chat functions, discussion forms and availability of teachers per mail were the tools to create an environment similar to traditional teaching. In this respect, two observations could be made: students did not like to discuss when they had to (that is, within the frame of pre-programmed discussion forums) and rather engaged in spontaneous chats to solve specific problems. For instance, they discussed the solutions of the gross morphology module, as some students were less experienced in this topic than others. Therefore, the possibility to discuss via a chat function is highly recommended in a web-based course. Furthermore, it is important that a teacher is leading the conversation in the background and is available when needed. Another interesting point was that students preferred voice-overed lectures, which were always available, to live-lectures, where they had the possibility to ask questions and get live answers through direct interaction with the teacher. The most likely explanation is that students preferred to organize the learning process according to their own schedule and have the possibility to reflect on questions, which were then asked via email. Therefore, in our experience, a live lecture is not a mandatory tool in a web-based training course.

1.3.   Outlook

The implementation of this course in the routine education of scientific researchers working with mice should be achieved. A possible setting would be the participation of other universities in order to create a European or even global network for training in disease modeling.

Such a training program can improve the quality of translational medicine and

achieve a more efficient and ethical use of experimental animals.

2.   PDAC and TNC

In the second part of the project I aimed at showing an example of practical application of the knowledge gained by attending the course in disease modeling. Here I focused on the role of TNC, a stromal glycoprotein, in the development of precursor lesions and subsequent desmoplasia in pancreatic carcinogenesis. TNC is upregulated in PanIN progression to invasive PDAC, indicating a central role of this protein in cancer development (Paron and others 2011). The deposition of extracellular TNC in *KC* mice was found to be similar to the previous described human situation (Esposito and others 2006).

2.1.   Influence of TNC on PDAC and its precursor lesions.

To assess the influence of an ablation of TNC on the development of precancerous lesions, TNC mutant mice on a C57BL6/N background were used. The focus of this study was set on young mice at the age of three months, as these mice show low-grade precursor lesions, which then progress to higher advanced lesions. As previously stated, the role of the stromal reaction in PDAC is still being controversial discussed (Gore and Korc 2014) and no data are available about the relevance of the stromal reaction at the preinvasive stage.

The higher percentage of architectural distortion and more pronounced development of PanIN lesions found in *KC-TNChet* and *KC-TNCko* mice compared to *KC* mice seem to suggest a protective role of TNC for $KRAS^{G12D}$-targeted epithelial cells. The known interactions between TNC and epithelial cells via indirect pathways activation of transmembrane receptor proteins (e.g. integrins) or via the cytoskeleton (Brellier and Chiquet-Ehrismann 2012) could represent the basis for this function of TNC. In addition, this apparent tumor-preventing role of stromal TNC in early precursor lesions indicates that the stroma reaction itself cannot be seen only as tumor promoting, as suggested by others. For example, it has been recently shown that by knocking out the sonic hedgehog pathway in a mouse model of PDAC and thereby targeting the desmoplastic stroma, a higher rate of ADM areas and PanIN lesions is observed in Shh$^{fl/fl}$;Pdx1-Cre;Kras$^{LSL-G12D/+}$;p53$^{fl/+}$;Rosa26$^{LSL-YFP}$ (ShhPKCY) mice when compared to control animals (Rhim and others 2014). These results raise the question if one underestimates the several functions of the desmoplastic stromal components - seemingly not only in

tumor support but tumor prevention (Rhim and others 2014). Özdemir and others observed a similar phenomenon, as conditionally abrogated α-SMA induced comparable effects, favoring the hypothesis that the desmoplastic stroma protects against rather than accelerates PDAC development (Ozdemir and others 2014). Taken together, these results support the concept that the tumor stroma with its extracellular components might not only be the driver of tumorigenesis in PDAC, but it also seems to exert a different, tumor suppressive role under different conditions. One should consider a role of TNC on epithelial regeneration, in particular the regeneration of acinar cells, as these cells differentiate to a ductal phenotype upon injury (Houbracken and others 2011). The molecular mechanisms underlying the effects of TNC on regeneration of acinar cells do not seem to be related to the Notch- or Wnt-pathways according to our expression data, but this aspect needs more detailed molecular investigation. Interestingly, the function of TNC seems to differ in already developed cancer.

Paron and others could show that pancreatic cancer lines grown on a TNC substrate tend to proliferate and migrate more. This might play a role in the invasion and metastasis in patients (Paron and others 2011). PDAC was detected in only a subgroup of twelve months-old mice in this study. In this age group, 66.7 % of *KC-TNChet* and 66.0 %*KC-TNCko* mice developed invasive, metastatic PDAC, meanwhile in the KC (TNC wt) group only 33.3 % mice had invasive, metastatic PDAC. Interestingly, in many cancer types as prostate and breast, TNC expression is linked with a poor prognosis (Emoto and others 2001, Ioachim and others 2002). In breast cancer, TNC seems to promote metastasis development (Oskarsson and others 2011). On the other hand, it was shown that in gliomas TNC has a role in tumor initiation, but not in tumor progression (Midwood and others 2011), which is more in line with the results of this study. In PDAC, no correlation between expression levels of TNC and prognosis could be found (Juuti and others 2004). Therefore, TNC might protect epithelia during stress but exert different functions once the tumor is evolved. Another explanation for these contradicting findings might be that the functions of TNC are not only context-dependent but also organ-dependent. Finally, a down-regulation of TNC expression within advanced carcinomas may explain why TNC negative tumors have a worse prognosis in breast cancer and colorectal cancer (Chiquet-Ehrismann and others 2014).

TNC might influence proliferation, even though there are contradictory findings (Midwood and Orend 2009). Therefore, when comparing the proliferation rates of

cells in ADM areas, PanIN and AFL between *KC* and *KC-TNChet* and *KC-TNCko* mice it could be shown that an absence or reduction of TNC protein does not only influence the architectural distortion but also enhances proliferation activity in areas of ADM. The fact that PanIN-1 lesions did not show any difference in proliferation compared to *KC* mice might be due to the small amount of cells that proliferate in PanIN-1 lesions (Aichler and others 2012). A possible way by which TNC could induce proliferation in epithelial cells is through its known function as an anti-adhesive protein to promote wound healing in *Kras* challenged epithelial cells, herby exerting similar function as described in wound healing (Sible and others 1995). Adhesion modulation is a key feature to influence cell proliferation, migration and differentiation. More specifically, TNC is able to influence cell spreading and proliferation by interactions with fibronectin (Chiquet-Ehrismann and Tucker 2011). Moreover, large splice variants of TNC regulate the proliferation of for instance neural stem cells through the modulation of the expression level of epidermal growth factor (EGF) receptor (Brellier and Chiquet-Ehrismann 2012).

TNC might influence apoptosis, even though the mechanisms are unclear (Midwood and Orend 2009). Further, apoptosis is an important feature in PDAC (Ruckert and others 2010). Therefore, the influence of absent TNC on apoptosis in early precursor lesions of PDAC was investigated. The small amount of apoptotic cells found here is in accordance with previously reported data in a mouse model of pancreatic β-cell carcinogenesis with a TNC ablation compared to the TNC wild-type model. Interestingly, the TNC overexpressing model exhibited less apoptotic cells (Saupe and others 2013). This underlines the several and ambiguous functions of this protein and that a deregulated expression of TNC might influence tumor cell survival.

As for apoptosis, no significant difference could be seen concerning the expression of p16, which is consistent with the complexity of mechanisms regulating the expression of this protein. All together these data show that the complex functions of TNC are still not completely understood and future work is needed to highlight the several function of this highly preserved protein (Chiquet-Ehrismann and others 1986, Matei and others 2011).

In TNC knockout mice, TNC is ablated in the complete organism and it is likely that other proteins are differentially regulated to compensate for the loss of TNC as for instance other members of the TN family (Chiquet-Ehrismann and Tucker

2011). An organ-specific ablation of TNC in the pancreas would give further insights in the role of TNC in pancreatic regeneration and, by crossing with PDAC-mouse models, in pancreatic carcinogenesis. Furthermore, mouse models with a complete abrogation of the TN family or an overexpression of different splice variants of TNC could further help to clarify these points.

3.   The PDAC project as a practical application of the course

After the successful completion of the web-based training course, students should have the basic knowledge to perform their own experiments with laboratory animals. To test this, this work serves as a test run for a student finishing the course and performing own mouse experiments afterwards. Together with the feedback collected from the students, this test system may serve as a quality control of the course. Several aspects learned during the preparation of the course could be used in the mouse experiments. For example, the C57BL6N background was chosen to generate the triple mutant animals, as this strains has no reported background lesions in the unchallenged pancreas and it is known for its secure expression of many mutations and exhibits a low spontaneous tumor incidence (Serpi and others 2013). Furthermore, knowledge of necropsy and sampling techniques and of murine pancreatic histology was extremely useful for detection of early changes in pancreatic parenchyma. On the other side, the course was focused on basic aspects and detailed histopathological examination and immunohistochemical characterization of the specific model was achieved by working with the supervisor. Sundberg and others underscored that the training of a researcher investigating histopathological changes should be beyond the basics offered by this kind of courses and that it is very important to find a mentor (Sundberg and others 2012).

VI.   SUMMARY

Development of a training program for disease modeling and its practical application: morphological characterization of a genetically engineered mouse model for pancreatic cancer

Animal models of human disease are increasingly used from basic science to preclinical drug development. This implicates a clear need for experts in histopathology of mouse models for human diseases and of specific programs to train these experts. The aim of this project was to develop an international, web-based disease model training program for students with a higher university degree. Already existing national training programs from a consortium consisting of experts from Finland, Germany and Scotland were merged and included specialist in pedagogy, human and veterinary pathology, biochemistry and mouse models of human disease.

The course comprised of a wide range of spontaneous background lesions in mouse strains (e.g. 129P2OlaHsd or C57BL6J), their gender and age differences, and physiological correlations. Similarities as well as differences with human pathology were highlighted. Moreover, the course included examples of basic lesions like cell adaptation, cell injury and cell death to the presentation of mouse models of human disease like the ductal adenocarcinoma of the pancreas (PDAC). By hosting a Pilot Course in spring 2013, the program was tested and feedback from student had been collected. Comparison of natural science students and medical students revealed a need for a tailored program depending on the basic education of the students.

Based on this training program, a phenotyping of a mouse model of PDAC was performed using immunohistochemistry and morphometric analysis. This analysis was also used as a test run to evaluate the web-based training program. Tumor-stroma interactions in PDAC, which is a very lethal disease, plays a key role and contributes to the highly aggressive nature of this cancer type. Tenascin-C (TNC), a protein of the extracellular matrix (EMC), is already overexpressed surrounding precursor lesions of PDAC. To investigate the impact of TNC on precursor lesions of PDAC and PDAC development *in vivo*, *LSL-KRAS*$^{G12D/+}$*;Ptf1a*$^{+/Cre(ex1)}$*;TNC*$^{-/-}$ (*KC-TNCko*) and *LSL-KRAS*$^{G12D/+}$*;Ptf1a*$^{+/Cre(ex1)}$*; TNC*$^{+/-}$ (*KC-TNChet*) mice where compared to *LSL-KRAS*$^{G12D/+}$*;Ptf1a*$^{+/Cre(ex1)}$ (*KC*) mice at the age groups 1, 2, 3 6, 9, 12 and 15 months. An earlier architectural distortion of pancreatic tissue

with fibrosis and inflammation was found in the *KC-TNCko* and *KC-TNChet* mice. To investigate the impact of TNC on precursor lesions, the focus of the investigation was set on young animals at the age of three months. The phenotype of precursor lesions and carcinomas were not influenced by the absence of TNC, but a higher frequency of PanIN lesions and carcinomas could be observed in *KC-TNCko* and *KC-TNChet* mice. Moreover, proliferation was elevated in *KC-TNChet* and *KC-TNCko* animals in areas of acinar-ductal metaplasia; meanwhile no differences in apoptosis could be detected between the genotypes. These results implicate that of TNC might influence tumors cells only in later stages; meanwhile in early carcinogenesis it might be tempting to suspect an influence of TNC on epithelial regeneration.

VII.   Zusammenfassung

Entwicklung eines Trainingsprogrammes für Tiermodellpathologie und dessen praktische Anwendung: morphologische Charakterisierung eines genetisch veränderten Mausmodelles des Pankreaskarzinoms

Da Tiermodelle zur Darstellung humaner Erkrankungen zunehmend sowohl in der Grundlagenforschung als auch in der präklinischen Medikamentenentwicklung verwendet werden, resultiert daraus ein klarer Bedarf an Experten, welche speziell ausgebildet sind, um pathophysiologische Veränderungen dieser Tiermodelle zu untersuchen. Ziel dieses Projekts war es, eine internationale, web-basierte Tiermodellplattform für das Pathologietraining für Studenten mit höherem Studienabschluss zu entwickeln. Hierzu wurden die nationalen und internationalen Trainingsprogramme der verschiedenen Teilnehmer des Konsortiums verbunden. Das Konsortium besteht aus Experten aus Finnland, Deutschland und Schottland mit Expertise in Pädagogik, humaner und Tierpathologie, Biochemie und Tiermodellen für humane Erkrankungen.

Das Kursprogramm besteht zum einem aus einer großen Auswahl von spontanen Hintergrundläsionen, wie sie in bestimmten Mauslinien (z.B. 129P2OlaHsd oder C57BL6J) häufiger vorkommen, deren geschlechter- sowie altersbedingten Unterschiede, physiologische Zusammenhänge sowie Unterschiede zum Mensch. Zudem beinhaltet der Kurs Beispiele für grundlegende pathologische Läsionen wie Zellanpassungsreaktionen, Zellschäden und Zelltod. Des Weiteren erfolgt eine Präsentation von Mausmodellen und den zugehörigen humanen Erkrankungen wie dem duktalen Adenokarzinom des Pankreas (PDAC). Das Programm wurde durch einen im Frühjahr 2013 durchgeführten Pilot Course getestet, sowie der Feedback der Studenten gesammelt. Die Studenten äußerten sich sehr zufrieden über den Kurs sowie den Kursinhalt. Ein Vergleich von naturwissenschaftlichen und medizinischen Studenten ergab, dass das Programm auf die jeweilige Grundausbildung des Studenten zugeschnitten werden muss.

Basierend auf diesem Kurs erfolgte eine tiefgehende immunhistochemische und morphometrische Phänotypisierung eines Mausmodells für das duktale Pankreaskarzinom. Diese Charakterisierung wurde zudem auch als ein Testlauf zur Kontrolle des web-basierten Trainingsprogrammes genützt. Im Pankreaskarzinom,

welches immer noch eine tödlich verlaufende Krankheit darstellt, spielen Interaktionen zwischen Tumorzellen und stromalen Zellen eine Schlüsselrolle und tragen somit zu der höchst aggressiven Natur dieses Tumors bei. Tenascin-C (TNC), ein Glykoprotein der extrazellulären Matrix, ist bereits im Stroma, welches Vorläuferläsionen das Pankreaskarzinoms umgibt, exprimiert.

Um die Rolle von TNC auf die Vorläufer und die Entstehung des Pankreaskarzinoms in *vivo* zu untersuchen, wurden *LSL-KRAS$^{G12D/+}$;Ptf1a$^{+/Cre(ex1)}$;TNC$^{-/-}$* (*KC-TNCko*) und *LSL-KRAS$^{G12D/+}$;Ptf1a$^{+/Cre(ex1)}$;TNC$^{+/-}$* (*KC-TNChet*) Mäuse mit *LSL-KRAS$^{G12D/+}$;Ptf1a$^{+/Cre(ex1)}$* (*KC*) Mäusen in den Altersgruppen 1, 2, 3, 6, 9, 12 und 15 Monaten verglichen.

Hierbei konnte ein schnellerer Umbau des Pankreasgewebes mit Fibrose und Entzündung in den *KC-TNCko* und *KC-TNChet* Mäusen festgestellt werden. Um die Rolle von TNC auf die Vorläuferläsionen des Pankreaskarzinoms zu untersuchen, wurde der Fokus auf junge Tiere im Alter von drei Monaten gelegt. Der Phänotyp der Vorläuferläsionen und Karzinome wurde nicht durch die Abwesenheit von TNC beeinflusst, allerdings konnte eine erhöhte Anzahl von PanIN und Karzinomen in *KC-TNCko* und *KC-TNChet* Mäusen beobachtet werden. Zudem wurde eine erhöhte Proliferation in *KC-TNCko* und *KC-TNChet* Mäusen in Arealen mit azinär-duktaler Metaplasie gefunden, allerdings ergaben sich keine Unterschiede in der Anzahl der Apoptosen zwischen den verschiedenen Genotypen.

Diese Ergebnisse implizieren, dass TNC die Tumorzellen erst in späteren Stadien beeinflusst, in der frühen Karzinogenese des Pankreaskarzinoms kann jedoch ein Einfluss von TNC auf die epitheliale Regeneration angenommen werden.

VIII. LITERATUR

Aguirre, A. J., Bardeesy, N., Sinha, M., Lopez, L., Tuveson, D. A., Horner, J., Redston, M. S. & DePinho, R. A. (2003) Activated Kras and Ink4a/Arf deficiency cooperate to produce metastatic pancreatic ductal adenocarcinoma. *Genes Dev* **17**, 3112-3126

Aichler, M., Seiler, C., Tost, M., Siveke, J., Mazur, P. K., Da Silva-Buttkus, P., Bartsch, D. K., Langer, P., Chiblak, S., Durr, A., Hofler, H., Kloppel, G., Muller-Decker, K., Brielmeier, M. & Esposito, I. (2012) Origin of pancreatic ductal adenocarcinoma from atypical flat lesions: a comparative study in transgenic mice and human tissues. *J Pathol* **226**, 723-734

Almoguera, C., Shibata, D., Forrester, K., Martin, J., Arnheim, N. & Perucho, M. (1988) Most human carcinomas of the exocrine pancreas contain mutant c-K-ras genes. *Cell* **53**, 549-554

Alsamarrai, A., Das, S. L., Windsor, J. A. & Petrov, M. S. (2014) Factors That Affect Risk for Pancreatic Disease in the General Population: a Systematic Review and Meta-analysis of Prospective Cohort Studies. *Clin Gastroenterol Hepatol*

Bardeesy, N., Aguirre, A. J., Chu, G. C., Cheng, K. H., Lopez, L. V., Hezel, A. F., Feng, B., Brennan, C., Weissleder, R., Mahmood, U., Hanahan, D., Redston, M. S., Chin, L. & Depinho, R. A. (2006) Both p16(Ink4a) and the p19(Arf)-p53 pathway constrain progression of pancreatic adenocarcinoma in the mouse. *Proc Natl Acad Sci U S A* **103**, 5947-5952

Baron, M., Main, A. L., Driscoll, P. C., Mardon, H. J., Boyd, J. & Campbell, I. D. (1992) 1H NMR assignment and secondary structure of the cell adhesion type III module of fibronectin. *Biochemistry* **31**, 2068-2073

Barthold, S. W., Borowsky, A. D., Brayton, C., Bronson, R., Cardiff, R. D., Griffey, S. M., Ince, T. A., Nikitin, A. Y., Sundberg, J., Valli, V. E. & Ward, J. M. (2007) From whence will they come? - A perspective on the acute shortage of pathologists

in biomedical research. *J Vet Diagn Invest* **19**, 455-456

Bayne, L. J., Beatty, G. L., Jhala, N., Clark, C. E., Rhim, A. D., Stanger, B. Z. & Vonderheide, R. H. (2012) Tumor-derived granulocyte-macrophage colony-stimulating factor regulates myeloid inflammation and T cell immunity in pancreatic cancer. *Cancer Cell* **21**, 822-835

Biankin, A. V., Waddell, N., Kassahn, K. S., Gingras, M. C., Muthuswamy, L. B., Johns, A. L., Miller, D. K., Wilson, P. J., Patch, A. M., Wu, J., Chang, D. K., Cowley, M. J., Gardiner, B. B., Song, S., Harliwong, I., Idrisoglu, S., Nourse, C., Nourbakhsh, E., Manning, S., Wani, S., Gongora, M., Pajic, M., Scarlett, C. J., Gill, A. J., Pinho, A. V., Rooman, I., Anderson, M., Holmes, O., Leonard, C., Taylor, D., Wood, S., Xu, Q., Nones, K., Fink, J. L., Christ, A., Bruxner, T., Cloonan, N., Kolle, G., Newell, F., Pinese, M., Mead, R. S., Humphris, J. L., Kaplan, W., Jones, M. D., Colvin, E. K., Nagrial, A. M., Humphrey, E. S., Chou, A., Chin, V. T., Chantrill, L. A., Mawson, A., Samra, J. S., Kench, J. G., Lovell, J. A., Daly, R. J., Merrett, N. D., Toon, C., Epari, K., Nguyen, N. Q., Barbour, A., Zeps, N., Australian Pancreatic Cancer Genome, I., Kakkar, N., Zhao, F., Wu, Y. Q., Wang, M., Muzny, D. M., Fisher, W. E., Brunicardi, F. C., Hodges, S. E., Reid, J. G., Drummond, J., Chang, K., Han, Y., Lewis, L. R., Dinh, H., Buhay, C. J., Beck, T., Timms, L., Sam, M., Begley, K., Brown, A., Pai, D., Panchal, A., Buchner, N., De Borja, R., Denroche, R. E., Yung, C. K., Serra, S., Onetto, N., Mukhopadhyay, D., Tsao, M. S., Shaw, P. A., Petersen, G. M., Gallinger, S., Hruban, R. H., Maitra, A., Iacobuzio-Donahue, C. A., Schulick, R. D., Wolfgang, C. L., Morgan, R. A., Lawlor, R. T., Capelli, P., Corbo, V., Scardoni, M., Tortora, G., Tempero, M. A., Mann, K. M., Jenkins, N. A., Perez-Mancera, P. A., Adams, D. J., Largaespada, D. A., Wessels, L. F., Rust, A. G., Stein, L. D., Tuveson, D. A., Copeland, N. G., Musgrove, E. A., Scarpa, A., Eshleman, J. R., Hudson, T. J., Sutherland, R. L., Wheeler, D. A., Pearson, J. V., McPherson, J. D., Gibbs, R. A. & Grimmond, S. M. (2012) Pancreatic cancer genomes reveal aberrations in axon guidance pathway genes. *Nature* **491**, 399-405

Bilimoria, K. Y., Bentrem, D. J., Ko, C. Y., Ritchey, J., Stewart, A. K., Winchester, D. P. & Talamonti, M. S. (2007) Validation of the 6th edition AJCC Pancreatic

Cancer Staging System: report from the National Cancer Database. *Cancer* **110**, 738-744

Bockman, D. E. (1997) Morphology of the exocrine pancreas related to pancreatitis. *Microsc Res Tech* **37**, 509-519

Boeker, M. & Klar, R. (2006) [E-learning in the education and training of physicians. Methods, results, evaluation]. *Bundesgesundheitsblatt Gesundheitsforschung Gesundheitsschutz* **49**, 405-411

Bolon, B., Couto, S., Fiette, L. & Perle, K. L. (2012) Internet and print resources to facilitate pathology analysis when phenotyping genetically engineered rodents. *Vet Pathol* **49**, 224-235

Borchers, M., Tipold, A., Pfarrer, C., Fischer, M. R. & Ehlers, J. P. (2010) [Acceptance of case-based, interactive e-learning in veterinary medicine on the example of the CASUS system]. *Tierarztl Prax Ausg K Kleintiere Heimtiere* **38**, 379-388

Borsi, L., Allemanni, G., Gaggero, B. & Zardi, L. (1996) Extracellular pH controls pre-mRNA alternative splicing of tenascin-C in normal, but not in malignantly transformed, cells. *Int J Cancer* **66**, 632-635

Bosman, F. T., Carneiro, F., Hruban, R.H., Theise, N.D. (2010) WHO Classification of Tumours of the Digestive System, Fourth Edition

Bouley, D., Meyerholz, D., Sellers, R., Boyd, K. & La Perle, K. (2009) Where's the mouse pathology training? *Vet Pathol* **46**, 1245-1247

Bourdon, M. A., Wikstrand, C. J., Furthmayr, H., Matthews, T. J. & Bigner, D. D. (1983) Human glioma-mesenchymal extracellular matrix antigen defined by monoclonal antibody. *Cancer Res* **43**, 2796-2805

Brellier, F. & Chiquet-Ehrismann, R. (2012) How do tenascins influence the birth and life of a malignant cell? *J Cell Mol Med* **16**, 32-40

Bussieres, J. F., Metras, M. E. & Leclerc, G. (2012) Use of Moodle, ExamSoft, and Twitter in a first-year pharmacy course. *Am J Pharm Educ* **76**, 94

Bustad, L. K., Gorham, J. R., Hegreberg, G. A. & Padgett, G. A. (1976) Comparative medicine: progress and prospects. *J Am Vet Med Assoc* **169**, 90-105

Capella, G., Farre, L., Villanueva, A., Reyes, G., Garcia, C., Tarafa, G. & Lluis, F. (1999) Orthotopic models of human pancreatic cancer. *Ann N Y Acad Sci* **880**, 103-109

Cardiff, R. D. (2009) How to phenotype a mouse. *Dis Model Mech* **2**, 317-321

Cardiff, R. D., Ward, J. M. & Barthold, S. W. (2008) 'One medicine---one pathology': are veterinary and human pathology prepared? *Lab Invest* **88**, 18-26

Carr, P. A., Erickson, H. P. & Palmer, A. G., 3rd (1997) Backbone dynamics of homologous fibronectin type III cell adhesion domains from fibronectin and tenascin. *Structure* **5**, 949-959

Chiquet-Ehrismann, R. & Chiquet, M. (2003) Tenascins: regulation and putative functions during pathological stress. *J Pathol* **200**, 488-499

Chiquet-Ehrismann, R., Hagios, C. & Schenk, S. (1995) The complexity in regulating the expression of tenascins. *Bioessays* **17**, 873-878

Chiquet-Ehrismann, R., Mackie, E. J., Pearson, C. A. & Sakakura, T. (1986) Tenascin: an extracellular matrix protein involved in tissue interactions during fetal development and oncogenesis. *Cell* **47**, 131-139

Chiquet-Ehrismann, R., Orend, G., Chiquet, M., Tucker, R. P. & Midwood, K. S.

(2014) Tenascins in stem cell niches. *Matrix Biol*

Chiquet-Ehrismann, R. & Tucker, R. P. (2011) Tenascins and the importance of adhesion modulation. *Cold Spring Harb Perspect Biol* **3**

Chiquet, M. & Fambrough, D. M. (1984) Chick myotendinous antigen. II. A novel extracellular glycoprotein complex consisting of large disulfide-linked subunits. *J Cell Biol* **98**, 1937-1946

Chung, C. Y. & Erickson, H. P. (1994) Cell surface annexin II is a high affinity receptor for the alternatively spliced segment of tenascin-C. *J Cell Biol* **126**, 539-548

Cifuentes-Diaz, C., Faille, L., Goudou, D., Schachner, M., Rieger, F. & Angaut-Petit, D. (2002) Abnormal reinnervation of skeletal muscle in a tenascin-C-deficient mouse. *J Neurosci Res* **67**, 93-99

Collins, M. A., Bednar, F., Zhang, Y., Brisset, J. C., Galban, S., Galban, C. J., Rakshit, S., Flannagan, K. S., Adsay, N. V. & Pasca di Magliano, M. (2012a) Oncogenic Kras is required for both the initiation and maintenance of pancreatic cancer in mice. *J Clin Invest* **122**, 639-653

Collins, M. A., Brisset, J. C., Zhang, Y., Bednar, F., Pierre, J., Heist, K. A., Galban, C. J., Galban, S. & di Magliano, M. P. (2012b) Metastatic pancreatic cancer is dependent on oncogenic Kras in mice. *PLoS One* **7**, e49707

Conway, J. F. & Parry, D. A. (1991) Three-stranded alpha-fibrous proteins: the heptad repeat and its implications for structure. *Int J Biol Macromol* **13**, 14-16

Crippa, S., Salvia, R., Warshaw, A. L., Dominguez, I., Bassi, C., Falconi, M., Thayer, S. P., Zamboni, G., Lauwers, G. Y., Mino-Kenudson, M., Capelli, P., Pederzoli, P. & Castillo, C. F. (2008) Mucinous cystic neoplasm of the pancreas is not an aggressive entity: lessons from 163 resected patients. *Ann Surg* **247**, 571-579

de Chevigny, A., Lemasson, M., Saghatelyan, A., Sibbe, M., Schachner, M. & Lledo, P. M. (2006) Delayed onset of odor detection in neonatal mice lacking tenascin-C. *Mol Cell Neurosci* **32**, 174-186

Dee, F. R. (2009) Virtual microscopy in pathology education. *Hum Pathol* **40**, 1112-1121

Dev, H., Barnett (2006) Computers in medical education. Springer New York, New York

Dictionaries, E. o. t. A. H. (2008) The American Heritage Medical Dictionary. Houghton Mifflin

DiMagno, E. P. (1999) Pancreatic cancer: clinical presentation, pitfalls and early clues. *Ann Oncol* **10 Suppl 4**, 140-142

Ding, Y., Cravero, J. D., Adrian, K. & Grippo, P. (2010) Modeling pancreatic cancer in vivo: from xenograft and carcinogen-induced systems to genetically engineered mice. *Pancreas* **39**, 283-292

Doello, K. (2014) A new pentachrome method for the simultaneous staining of collagen and sulfated mucopolysaccharides. *Yale J Biol Med* **87**, 341-347

El-Karef, A., Yoshida, T., Gabazza, E. C., Nishioka, T., Inada, H., Sakakura, T. & Imanaka-Yoshida, K. (2007) Deficiency of tenascin-C attenuates liver fibrosis in immune-mediated chronic hepatitis in mice. *J Pathol* **211**, 86-94

Emoto, K., Yamada, Y., Sawada, H., Fujimoto, H., Ueno, M., Takayama, T., Kamada, K., Naito, A., Hirao, S. & Nakajima, Y. (2001) Annexin II overexpression correlates with stromal tenascin-C overexpression: a prognostic marker in colorectal carcinoma. *Cancer* **92**, 1419-1426

Erickson, H. P. & Inglesias, J. L. (1984) A six-armed oligomer isolated from cell

surface fibronectin preparations. *Nature* **311**, 267-269

Esposito, I., Penzel, R., Chaib-Harrireche, M., Barcena, U., Bergmann, F., Riedl, S., Kayed, H., Giese, N., Kleeff, J., Friess, H. & Schirmacher, P. (2006) Tenascin C and annexin II expression in the process of pancreatic carcinogenesis. *J Pathol* **208**, 673-685

Fickert, P., Zollner, G., Fuchsbichler, A., Stumptner, C., Weiglein, A. H., Lammert, F., Marschall, H. U., Tsybrovskyy, O., Zatloukal, K., Denk, H. & Trauner, M. (2002) Ursodeoxycholic acid aggravates bile infarcts in bile duct-ligated and Mdr2 knockout mice via disruption of cholangioles. *Gastroenterology* **123**, 1238-1251

Fischer, D., Brown-Ludi, M., Schulthess, T. & Chiquet-Ehrismann, R. (1997) Concerted action of tenascin-C domains in cell adhesion, anti-adhesion and promotion of neurite outgrowth. *J Cell Sci* **110 (Pt 13)**, 1513-1522

Forsberg, E., Hirsch, E., Frohlich, L., Meyer, M., Ekblom, P., Aszodi, A., Werner, S. & Fassler, R. (1996) Skin wounds and severed nerves heal normally in mice lacking tenascin-C. *Proc Natl Acad Sci U S A* **93**, 6594-6599

Fox, J. G. (1985) Laboratory animal medicine. Changes and challenges. *Cornell Vet* **75**, 159-170

Fu, L., Pelicano, H., Liu, J., Huang, P. & Lee, C. (2002) The circadian gene Period2 plays an important role in tumor suppression and DNA damage response in vivo. *Cell* **111**, 41-50

Fukamauchi, F., Mataga, N., Wang, Y. J., Sato, S., Youshiki, A. & Kusakabe, M. (1996) Abnormal behavior and neurotransmissions of tenascin gene knockout mouse. *Biochem Biophys Res Commun* **221**, 151-156

Furukawa, T., Hatori, T., Fujita, I., Yamamoto, M., Kobayashi, M., Ohike, N., Morohoshi, T., Egawa, S., Unno, M., Takao, S., Osako, M., Yonezawa, S., Mino-

Kenudson, M., Lauwers, G. Y., Yamaguchi, H., Ban, S. & Shimizu, M. (2011) Prognostic relevance of morphological types of intraductal papillary mucinous neoplasms of the pancreas. *Gut* **60**, 509-516

Furukawa, T., Kloppel, G., Volkan Adsay, N., Albores-Saavedra, J., Fukushima, N., Horii, A., Hruban, R. H., Kato, Y., Klimstra, D. S., Longnecker, D. S., Luttges, J., Offerhaus, G. J., Shimizu, M., Sunamura, M., Suriawinata, A., Takaori, K. & Yonezawa, S. (2005) Classification of types of intraductal papillary-mucinous neoplasm of the pancreas: a consensus study. *Virchows Arch* **447**, 794-799

Garcion, E., Halilagic, A., Faissner, A. & ffrench-Constant, C. (2004) Generation of an environmental niche for neural stem cell development by the extracellular matrix molecule tenascin C. *Development* **131**, 3423-3432

Garwood, J., Garcion, E., Dobbertin, A., Heck, N., Calco, V., ffrench-Constant, C. & Faissner, A. (2004) The extracellular matrix glycoprotein Tenascin-C is expressed by oligodendrocyte precursor cells and required for the regulation of maturation rate, survival and responsiveness to platelet-derived growth factor. *Eur J Neurosci* **20**, 2524-2540

Gay, W. I. (1967) Comparative medicine. *Science* **158**, 1220-1237

Gong, X. G., Lv, Y. F., Li, X. Q., Xu, F. G. & Ma, Q. Y. (2010) Gemcitabine resistance induced by interaction between alternatively spliced segment of tenascin-C and annexin A2 in pancreatic cancer cells. *Biol Pharm Bull* **33**, 1261-1267

Gore, J. & Korc, M. (2014) Pancreatic cancer stroma: friend or foe? *Cancer Cell* **25**, 711-712

Grumet, M., Hoffman, S., Crossin, K. L. & Edelman, G. M. (1985) Cytotactin, an extracellular matrix protein of neural and non-neural tissues that mediates glia-neuron interaction. *Proc Natl Acad Sci U S A* **82**, 8075-8079

Guerra, C., Schuhmacher, A. J., Canamero, M., Grippo, P. J., Verdaguer, L., Perez-Gallego, L., Dubus, P., Sandgren, E. P. & Barbacid, M. (2007) Chronic pancreatitis is essential for induction of pancreatic ductal adenocarcinoma by K-Ras oncogenes in adult mice. *Cancer Cell* **11**, 291-302

Hamilton, P. W., Wang, Y. & McCullough, S. J. (2012) Virtual microscopy and digital pathology in training and education. *APMIS* **120**, 305-315

Haneder, S., J.C. Patterson-Kane, C.G. Lamm, T. Linnakylä, E. Kuittinen, L. Strauss, S. Mäkelä, M. Poutanen, M. Schlitter, Steiger, K. & Esposito, I. (2013) Development of an international web-based pathology trainng program in disease modeling. In: 97. Jahrestagung der Deutschen Gesellschaft für Pathologie e.V., 2013, Heidelberg

Haneder, S., Steiger, K., Schlitter, A., Pouttanen, M., Strauss, L., Kane-Patterson, J., T., L., Höfler, H. & Esposito, I. (2014) Entwicklung einer internationalen, webbasierten Lernplattform für Tiermodellpathologie. 57. JAHRESTAGUNG DER FACHGRUPPE "PATHOLOGIE", DVG. Fulda

Heinemann, V., Haas, M. & Boeck, S. (2012) Systemic treatment of advanced pancreatic cancer. *Cancer Treat Rev* **38**, 843-853

Hendaoui, I., Tucker, R. P., Zingg, D., Bichet, S., Schittny, J. & Chiquet-Ehrismann, R. (2014) Tenascin-C is required for normal Wnt/beta-catenin signaling in the whisker follicle stem cell niche. *Matrix Biol* **40**, 46-53

Hidalgo, M. (2010) Pancreatic cancer. *N Engl J Med* **362**, 1605-1617

Hingorani, S. R., Petricoin, E. F., Maitra, A., Rajapakse, V., King, C., Jacobetz, M. A., Ross, S., Conrads, T. P., Veenstra, T. D., Hitt, B. A., Kawaguchi, Y., Johann, D., Liotta, L. A., Crawford, H. C., Putt, M. E., Jacks, T., Wright, C. V., Hruban, R. H., Lowy, A. M. & Tuveson, D. A. (2003) Preinvasive and invasive ductal pancreatic cancer and its early detection in the mouse. *Cancer Cell* **4**, 437-450

Hingorani, S. R., Wang, L., Multani, A. S., Combs, C., Deramaudt, T. B., Hruban, R. H., Rustgi, A. K., Chang, S. & Tuveson, D. A. (2005) Trp53R172H and KrasG12D cooperate to promote chromosomal instability and widely metastatic pancreatic ductal adenocarcinoma in mice. *Cancer Cell* **7**, 469-483

Houbracken, I., de Waele, E., Lardon, J., Ling, Z., Heimberg, H., Rooman, I. & Bouwens, L. (2011) Lineage tracing evidence for transdifferentiation of acinar to duct cells and plasticity of human pancreas. *Gastroenterology* **141**, 731-741, 741 e731-734

Hruban, R. H., Adsay, N. V., Albores-Saavedra, J., Anver, M. R., Biankin, A. V., Boivin, G. P., Furth, E. E., Furukawa, T., Klein, A., Klimstra, D. S., Kloppel, G., Lauwers, G. Y., Longnecker, D. S., Luttges, J., Maitra, A., Offerhaus, G. J., Perez-Gallego, L., Redston, M. & Tuveson, D. A. (2006) Pathology of genetically engineered mouse models of pancreatic exocrine cancer: consensus report and recommendations. *Cancer Res* **66**, 95-106

Hruban, R. H., Adsay, N. V., Albores-Saavedra, J., Compton, C., Garrett, E. S., Goodman, S. N., Kern, S. E., Klimstra, D. S., Kloppel, G., Longnecker, D. S., Luttges, J. & Offerhaus, G. J. (2001) Pancreatic intraepithelial neoplasia: a new nomenclature and classification system for pancreatic duct lesions. *Am J Surg Pathol* **25**, 579-586

Hruban, R. H. & Fukushima, N. (2008) Cystic lesions of the pancreas. *Diagn Histopathol (Oxf)* **14**, 260-265

Hruban, R. H., Goggins, M., Parsons, J. & Kern, S. E. (2000) Progression model for pancreatic cancer. *Clin Cancer Res* **6**, 2969-2972

Hwang, R. F., Moore, T., Arumugam, T., Ramachandran, V., Amos, K. D., Rivera, A., Ji, B., Evans, D. B. & Logsdon, C. D. (2008) Cancer-associated stromal fibroblasts promote pancreatic tumor progression. *Cancer Res* **68**, 918-926

Ince, T. A., Ward, J. M., Valli, V. E., Sgroi, D., Nikitin, A. Y., Loda, M., Griffey,

S. M., Crum, C. P., Crawford, J. M., Bronson, R. T. & Cardiff, R. D. (2008) Do-it-yourself (DIY) pathology. *Nat Biotechnol* **26**, 978-979; discussion 979

Ioachim, E., Charchanti, A., Briasoulis, E., Karavasilis, V., Tsanou, H., Arvanitis, D. L., Agnantis, N. J. & Pavlidis, N. (2002) Immunohistochemical expression of extracellular matrix components tenascin, fibronectin, collagen type IV and laminin in breast cancer: their prognostic value and role in tumour invasion and progression. *Eur J Cancer* **38**, 2362-2370

Ishii, K., Imanaka-Yoshida, K., Yoshida, T. & Sugimura, Y. (2008) Role of stromal tenascin-C in mouse prostatic development and epithelial cell differentiation. *Dev Biol* **324**, 310-319

J.C. Patterson-Kane, C.G. Lamm, T. Linnakylä, E. Kuittinen, L. Strauss, S. Mäkelä, M. Poutanen, M. Schlitter, S. Haneder, K., Steiger & Esposito, I. (2013) An e-learning course in genetically engineered mouse model pathology: the european experience. ACVP and ACVCP 2013 concurrent annual meeting. Montreal

Jain, R., Fischer, S., Serra, S. & Chetty, R. (2010) The use of Cytokeratin 19 (CK19) immunohistochemistry in lesions of the pancreas, gastrointestinal tract, and liver. *Appl Immunohistochem Mol Morphol* **18**, 9-15

Jensen, J., Pedersen, E. E., Galante, P., Hald, J., Heller, R. S., Ishibashi, M., Kageyama, R., Guillemot, F., Serup, P. & Madsen, O. D. (2000) Control of endodermal endocrine development by Hes-1. *Nat Genet* **24**, 36-44

Jones, F. S., Hoffman, S., Cunningham, B. A. & Edelman, G. M. (1989) A detailed structural model of cytotactin: protein homologies, alternative RNA splicing, and binding regions. *Proc Natl Acad Sci U S A* **86**, 1905-1909

Jones, F. S. & Jones, P. L. (2000a) The tenascin family of ECM glycoproteins: structure, function, and regulation during embryonic development and tissue remodeling. *Dev Dyn* **218**, 235-259

Jones, P. L. & Jones, F. S. (2000b) Tenascin-C in development and disease: gene regulation and cell function. *Matrix Biol* **19**, 581-596

Juuti, A., Nordling, S., Louhimo, J., Lundin, J. & Haglund, C. (2004) Tenascin C expression is upregulated in pancreatic cancer and correlates with differentiation. *J Clin Pathol* **57**, 1151-1155

Kanda, M., Matthaei, H., Wu, J., Hong, S. M., Yu, J., Borges, M., Hruban, R. H., Maitra, A., Kinzler, K., Vogelstein, B. & Goggins, M. (2012) Presence of somatic mutations in most early-stage pancreatic intraepithelial neoplasia. *Gastroenterology* **142**, 730-733 e739

Katoh, D., Nagaharu, K., Shimojo, N., Hanamura, N., Yamashita, M., Kozuka, Y., Imanaka-Yoshida, K. & Yoshida, T. (2013) Binding of alphavbeta1 and alphavbeta6 integrins to tenascin-C induces epithelial-mesenchymal transition-like change of breast cancer cells. *Oncogenesis* **2**, e65

Kern, S., Hruban, R., Hollingsworth, M. A., Brand, R., Adrian, T. E., Jaffee, E. & Tempero, M. A. (2001) A white paper: the product of a pancreas cancer think tank. *Cancer Res* **61**, 4923-4932

Kerres, M. (2013) Mediendidaktik : Konzeption und Entwicklung mediengestützter Lernangebote. Oldenbourg

Kloppel, G., Detlefsen, S. & Feyerabend, B. (2004) Fibrosis of the pancreas: the initial tissue damage and the resulting pattern. *Virchows Arch* **445**, 1-8

Kojima, K., Vickers, S. M., Adsay, N. V., Jhala, N. C., Kim, H. G., Schoeb, T. R., Grizzle, W. E. & Klug, C. A. (2007) Inactivation of Smad4 accelerates Kras(G12D)-mediated pancreatic neoplasia. *Cancer Res* **67**, 8121-8130

Koorstra, J. B., Hustinx, S. R., Offerhaus, G. J. & Maitra, A. (2008) Pancreatic carcinogenesis. *Pancreatology* **8**, 110-125

Korc, M. (2007) Pancreatic cancer-associated stroma production. *Am J Surg* **194**, S84-86

Kruse, J., Keilhauer, G., Faissner, A., Timpl, R. & Schachner, M. (1985) The J1 glycoprotein--a novel nervous system cell adhesion molecule of the L2/HNK-1 family. *Nature* **316**, 146-148

Kuribayashi, K., Mayes, P. A. & El-Deiry, W. S. (2006) What are caspases 3 and 7 doing upstream of the mitochondria? *Cancer Biol Ther* **5**, 763-765

Linder, S., Blasjo, M., von Rosen, A., Parrado, C., Falkmer, U. G. & Falkmer, S. (2001) Pattern of distribution and prognostic value of angiogenesis in pancreatic duct carcinoma: a semiquantitative immunohistochemical study of 45 patients. *Pancreas* **22**, 240-247

Locker, G. Y., Hamilton, S., Harris, J., Jessup, J. M., Kemeny, N., Macdonald, J. S., Somerfield, M. R., Hayes, D. F., Bast, R. C., Jr. & Asco (2006) ASCO 2006 update of recommendations for the use of tumor markers in gastrointestinal cancer. *J Clin Oncol* **24**, 5313-5327

Mackie, E. J. (1997) Molecules in focus: tenascin-C. *Int J Biochem Cell Biol* **29**, 1133-1137

Maitra, A. & Hruban, R. H. (2008) Pancreatic cancer. *Annu Rev Pathol* **3**, 157-188

Malvezzi, M., Bertuccio, P., Levi, F., La Vecchia, C. & Negri, E. (2013) European cancer mortality predictions for the year 2013. *Ann Oncol* **24**, 792-800

Masic, I. (2008) E-learning as new method of medical education. *Acta Inform Med* **16**, 102-117

Matei, I., Ghajar, C. M. & Lyden, D. (2011) A TeNaCious foundation for the metastatic niche. *Cancer Cell* **20**, 139-141

Maxwell, S. & Mucklow, J. (2012) e-Learning initiatives to support prescribing. *Br J Clin Pharmacol* **74**, 621-631

McDonald, O. G., Maitra, A. & Hruban, R. H. (2012) Human correlates of provocative questions in pancreatic pathology. *Adv Anat Pathol* **19**, 351-362

McKimm, J., Jollie, C. & Cantillon, P. (2003) ABC of learning and teaching: Web based learning. *BMJ* **326**, 870-873

Midwood, K. S., Hussenet, T., Langlois, B. & Orend, G. (2011) Advances in tenascin-C biology. *Cell Mol Life Sci* **68**, 3175-3199

Midwood, K. S. & Orend, G. (2009) The role of tenascin-C in tissue injury and tumorigenesis. *J Cell Commun Signal* **3**, 287-310

Milev, P., Fischer, D., Haring, M., Schulthess, T., Margolis, R. K., Chiquet-Ehrismann, R. & Margolis, R. U. (1997) The fibrinogen-like globe of tenascin-C mediates its interactions with neurocan and phosphacan/protein-tyrosine phosphatase-zeta/beta. *J Biol Chem* **272**, 15501-15509

Miyamoto, Y., Maitra, A., Ghosh, B., Zechner, U., Argani, P., Iacobuzio-Donahue, C. A., Sriuranpong, V., Iso, T., Meszoely, I. M., Wolfe, M. S., Hruban, R. H., Ball, D. W., Schmid, R. M. & Leach, S. D. (2003) Notch mediates TGF alpha-induced changes in epithelial differentiation during pancreatic tumorigenesis. *Cancer Cell* **3**, 565-576

Mossbrugger, I., Hoelzlwimmer, G., Calzada-Wack, J. & Quintanilla-Martinez, L. (2007) Standardized morphological phenotyping of mouse models of human diseases within the German Mouse Clinic. *Verh Dtsch Ges Pathol* **91**, 98-103

Mouse Genome Sequencing, C., Waterston, R. H., Lindblad-Toh, K., Birney, E., Rogers, J., Abril, J. F., Agarwal, P., Agarwala, R., Ainscough, R., Alexandersson, M., An, P., Antonarakis, S. E., Attwood, J., Baertsch, R., Bailey, J., Barlow, K.,

Beck, S., Berry, E., Birren, B., Bloom, T., Bork, P., Botcherby, M., Bray, N., Brent, M. R., Brown, D. G., Brown, S. D., Bult, C., Burton, J., Butler, J., Campbell, R. D., Carninci, P., Cawley, S., Chiaromonte, F., Chinwalla, A. T., Church, D. M., Clamp, M., Clee, C., Collins, F. S., Cook, L. L., Copley, R. R., Coulson, A., Couronne, O., Cuff, J., Curwen, V., Cutts, T., Daly, M., David, R., Davies, J., Delehaunty, K. D., Deri, J., Dermitzakis, E. T., Dewey, C., Dickens, N. J., Diekhans, M., Dodge, S., Dubchak, I., Dunn, D. M., Eddy, S. R., Elnitski, L., Emes, R. D., Eswara, P., Eyras, E., Felsenfeld, A., Fewell, G. A., Flicek, P., Foley, K., Frankel, W. N., Fulton, L. A., Fulton, R. S., Furey, T. S., Gage, D., Gibbs, R. A., Glusman, G., Gnerre, S., Goldman, N., Goodstadt, L., Grafham, D., Graves, T. A., Green, E. D., Gregory, S., Guigo, R., Guyer, M., Hardison, R. C., Haussler, D., Hayashizaki, Y., Hillier, L. W., Hinrichs, A., Hlavina, W., Holzer, T., Hsu, F., Hua, A., Hubbard, T., Hunt, A., Jackson, I., Jaffe, D. B., Johnson, L. S., Jones, M., Jones, T. A., Joy, A., Kamal, M., Karlsson, E. K., Karolchik, D., Kasprzyk, A., Kawai, J., Keibler, E., Kells, C., Kent, W. J., Kirby, A., Kolbe, D. L., Korf, I., Kucherlapati, R. S., Kulbokas, E. J., Kulp, D., Landers, T., Leger, J. P., Leonard, S., Letunic, I., Levine, R., Li, J., Li, M., Lloyd, C., Lucas, S., Ma, B., Maglott, D. R., Mardis, E. R., Matthews, L., Mauceli, E., Mayer, J. H., McCarthy, M., McCombie, W. R., McLaren, S., McLay, K., McPherson, J. D., Meldrim, J., Meredith, B., Mesirov, J. P., Miller, W., Miner, T. L., Mongin, E., Montgomery, K. T., Morgan, M., Mott, R., Mullikin, J. C., Muzny, D. M., Nash, W. E., Nelson, J. O., Nhan, M. N., Nicol, R., Ning, Z., Nusbaum, C., O'Connor, M. J., Okazaki, Y., Oliver, K., Overton-Larty, E., Pachter, L., Parra, G., Pepin, K. H., Peterson, J., Pevzner, P., Plumb, R., Pohl, C. S., Poliakov, A., Ponce, T. C., Ponting, C. P., Potter, S., Quail, M., Reymond, A., Roe, B. A., Roskin, K. M., Rubin, E. M., Rust, A. G., Santos, R., Sapojnikov, V., Schultz, B., Schultz, J., Schwartz, M. S., Schwartz, S., Scott, C., Seaman, S., Searle, S., Sharpe, T., Sheridan, A., Shownkeen, R., Sims, S., Singer, J. B., Slater, G., Smit, A., Smith, D. R., Spencer, B., Stabenau, A., Stange-Thomann, N., Sugnet, C., Suyama, M., Tesler, G., Thompson, J., Torrents, D., Trevaskis, E., Tromp, J., Ucla, C., Ureta-Vidal, A., Vinson, J. P., Von Niederhausern, A. C., Wade, C. M., Wall, M., Weber, R. J., Weiss, R. B., Wendl, M. C., West, A. P., Wetterstrand, K., Wheeler, R., Whelan, S., Wierzbowski, J., Willey, D., Williams, S., Wilson, R. K., Winter, E., Worley, K. C., Wyman, D., Yang, S., Yang, S. P., Zdobnov, E. M., Zody, M. C. & Lander, E. S. (2002) Initial sequencing and comparative analysis of the mouse genome. *Nature* **420**, 520-562

Muller-Decker, K., Furstenberger, G., Annan, N., Kucher, D., Pohl-Arnold, A., Steinbauer, B., Esposito, I., Chiblak, S., Friess, H., Schirmacher, P. & Berger, I. (2006) Preinvasive duct-derived neoplasms in pancreas of keratin 5-promoter cyclooxygenase-2 transgenic mice. *Gastroenterology* **130**, 2165-2178

Nakao, N., Hiraiwa, N., Yoshiki, A., Ike, F. & Kusakabe, M. (1998) Tenascin-C promotes healing of Habu-snake venom-induced glomerulonephritis: studies in knockout congenic mice and in culture. *Am J Pathol* **152**, 1237-1245

Neesse, A., Michl, P., Frese, K. K., Feig, C., Cook, N., Jacobetz, M. A., Lolkema, M. P., Buchholz, M., Olive, K. P., Gress, T. M. & Tuveson, D. A. (2011) Stromal biology and therapy in pancreatic cancer. *Gut* **60**, 861-868

Nielsen, N. O. (1983) Comparative medicine. *Can Vet J* **24**, 269-277

Orend, G. (2005) Potential oncogenic action of tenascin-C in tumorigenesis. *Int J Biochem Cell Biol* **37**, 1066-1083

Orend, G. & Chiquet-Ehrismann, R. (2006) Tenascin-C induced signaling in cancer. *Cancer Lett* **244**, 143-163

Oskarsson, T., Acharyya, S., Zhang, X. H., Vanharanta, S., Tavazoie, S. F., Morris, P. G., Downey, R. J., Manova-Todorova, K., Brogi, E. & Massague, J. (2011) Breast cancer cells produce tenascin C as a metastatic niche component to colonize the lungs. *Nat Med* **17**, 867-874

Oskarsson, T. & Massague, J. (2012) Extracellular matrix players in metastatic niches. *EMBO J* **31**, 254-256

Ottenhof, N. A., de Wilde, R. F., Maitra, A., Hruban, R. H. & Offerhaus, G. J. (2011) Molecular characteristics of pancreatic ductal adenocarcinoma. *Patholog Res Int* **2011**, 620601

Ozdemir, B. C., Pentcheva-Hoang, T., Carstens, J. L., Zheng, X., Wu, C. C., Simpson, T. R., Laklai, H., Sugimoto, H., Kahlert, C., Novitskiy, S. V., De Jesus-Acosta, A., Sharma, P., Heidari, P., Mahmood, U., Chin, L., Moses, H. L., Weaver, V. M., Maitra, A., Allison, J. P., LeBleu, V. S. & Kalluri, R. (2014) Depletion of carcinoma-associated fibroblasts and fibrosis induces immunosuppression and accelerates pancreas cancer with reduced survival. *Cancer Cell* **25**, 719-734

Parisky, A. & Boulay, R. (2013) Designing and Developing Open Education Resources in Higher Education: A Molecular Biology Project. *Int J Technol Knowl Soc* **9**, 145-155

Paron, I., Berchtold, S., Voros, J., Shamarla, M., Erkan, M., Hofler, H. & Esposito, I. (2011) Tenascin-C enhances pancreatic cancer cell growth and motility and affects cell adhesion through activation of the integrin pathway. *PLoS One* **6**, e21684

Pas, J., Wyszko, E., Rolle, K., Rychlewski, L., Nowak, S., Zukiel, R. & Barciszewski, J. (2006) Analysis of structure and function of tenascin-C. *Int J Biochem Cell Biol* **38**, 1594-1602

Pathmanathan, N. & Balleine, R. L. (2013) Ki67 and proliferation in breast cancer. *J Clin Pathol* **66**, 512-516

Rader, K. A. (2004) Making Mice: Standardizing Animals for American Biomedical Research, 1900-1955. Princeton University Press

Rayess, H., Wang, M. B. & Srivatsan, E. S. (2012) Cellular senescence and tumor suppressor gene p16. *Int J Cancer* **130**, 1715-1725

Rhim, A. D., Oberstein, P. E., Thomas, D. H., Mirek, E. T., Palermo, C. F., Sastra, S. A., Dekleva, E. N., Saunders, T., Becerra, C. P., Tattersall, I. W., Westphalen, C. B., Kitajewski, J., Fernandez-Barrena, M. G., Fernandez-Zapico, M. E., Iacobuzio-Donahue, C., Olive, K. P. & Stanger, B. Z. (2014) Stromal elements act to restrain, rather than support, pancreatic ductal adenocarcinoma. *Cancer Cell* **25**,

735-747

Roberts, D. D. (2011) Emerging functions of matricellular proteins. *Cell Mol Life Sci* **68**, 3133-3136

Rocchi, M., Archidiacono, N., Romeo, G., Saginati, M. & Zardi, L. (1991) Assignment of the gene for human tenascin to the region q32-q34 of chromosome 9. *Hum Genet* **86**, 621-623

Rosenthal, N. & Brown, S. (2007) The mouse ascending: perspectives for human-disease models. *Nat Cell Biol* **9**, 993-999

Roth-Kleiner, M., Hirsch, E. & Schittny, J. C. (2004) Fetal lungs of tenascin-C-deficient mice grow well, but branch poorly in organ culture. *Am J Respir Cell Mol Biol* **30**, 360-366

Rozenblum, E., Schutte, M., Goggins, M., Hahn, S. A., Panzer, S., Zahurak, M., Goodman, S. N., Sohn, T. A., Hruban, R. H., Yeo, C. J. & Kern, S. E. (1997) Tumor-suppressive pathways in pancreatic carcinoma. *Cancer Res* **57**, 1731-1734

Ruckert, F., Dawelbait, G., Winter, C., Hartmann, A., Denz, A., Ammerpohl, O., Schroeder, M., Schackert, H. K., Sipos, B., Kloppel, G., Kalthoff, H., Saeger, H. D., Pilarsky, C. & Grutzmann, R. (2010) Examination of apoptosis signaling in pancreatic cancer by computational signal transduction analysis. *PLoS One* **5**, e12243

Ruf, D., Berner, M. M., Kriston, L. & Harter, M. (2008) [E-Learning--an important contribution to general medical training and continuing education?]. *Bundesgesundheitsblatt Gesundheitsforschung Gesundheitsschutz* **51**, 1061-1069

Ruifrok, A. C. & Johnston, D. A. (2001) Quantification of histochemical staining by color deconvolution. *Anal Quant Cytol Histol* **23**, 291-299

Saga, Y., Tsukamoto, T., Jing, N., Kusakabe, M. & Sakakura, T. (1991) Murine tenascin: cDNA cloning, structure and temporal expression of isoforms. *Gene* **104**, 177-185

Saga, Y., Yagi, T., Ikawa, Y., Sakakura, T. & Aizawa, S. (1992) Mice develop normally without tenascin. *Genes Dev* **6**, 1821-1831

Salter, S. M., Karia, A., Sanfilippo, F. M. & Clifford, R. M. (2014) Effectiveness of E-learning in pharmacy education. *Am J Pharm Educ* **78**, 83

Samuel, N. & Hudson, T. J. (2012) The molecular and cellular heterogeneity of pancreatic ductal adenocarcinoma. *Nat Rev Gastroenterol Hepatol* **9**, 77-87

Saupe, F., Schwenzer, A., Jia, Y., Gasser, I., Spenle, C., Langlois, B., Kammerer, M., Lefebvre, O., Hlushchuk, R., Rupp, T., Marko, M., van der Heyden, M., Cremel, G., Arnold, C., Klein, A., Simon-Assmann, P., Djonov, V., Neuville-Mechine, A., Esposito, I., Slotta-Huspenina, J., Janssen, K. P., de Wever, O., Christofori, G., Hussenet, T. & Orend, G. (2013) Tenascin-C downregulates wnt inhibitor dickkopf-1, promoting tumorigenesis in a neuroendocrine tumor model. *Cell Rep* **5**, 482-492

Schlitter, A. M. & Esposito, I. (2012) [Pathology and classification of intraductal papillary mucinous neoplasms of the pancreas]. *Chirurg* **83**, 110-115

Schmitz-Winnenthal, F. H., Escobedo, L. V., Beckhove, P., Schirrmacher, V., Bucur, M., Ziouta, Y., Volk, C., Schmied, B., Koch, M., Antolovic, D., Weitz, J., Buchler, M. W. & Z'Graggen, K. (2006) Specific immune recognition of pancreatic carcinoma by patient-derived CD4 and CD8 T cells and its improvement by interferon-gamma. *Int J Oncol* **28**, 1419-1428

Schutte, M., Hruban, R. H., Geradts, J., Maynard, R., Hilgers, W., Rabindran, S. K., Moskaluk, C. A., Hahn, S. A., Schwarte-Waldhoff, I., Schmiegel, W., Baylin, S. B., Kern, S. E. & Herman, J. G. (1997) Abrogation of the Rb/p16 tumor-suppressive pathway in virtually all pancreatic carcinomas. *Cancer Res* **57**, 3126-

3130

Segen, J. C. (2005) Concise Dictionary of Modern Medicine. McGraw-Hill Professional Publishing p765

Sellers, R. S. & Ward, J. M. (2012) Toward a better understanding of mouse models of disease. *Vet Pathol* **49**, 4

Seluakumaran, K., Jusof, F. F., Ismail, R. & Husain, R. (2011) Integrating an open-source course management system (Moodle) into the teaching of a first-year medical physiology course: a case study. *Adv Physiol Educ* **35**, 369-377

Serpi, R., Klein-Rodewald, T., Calzada-Wack, J., Neff, F., Schuster, T., Gailus-Durner, V., Fuchs, H., Poutanen, M., Hrabre de Angelis, M. & Esposito, I. (2013) Inbred wild type mouse strains have distinct spontaneous morphological phenotypes. *Histol Histopathol* **28**, 79-88

Sible, J. C., Rettig, W. J., Eriksson, E., Smith, S. P. & Oliver, N. (1995) Gene expression of tenascin is altered in normal scars and keloids. *Wound Repair Regen* **3**, 37-48

Siegel, R., Naishadham, D. & Jemal, A. (2012) Cancer statistics, 2012. *CA Cancer J Clin* **62**, 10-29

Siegel, R., Naishadham, D. & Jemal, A. (2013) Cancer statistics, 2013. *CA Cancer J Clin* **63**, 11-30

Simmons, D. (2008) The use of animal models in studying genetic disease: transgenesis and induced mutation. *Nature Education* **1(1):70**

Siveke, J. T., Einwachter, H., Sipos, B., Lubeseder-Martellato, C., Kloppel, G. & Schmid, R. M. (2007) Concomitant pancreatic activation of Kras(G12D) and Tgfa results in cystic papillary neoplasms reminiscent of human IPMN. *Cancer Cell* **12**,

266-279

Strauss, L., J.C. Patterson-Kane, C.G. Lamm, T. Linnakylä, E. Kuittinen, S. Mäkelä, M. Poutanen, M. Schlitter, S. Haneder, Steiger, K. & Esposito, I. (2013) Mouse model pathology training for scientists: the results of a European Commission-funded e-learning pilot course. Special Seminar September 13, 2013. University of Glasgow, College of Medical, Veterinary & Life Sciences, Scotland

Sultana, A., Cox, T., Ghaneh, P. & Neoptolemos, J. P. (2012) Adjuvant therapy for pancreatic cancer. *Recent Results Cancer Res* **196**, 65-88

Sundberg, J. P., Ward, J. M., HogenEsch, H., Nikitin, A. Y., Treuting, P. M., Macauley, J. B. & Schofield, P. N. (2012) Training pathologists in mouse pathology. *Vet Pathol* **49**, 393-397

Szymas, J. & Lundin, M. (2011) Five years of experience teaching pathology to dental students using the WebMicroscope. *Diagn Pathol* **6 Suppl 1**, S13

Tanaka, M., Shibahara, J., Fukushima, N., Shinozaki, A., Umeda, M., Ishikawa, S., Kokudo, N. & Fukayama, M. (2011) Claudin-18 is an early-stage marker of pancreatic carcinogenesis. *J Histochem Cytochem* **59**, 942-952

Tascilar, M., Skinner, H. G., Rosty, C., Sohn, T., Wilentz, R. E., Offerhaus, G. J., Adsay, V., Abrams, R. A., Cameron, J. L., Kern, S. E., Yeo, C. J., Hruban, R. H. & Goggins, M. (2001) The SMAD4 protein and prognosis of pancreatic ductal adenocarcinoma. *Clin Cancer Res* **7**, 4115-4121

Tian, X., Liu, Z., Niu, B., Zhang, J., Tan, T. K., Lee, S. R., Zhao, Y., Harris, D. C. & Zheng, G. (2011) E-cadherin/beta-catenin complex and the epithelial barrier. *J Biomed Biotechnol* **2011**, 567305

Valli, T., Barthold, S. W., Ward, J. E., Brayton, C., Nikitin, A., Borowsky, A. D., Bronson, R. T., Cardiff, R. D., Sundberg, J. & Ince, T. (2007) Over 60% of NIH

extramural funding involves animal-related research. *Vet Pathol* **44**, 962-963, author reply 963-964

Vaughan, L., Huber, S., Chiquet, M. & Winterhalter, K. H. (1987) A major, six-armed glycoprotein from embryonic cartilage. *EMBO J* **6**, 349-353

Wang, Y., Schrag, D., Brooks, G. A. & Dominici, F. (2013) National trends in pancreatic cancer outcomes and pattern of care among Medicare beneficiaries, 2000 through 2010. *Cancer*

Wilson, J. S., Pirola, R. C. & Apte, M. V. (2014) Stars and stripes in pancreatic cancer: role of stellate cells and stroma in cancer progression. *Front Physiol* **5**, 52

Woll, S., Schlitter, A. M., Dhaene, K., Roller, M., Esposito, I., Sahin, U. & Tureci, O. (2014) Claudin 18.2 is a target for IMAB362 antibody in pancreatic neoplasms. *Int J Cancer* **134**, 731-739

Wormann, S. M. & Algul, H. (2013) Risk Factors and Therapeutic Targets in Pancreatic Cancer. *Front Oncol* **3**, 282

Yadav, D. & Lowenfels, A. B. (2013) The epidemiology of pancreatitis and pancreatic cancer. *Gastroenterology* **144**, 1252-1261

Zischka, H., Lichtmannegger, J., Schmitt, S., Jagemann, N., Schulz, S., Wartini, D., Jennen, L., Rust, C., Larochette, N., Galluzzi, L., Chajes, V., Bandow, N., Gilles, V. S., DiSpirito, A. A., Esposito, I., Goettlicher, M., Summer, K. H. & Kroemer, G. (2011) Liver mitochondrial membrane crosslinking and destruction in a rat model of Wilson disease. *J Clin Invest* **121**, 1508-1518

IX. ANNEX

1. Web-based learning platform for comparative histology

1.1. Material

1.1.1. Laboratory equipment

Unless indicated the companies or distributors were located in Germany.

Product	Company
Axioskop 20	Carl Zeiss AG, Jena
Aperio ScanScope CS	Aperio, Vista (USA)
Iomega LDHD UP external storage	Lenovo GmbH, Stuttgart
Intenso 8GB USB stick	Intenso GmbH, Vechta

1.1.2. Software

Product	Company
Adobe Acrobat 9 Pro	Adobe Systems GmbH, Munich
Adobe® Connect™	Adobe Systems GmbH, Munich
Adobe Photoshop Elements 5.0	Adobe Systems GmbH, Munich
Aperio ImageScope	Aperio, Vista (USA)
Doodle	Doodle AG, Zurich (CH)
Moodle 2.5.1	eLeDia - E-Learning im Dialog GmbH, Berlin
Skype 6.13	Microsoft, Redmond (USA)
WebMicroscope	University of Helsinki, Helsinki (FI)

2. Example for phenotyping of a mouse strain: The TNC

model

2.1.   Material

2.1.1.   Reagents

Product	*Company*
3,3'-Diaminobenzidin	Medac GmbH, Wedel
Acetic acid	Merck KGaA, Darmstadt
Acid Fuchsin	Sigma-Aldrich Chemie GmbH, Steinheim
Agarose LE for gel electrophoresis	Biozym Scientific GmbH, Hessisch Oldendorf
Alcian Blue 8GX powder	Sigma-Aldrich Chemie GmbH, Steinheim
Alcin Blue 1 %	MORPHISTO® Evolutionsforschung und Anwendung GmbH, Frankfurt am Main
Antibody diluent Dako REAL™	Dako Deutschland GmbH, Hamburg
Basic Fuchsin	Sigma-Aldrich Chemie GmbH, Steinheim
Bromophenol blue	Sigma-Aldrich Chemie GmbH, Steinheim
Chloroform	Merck KGaA , Darmstadt
Citric acid	Merck KGaA , Darmstadt
Crocein scarlet-acid fuchsin	MORPHISTO® Evolutionsforschung und Anwendung GmbH, Frankfurt am Main
Dako Pen	Dako Deutschland GmbH, Hamburg
Dimethylsulfoxid	Sigma-Aldrich Chemie GmbH, Steinheim
Discovery® MoMap™ Kit	Roche Diagnostics, Mannheim,
DNA-Loading dye 6X	Thermo Fisher Scientific, Schwerte
dNTP Set, 100 mM Solutions	Life Technologies GmbH, Darmstadt
Eosin	Sigma-Aldrich Chemie GmbH, Steinheim
Ethanol	Merck KGaA , Darmstadt
Ethidium bromide	Amresco, Solon (USA)
Ferric chlorid	MORPHISTO® Evolutionsforschung und Anwendung GmbH, Frankfurt am Main
Forene Isofluran	Abbott GmbH & Co. KG, Wiesbaden
Formalin	Staub & Co. GmbH, Munich
Generuler 100 bp DNA-Ladder ready to use	Thermo Fisher Scientific, Schwerte
Goat serum	Abcam plc, Cambridge, (UK)
Hemalm	AppliChem GmbH, Darmstadt
Hematoxylin Solution, Mayer's	Sigma-Aldrich Chemie GmbH, Steinheim

HistoMark Biotin-Streptavidin Peroxidase Kit	KPL, Inc., Gaithersburg (USA)
Hydrogen chloride	neoLab, Heidelberg
Hydrogen peroxide 30 %	Merck KGaA , Darmstadt
Isoamyl alcohol	Sigma-Aldrich Chemie GmbH, Steinheim
Isopropanol	Merck KGaA , Darmstadt
Light green SF yellowish	Merck KGaA, Darmstadt
Methanol	Merck KGaA , Darmstadt
Nuclear fast red-aluminum sulfate solution 0.1 %	Merck KGaA , Darmstadt
Orange G	Sigma-Aldrich Chemie GmbH, Steinheim
Peroxidase-labeled Streptavidin	KPL, Inc., Gaithersburg (USA)
Pertex mounting medium	Medite GmbH, Burgdorf
Phenol:Chloroform:Isoamyl alcohol 25:24:1	AppliChem GmbH, Darmstadt
Phosphotungstic acid hydrate	Sigma-Aldrich Chemie GmbH, Steinheim
Picric acid	Sigma-Aldrich Chemie GmbH, Steinheim
Ponceau Xylidine	Sigma-Aldrich Chemie GmbH, Steinheim
Potassium chloride	Sigma-Aldrich Chemie GmbH, Steinheim
Proteinase K	Roche Diagnostics, Mannheim
Rabbit Serum (10 %)	KPL, Inc., Gaithersburg (USA)
RNAlater®	Life Technologies GmbH, Darmstadt
Safron du Gatinais	MORPHISTO® Evolutionsforschung und Anwendung GmbH, Frankfurt am Main
Schiff's reagent	Sigma-Aldrich Chemie GmbH, Steinheim
Sodium chloride	Merck KGaA , Darmstadt
Sodium dodecyl sulfate 20 % (w/v) solution	AppliChem GmbH, Darmstadt
Sodium periodate	Sigma-Aldrich Chemie GmbH, Steinheim
Taq DNA Polymerase BioTherm™	Ares Bioscience GmbH, Köln
Trizma® base	Sigma-Aldrich Chemie GmbH, Steinheim
Verhoeff stock solution A, B, C	MORPHISTO® Evolutionsforschung und Anwendung GmbH, Frankfurt am Main
Wash Buffer 10x	Dako Deutschland GmbH, Hamburg
Water, Aqua ad iniectabilia	AlleMan Pharma GmbH, Rimbach
Weigert's iron hematoxylin kit	Merck KGaA , Darmstadt
Xylene	Merck KGaA , Darmstadt

2.1.2.   Consumables

Product	*Company*
Corning®DeckWorks® Pipette tips, 10 µl	Sigma-Aldrich Chemie GmbH, Steinheim
Corning®DeckWorks® Pipette tips, 1000 µl	Sigma-Aldrich Chemie GmbH, Steinheim
Corning®DeckWorks® Pipette tips, 20 µl	Sigma-Aldrich Chemie GmbH, Steinheim
Corning®DeckWorks® Pipette tips, 200 µl	Sigma-Aldrich Chemie GmbH, Steinheim
Coverslips	Carl Roth GmbH & Co.KG, Karlsruhe
Cryotubes	A. Hartenstein, Würzburg
Dako Tube with cap	Dako Deutschland GmbH, Hamburg
Embedding cassettes	A. Hartenstein, Würzburg
Microscope Slides	Gerhard Menzel GmbH, Braunschweig
Injekt™ 2 mL LL Syringe	B. Braun Melsungen AG, Melsungen
Injekt™ 5 mL LL Syringe	B. Braun Melsungen AG, Melsungen
SuperFrost® Microscope Slides	Gerhard Menzel GmbH, Braunschweig
PCR tube strips 0.2 ml	Eppendorf AG, Hamburg
PowerPac Basic Power Supply	Bio-Rad Laboratories GmbH, Munich
Reaction tubes 1.5 ml	Eppendorf AG, Hamburg
Reaction tubes 2 ml	Eppendorf AG, Hamburg
Reaction tubes Falcon™ Blue Max 15 ml	BD Bioscience, Heidelberg
Reaction tubes Falcon™ Blue Max 50 ml	BD Bioscience, Heidelberg
Safe seal microtubes	Eppendorf AG, Hamburg
Slide Storage Box	A. Hartenstein, Würzburg
Sterican® Hypodermic needle, 20G x 1 ½"	B. Braun Melsungen AG, Melsungen
Sterile Surgical Blade figure 26	C. Bruno Bayha GmbH, Tuttlingen

2.1.3.   Laboratory equipment

Product	*Company*
Aperio ScanScope CS	Aperio, Vista (USA)
Axioskop 20	Carl Zeiss AG, Jena
Centrifuge 5415D	Eppendorf AG, Hamburg
Centrifuge 5417R	Eppendorf AG, Hamburg

Dako Autostainer Universal Staining System	Dako Deutschland GmbH, Hamburg
Dissecting set type Ratisbon	Medax-lithomed, Schweinfurt
Eppendorf Mastercycler gradient	Eppendorf AG, Hamburg
Eppendorf research pipettes	Eppendorf AG, Hamburg
Gel documentation system	Vilber Lourmat, Eberhardzell
Glass coverslipper Promounter RCM2000	Medite GmbH , Burgdorf
Heating block Thermomixer® comfort 1.5 ml	Eppendorf AG, Hamburg
Heating block ThermoStat plus 1.5 ml	Eppendorf AG, Hamburg
Heating oven type BE400	Memmert, Schwabach
Heating plate HP 30 digital IKATHERM	IKA®-Werke GmbH & CO. KG, Staufen
Hotplate stirrer IKAMAG® RCT	IKA® Werke GmbH und Co.KG, Staufen
IKA® MS1 Minishaker	IKA® Werke GmbH und Co.KG, Staufen
Ikamage® RCT magnetic stirrer	IKA® Werke GmbH und Co.KG, Staufen
Incubator shaker Model G25	New Brunswick Sci., Edison (NJ, USA)
Lab centrifuge 4K15	Sigma-Aldrich Chemie GmbH, Steinheim
Laboratory balance BP 310 S	Sartorius AG, Göttingen
Magnetic stir bars, various sizes	NeoLab, Heidelberg
Magnetic stirrer MR2000	Heidolph Instruments, Schwabach
Microm HM 335 E	Thermo Fisher Scientific, Schwerte
Microtome blade	Pfm medical AG, Köln
Microwave Privileg 1034HGD	Otto, Hamburg
Mitsubishi P95 printer	Mitsubishi Electric, Ratingen
Nanodrop ND 2000c	Peqlab Biotechnology GmbH, Erlangen
Paraffin Embedding System Medite TBS 88	Medite GmbH, Burgdorf
pH-Meter (pH 211)	HANNA Instruments GmbH, Kehl am Rhein
Pressure cooker	WMF, Geislingen/Steige
Rocker table Rocky®	Fröbel Labortechnik, Lindau
Scales Sartorius universal	Sartorius AG, Göttingen
Shandon Excelsior ES	Thermo Fisher Scientific, Schwerte
Spectrophotometer NanoDrop® ND-1000	Thermo Fisher Scientific, Schwerte
Spectrophotometer UV/VIS Novaspec II	Pharmacia LKB, Uppsala (S)
Stuart Scientific SD Rocking Platform STR	Keison products, Chelmsford (GB)

Thermomixer compact	Eppendorf AG, Hamburg
Tissue Cool Plate COP 20	Medite GmbH, Burgdorf
Tissue Floatation Baths TFB 35	Medite GmbH, Burgdorf
Vacuum Concentrator plus	Eppendorf AG, Hamburg
Vortexer MS1 Minishaker	IKA®-Werke GmbH & CO. KG, Staufen
Wide Mini Subset GT electrophoresis system	Bio-Rad Laboratories GmbH , Munich

2.1.4.   Buffer

Citrate buffer for IHC

| Citric acid | 10 mM |
| pH 6 | |

Lysis buffer for DNA extraction

TRIS-HCL, pH 8.0	50 mM
NaCl	100 mM
EDTA	100 mM
SDS	1 %
Proteinase K	0.5 mg/ml

EDTA buffer for IHC

| EDTA | 1 mM |
| pH 8.0 | |

TBS 10X for IHC

TRIS base	250 mM
NaCl	1400 mM
pH 7.5	

2.1.5.   Software

Product   *Company*

Adobe Acrobat 9 Pro	Adobe Systems GmbH, Munich
Adobe Photoshop Elements 5.0	Adobe Systems GmbH, Munich
Aperio ImageScope	Aperio, Vista (USA)
Aperio Spectrum™ Plus	Aperio, Vista (USA)
Definiens Developer XD	Definiens AG, Munich
Definiens TissueStudio	Definiens AG, Munich

Endnote X6   Endnote, Carlsbad (USA)

IBM SPSS Statistics 21   IBM Deutschland GmbH, Ehningen

Image J   National Institutes of Health, Bethesda (USA)

Microsoft Office 2010   Microsoft, Redmond (USA)

X. ACKNOWLEDGEMENTS